

DISSERTATION

**TWO NOVEL FLUORESCENT IMMUNOASSAYS FOR MULTIANALYTE
DETECTION**

Submitted by

Brian M. Murphy

Department of Chemistry

In partial fulfillment of the requirements

For the Degree of Doctor of Philosophy

Colorado State University

Fort Collins, Colorado

Spring 2009

UMI Number: 3374634

INFORMATION TO USERS

The quality of this reproduction is dependent upon the quality of the copy submitted. Broken or indistinct print, colored or poor quality illustrations and photographs, print bleed-through, substandard margins, and improper alignment can adversely affect reproduction.

In the unlikely event that the author did not send a complete manuscript and there are missing pages, these will be noted. Also, if unauthorized copyright material had to be removed, a note will indicate the deletion.

UMI[®]

UMI Microform 3374634
Copyright 2009 by ProQuest LLC
All rights reserved. This microform edition is protected against
unauthorized copying under Title 17, United States Code.

ProQuest LLC
789 East Eisenhower Parkway
P.O. Box 1346
Ann Arbor, MI 48106-1346

COLORADO STATE UNIVERSITY

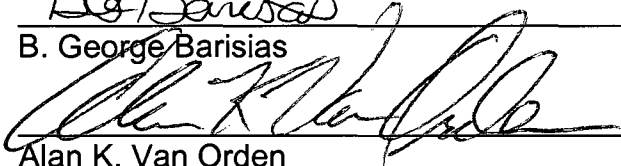
April 3, 2009

WE HEREBY RECOMMEND THAT THE DISSERTATION PREPARED UNDER OUR SUPERVISION BY BRIAN M. MURPHY ENTITLED "TWO NOVEL FLUORESCENT IMMUNOASSAYS FOR MULTIANALYTE DETECTION" BE ACCEPTED AS FULFILLING IN PART REQUIREMENTS FOR THE DEGREE OF DOCTOR OF PHILOSOPHY.

Committee on Graduate Work



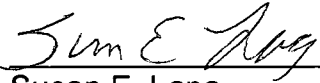
B. George Barisias



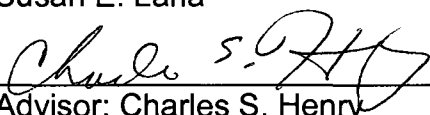
Alan K. Van Orden



Robert M. Williams



Susan E. Lana



Advisor: Charles S. Henry



Department Head: Anthony K. Rappe

ABSTRACT OF DISSERTATION
TWO NOVEL FLUORESCENT IMMUNOASSAYS FOR MULTIANALYTE
DETECTION

Since their inception several decades ago, immunoassays have become the workhorse technology for measuring both proteins and small molecules in complex biological matrices. Immunoassay technologies have become important tools in the field of medicine, where measurement of a variety of analytes in media such as urine, blood, or serum is essential. To diagnose many diseases and conditions, clinicians rely on the quantification of several biomarkers in a sample. However, common immunoassay systems such as ELISA can measure only a single analyte at a time, and can take hours to complete. This dissertation details two new immunoassay methods designed to simultaneously quantify several analytes from a single sample. Protein patterning on a silicon nitride wafer is performed for a micromosaic fluorescent immunoassay in which the thyroid hormone thyroxine (T4), inflammation biomarker CRP, and BSA-conjugated 3-nitrotyrosine (3NT) are assayed in the competitive format. The assay for 3NT is then combined with a sandwich immunoassay for superoxide

dismutase (SOD) and catalase (CAT), demonstrating that micromosaic immunoassays can be used to simultaneously quantitate small and large targets. In a second approach, a unique capillary electrophoresis immunoassay is performed for 3NT, carboxy-methyl lysine (CML), and thyroxine (T4). Termed a cleavable tag immunoassay (CTI), the method relies on bioconjugation of IgGs to unique chemically cleavable fluorophores which serve as reporter groups for each analyte. A novel method for bioconjugation of IgG to fluorophore to produce the conjugates is presented. Microchip CE with fluorescence detection is demonstrated and resolution is optimized for the separation of three different CTI conjugate fragments. This dissertation will argue for the viability of both methods as relevant in the development of true multianalyte clinical diagnosis assays.

Brian M. Murphy

Department of Chemistry

Colorado State University

Fort Collins, CO 80523

Spring 2009

ACKNOWLEDGEMENTS

I would like to thank everyone in the Henry Lab who helped me in one way or another. Whether it was through discussion of the science or just keeping good company, you are appreciated. I would like to thank Dr. Meghan Caulum for her pioneering work on the CTI project, and N. Scott Lynn for his help in collaboration on the micromosaics project.

I would like to acknowledge NIH, Synkera, and NBS group for funding opportunities.

I would like to give special thanks to those who have inspired me so much, including Dr. Alvin Frostad, Barbara Harding, Dr. Kevin Cantrell, Dr. Raymond Bard, Rob Conner, and of course my family Mom, Dad, and Kate. I attribute so much of my success to your positive influences.

TABLE OF CONTENTS

	<u>page</u>
ABSTRACT	iii
ACKNOWLEDGEMENTS	v
LIST OF FIGURES	ix
LIST OF TABLES	xii
CHAPTERS	
1. INTRODUCTION	1
1.1. Antibodies as Chemical Probes	1
1.2. Multi-Analyte Immunoassays	2
1.2.1. ELISA	3
1.2.2. Protein Array Technology	4
1.2.3. Capillary Electrophoresis Immunoassays	6
1.3. Micromosaic Immunoassays	11
1.4. Cleavable Tag Immunoassay	14
1.5. Dissertation Summary	16
1.6. References	18
2. COMPETITIVE IMMUNOASSAY METHODS FOR DETECTION FOR DETECTION OF METABOLITES AND PROTEINS USING MICROMOSAIC PATTERNING	23
2.1. Introduction	23
2.2. Materials and Methods	26
2.2.1. Chemicals and Materials	26
2.2.2. Fabrication of Microfluidic Networks	27
2.2.3. Preparation of Labeled Proteins and Protein Conjugates	27
2.2.4. Micromosaic Immunoassays on Silicon Nitride Substrates	28
2.3. Results and Discussion	29
2.3.1. Specificity of Fluorescent Tracers for Surface-Bound Capture Reagents	29
2.3.2. Optimization of Competitive Immunoassays	33
2.3.3. Competitive Immunoassays for T4, CRP, and BSA-3NT	34
2.3.4. Estimation of Affinity Constants	39
2.4. Conclusions	45
2.5. References	45

3. ANALYSIS OF OXIDATIVE STRESS BIOMARKERS USING A SIMULTANEOUS COMPETITIVE/NON-COMPETITIVE MICROMOSAIC IMMUNOASSAY	49
3.1. Introduction	49
3.2. Materials and Methods	51
3.2.1. Chemicals and Materials	51
3.2.2. Protein Labeling and Conjugation	52
3.2.3. Microfluidic Network Fabrication and Substrate Preparation	52
3.2.4. Micromosaic Immunoassays	53
3.3. Results and Discussion	55
3.3.1. Cross Reactivity Analysis	55
3.3.2. Multiplexed Immunoassay for CAT, 3NT, and SOD	56
3.3.3. Calculation of Limits of Detection	63
3.3.4. Mitigating Depletion Effect with Selective Geometries	64
3.4. Conclusions	67
3.5. Acknowledgements	69
3.6. References	69
4. FLUORESCENT CTI TAGS FOR AVIDIN-BIOTIN BASED IMMUNOCONJUGATION SCHEMES	
4.1. Introduction	72
4.2. Materials and Methods	73
4.2.1. Chemicals and Materials	73
4.2.2. Synthesis of FTHD and FAM Tags	73
4.2.3. Capillary Electrophoresis	74
4.3. Results and Discussion	77
4.3.1. Capillary Electrophoresis of CTI Tag Products	77
4.4. Conclusions	80
4.5. References	80
5. COMPETITIVE MICROPLATE CTI FOR 3NT, T4, AND BSA-CML	
5.1. Introduction	81
5.2. Materials and Methods	83
5.2.1. Chemicals and Materials	83
5.2.2. Preparation of IgGs for Conjugation	85
5.2.3. One Step CTI Conjugates Using DTSSP Crosslinker	85
5.2.4. Modification of IgG with SPDP Crosslinker	87
5.2.5. Thiol-Amine Conjugation to SPDP Modified IgG	88
5.2.6. Fluorescence Derivatization of Thiol-Amine Modified IgG	88
5.2.7. PDMS Microchip Fabrication	91
5.2.8. Microplate Competitive Immunoassay	92
5.2.9. Separation Parameters for Microchip Fluorescence CE	93
5.3. Results and Discussion	94
5.3.1. Examination of One Step CTI Conjugation Using DTSSP	94
5.3.2. Quantification of Crosslinking of IgG to SPDP	95
5.3.3. Primary Amine Concentration of Modified and Unmodified IgG	99

5.3.4. Molar F/P Ratio Quantification for FITC Labeled Conjugates	100
5.3.5. Competitive CTI for BSA-3NT	103
5.3.6. Three Analyte Competitive CTI	103
5.4. Conclusion	111
5.5. References	111
6. RESEARCH SUMMARY AND FUTURE DIRECTIONS	113
6.1. Research Summary	113
6.2. Future Work	115
APPENDIX 1: RESEARCH PROPOSAL	116

LIST OF FIGURES

Figure		Page
1.1	Schematic of micromosaic immunoassay. A. Substrate is sensitized during first dimension patterning. B. Substrate is blocked from non-specific binding with BSA. C. Second dimension pattern with fluorescent affinity reagent. D. Completed micromosaic.	13
1.2	CTI, sandwich immunoassay format. Step 1: targets are captured on antibody-conjugated particles. Step 2: Detection antibodies are introduced to particles. Step 3: TCEP is exposed to the particles, allowing diffusion of tracers into solution. Step 4: tracers are analyzed by CE.	17
2.1	Schematic of patterning steps for T4 immunoassay. (I) BSA-T4 is patterned through a microfluidic network on the substrate. (II) The substrate is washed, leaving the patterned feature. (III) Remaining reactive sites are blocked from non-specific adsorption using BSA. (IV) A sample containing FITC-labeled monoclonal antibody for T4 is patterned perpendicular to the first feature using a second microfluidic network. (V) Affinity interactions are observed in a mosaic pattern on the substrate using fluorescence imaging.	30
2.2	Specificity assessment of the three surface receptor/fluorescent ligand pairs. Receptors were immobilized to the substrate during first dimension patterning. Dilutions of fluorescent ligands patterned orthogonally to the first dimension demonstrate the affinity and specificity properties of the system. Cross-reactivity and non-specific binding were below the fluorescent detection limit employed here.	32
2.3	Fluorescent image of the competitive immunoassay for T4, CRP and BSA-3NT. Solutions containing each analyte were prepared with a fluorescent tracer for each analyte at a constant, empirically-determined concentration. Decreasing signal with increasing analyte concentration demonstrates the competitive effect for each analyte. An affinity purified serum sample was prepared at known concentrations of each analyte, which is analyzed in the far left column.	35
2.4	Dose-response curves for each analyte. Each fluorescent intensity plot was constructed from fluorescence data taken from the image in	36

Fig. 2.3 as described in the text.

2.5	Plots of $1/\Delta F$ versus $1/[L]$ for each antibody-antigen system shown in Fig. 2.2. The slope and intercept for each curve can be used to estimate the dissociation constants (K_D) between a tracer and its surface receptor.	42
3.1	Schematic showing microfluidic channel shape for first and second dimension patterning (a) and for third dimension pattern (b). Inset of 12 channel design is shown in (c), where each channel is 20 microns wide with 40 micron spacing.	54
3.2	Micromosaic demonstrating tracer specificity for patterned and captured proteins for each of the three analytical targets CAT, 3NT and SOD.	57
3.3	Micromosaic immunoassay for simultaneous detection of CAT, 3NT, and SOD. Solutions patterned in the first and second dimension are indicated. The entire mosaic was patterned in the third dimension with 50 μ g/ml AF pAb CAT and 50 μ g/ml AF pAb SOD detection antibodies.	59
3.4	Dose-response curves for CAT, 3NT, and SOD obtained from fluorescent signals in Fig. 3.3.	61
3.5	Fluorescence intensity profile of 100ng/ml CAT mosaics with direction of flow indicated. Depletion of analyte from solution occurs along the direction of flow.	62
3.6	Reagent depletion effect can be predicted using linear fluid dynamics. Cross section of microchannel with reagent flowing over reactive spots. Image courtesy of Scott Lynn, CSU Department of Chemical Engineering.	65
3.7	Examination of the effect of microchannel spacing on analyte depletion using AF mAb 3NT. BSA-3NT spacing of 0 (left) and 4 empty microchannels (right).	66
3.8	RSD versus channel spacing (in microns) for AF mAb 3NT geometrical optimization experiment.	68
4.1	Synthesis of FTHD and FHB.	74
4.2	Synthesis of FAM and FAMB.	76

4.3	Electropherograms for FTED and FTHD using caffeine as a neutral marker. Both products exhibit a single product peak, and can be easily resolved from one another.	77
4.4	Electropherograms for the reaction of FTHD and sulfo-NHS-SS-biotin. FTHD is consumed, and a new product peak is formed.	79
4.5	Formation of FAM using FITC and cystamine. Cleavage of the final product is observed after addition of disulfide reducing reagent TCEP.	79
5.1	Schematic for one-step CTI conjugation using the homobifunctional crosslinker DTSSP and FITC derived with a diamine.	86
5.2	Schematic for modification of target antibody with SPDP crosslinker. Exposure of the conjugate to DTT results in cleavage of the disulfide and release of pyridine-2-thione.	89
5.3	Conjugation of SPDP modified antibody to thiol-amine and FITC fluorophore.	90
5.4	Size-exclusion chromatogram of native pAb CAT and pAb CAT conjugated to FTED using DTSSP in a one-step procedure. Flow rate was 1 ml/min in 100 mM sodium phosphate pH 6 run buffer. Injection was 20 μ l of 1 mg/ml antibody.	96
5.5	Sample electropherogram for separation of FCAM and FCYS tags (A). CTI dose-response curve for BSA-3NT (B). Separation buffer was 10 mM HEPPSO, 5 mM SDS, 0.5 mM TDAPS pH 7.5. Cleavage buffer was 10 mM HEPPSO, 1 mM TCEP pH 7.5.	104
5.6	Electropherogram for separation of FCAM, FCYS, and FCG CTI fragments. Separation buffer was 10 mM TAPS, 5 mM SDS, 0.05% Triton-X 100, and 20% acetonitrile.	106
5.7	Specificity and peak identity experiment. Substrates were sensitized to only one analyte, but incubated with all three CTI immunoconjugates in the second step.	108
5.8	Competitive effect of 3NT, T4, and BSA-CML on cleaved tag peaks. Above: 0 μ M 3NT, 0 μ M T4, 0 μ g/mL BSA-CML. Below: 10 μ M 3NT, 10 μ M T4, 4 μ g/mL BSA-CML. Separation buffer was 10 mM TAPS, 5 mM SDS, 0.05% Triton-X 100.	109

5.8	Dose-response curve for 3NT in three analyte system. Error bars represent one standard deviation.	110
-----	---	-----

LIST OF TABLES

Table		Page
2.1	Detection limits and serum response for the analytes T4, CRP, and BSA-3NT.	38
2.2	Estimated K_D values for each affinity pair assayed.	44
5.1	CTI conjugates used for competitive immunoassays. Abbreviations used in the text are in the column to the far right.	102

Chapter 1

Introduction

1.1 Antibodies as Chemical Probes

Analytical chemists are constantly searching for differences in chemical properties which they can exploit in a way to differentiate one analyte from another. This concept of selectivity makes modern chemical analysis possible. Biological organisms must also possess mechanisms for differentiating between one species and another, although the consequences of their selective capacity can mean the difference between survival and death. This idea is exemplified by the mammalian immune system which is able to recognize foreign molecules and selectively rid them from the body. Upon recognition of a hazardous substance, the immune system produces immunoglobulin proteins, antibodies, which bind to their target with high selectivity and high affinity to prevent the target from damaging the host.

The same properties that make antibodies an essential element of our immune systems also make them incredibly attractive as chemical probes for quantification of analytes, particularly in complex media such as blood or serum where specificity is paramount to the success of the analysis. The antibody as a chemical probe was popularized by Yalow and Berson in the late 1950's.^{1,2} The researchers observed that the disappearance of radiolabeled insulin was slowed in patients who had received insulin previously, and theorized this was due to the presence of antibodies that would bind to insulin and prevent uptake. Low

concentrations of the suspected antibody prevented the use of immunoprecipitation for detection. Using paper electrophoresis, they were able to separate radiolabeled insulin from immunocomplex and developed the first radioimmunoassay for insulin in the process. This work showed that quantification of soluble immunocomplexes could be used for detection of antigens at levels much lower than other immunological methods at the time. During the same year, Ekins described a similar electrophoretic assay for the thyroid hormone thyroxine.³ Rosalyn S. Yalow was awarded the Nobel Prize for her work on radioimmunoassays in 1977.⁴ Decades later, immunoassay techniques have found mainstream use in clinical and research settings, and are a billion-dollar industry.⁵

1.2 Multi-Analyte Immunoassays

One of the modern challenges to improving immunoassay techniques is the advancement of multi-analyte immunoassays.⁵ The ability to simultaneously quantify several analytes from a sample can save time and money, and can improve the quality of diagnosis in clinical settings. Furthermore, conditions such as oxidative stress manifest themselves through changes in several macromolecular and metabolite concentrations.⁶ Oxidative stress cannot be accurately diagnosed by examining an individual biomarker, therefore the diagnosis of that condition would be improved using multianalyte techniques.^{7, 8} Multi-analyte immunoassay techniques would also be useful in drug discovery, where groups of clinically related analytes need to be measured in many

samples.⁹ A brief discussion of multianalyte immunoassays and standard assay techniques relevant to the dissertation is presented below, but is in no way an exhaustive review of the many immunoassay techniques described to date.

1.2.1 ELISA

Enzyme-linked immunosorbent assay (ELISA) is one of the most popular immunoassay techniques used today. ELISA is considered a solid-phase heterogeneous immunoassay as a reaction between antibody and target occurs on a solid phase after one of the reagents has been adsorbed to it. In early ELISA cellulose was used as a solid phase, which has been replaced with polystyrene microtiter plates.¹⁰ Detection of surface-bound immunocomplex is performed with an enzyme-conjugated anti-IgG.¹¹ Unbound reagents are washed away from the solid phase, which is then exposed to an enzyme substrate which typically produces a chromogenic product upon reaction with the enzyme.¹² In modern ELISA, microtiter plates on which the assay reaction occurs can be placed into a plate reading device to quantify the enzyme products, which can then be used to calculate the concentration of antigen in the sample.

ELISA is generally considered to be a single-analyte technique, meaning that only one analyte is analyzed at a time from a single sample. However, there have been attempts to multiplex ELISA. Wiese et al. used a microarrayer to localize capture antibodies in 250 micron spots in glass microplate wells before analyte capture and detection.¹³ This allowed for the detection of multiple analytes in a single microplate well. Similarly, Adrian et al. were able to detect 25

different antibiotics using spatial control of solid-phase receptors.¹⁴ Another approach is to utilize different enzyme labels for each immunochemical reaction. Multianalyte ELISA using different enzyme labels for different antibodies has seen little advancement.¹⁵ This approach has been limited because of discrepancy of conditions for which enzyme activity is optimal, such as pH. Another limiting factor is the number of different enzymes available for immunoassay. One possible solution to this problem involves sequential enzyme activity measurements. Spencer et al. performed a multianalyte ELISA using multiple enzymes by first measuring activity of captured alkaline phosphatase-bound antibody, then rinsed the well and measured captured peroxidase-bound antibody.¹⁶ Although multianalyte analysis using ELISA seems quite limited today, the method will likely remain the most heavily used immunodiagnostic technique for single-analyte analysis due to its versatility and acceptance in the scientific community.

1.2.2 Protein Array Technology

In the late 1980's, Roger Ekins advanced the "ambient analyte theory" which suggested that using a smaller and smaller amount of antibody to measure antigen in solution should result in a more sensitive immunoassay.¹⁷ When a large amount of antibody is exposed to sample, formation of the immunocomplex significantly reduces the amount of unbound antigen in solution. In this situation, the total number of immunocomplexes that can be formed in a given amount of time (and the total antigen in solution) is the limiting factor. Ekins postulated that

this behavior changes radically as the amount of capture antibody used is reduced. At low concentration of capture antibody, formation of the immunocomplex no longer significantly reduces the amount of antigen in solution. This occurs at an antibody concentration of less than $0.05/K$, where K is the affinity constant for immunocomplexation.¹⁸ Here, the “fractional occupancy” of the binding sites directly reflects the amount of antigen in solution. The assay is more sensitive because the immunocomplex is formed at a high antigen concentration. When an ambient analyte assay utilizes a “microspot” of antibody on a solid phase, an increased signal density (typically fluorescence) on the microspot can lead to further increases in sensitivity.¹⁹

Ekins's ambient analyte theory helped pave the way for the development of antibody microarrays.²⁰ Protein microarrays arrived as an offspring of DNA microarrays, which were designed to investigate the expression of thousands of genes at once.²¹ Because mRNA quantification cannot always predict protein levels, investigation of the proteome requires more direct measurement of proteins.^{19, 22, 23} Through the use of conventional robot arrayers, proteins were printed onto a substrate with micron-sized spots over which immunoassays and other affinity assays could be performed.^{24, 25} Using this technology, over 10,000 individual protein spots can be arrayed, providing a platform for proteomics with quantitative capabilities far exceeding that of conventional 2D gel electrophoresis.⁹ While protein arrays are a valuable research tool, limitations involving production of the arrays and high cost of the instrumentation required to perform the assays prevents widespread application as a clinical tool for

immunoassays.⁹ Protein microarrays would benefit from improved protein capture chemistry, standard labeling procedure for all proteins used for detection, and methods for arraying proteins with higher uniformity.^{9, 18, 26}

1.2.3. Capillary Electrophoresis Immunoassays

Capillary electrophoresis (CE) is an analytical technique that uses analyte migration in an electric field as a basis for separation. An analyte's electrophoretic mobility is dependent on its charge and its hydrated radius, which can be approximated using its mass.²⁷

$$\mu = q/6\pi\eta r \quad (1.1)$$

where q is the charge of the particle, η is the buffer viscosity, and r the Stokes' radius of the analyte. Assuming a spherical particle, the mass M is related to r by:

$$M = (4/3)\pi r^3 \rho \quad (1.2)$$

where V is the volume of the particle in solution.

Popular electrophoretic techniques such as SDS-PAGE use electrophoretic migration to separate protein and DNA sample components along the length of a gel matrix under an applied electric field. In this situation, migration of the solvent molecules does not drastically affect the performance of

the separation. However, when an electric field is applied along the length of an open tubular capillary filled with buffer, migration of solvent molecules at the wall-solvent interface causes movement of the bulk solution due to a favorable surface area to volume ratio. This is termed electroosmotic flow. During capillary electrophoresis, an analyte's velocity v_i is proportional to the product of its mobility and electroosmotic flow:

$$v_i = \mu_{app}E = (\mu_{ep}\mu_{eo})E \quad (1.3)$$

where μ_{app} is the observed mobility, E is the applied field, μ_{ep} is the mobility of the analyte due to the potential alone, and μ_{eo} is the mobility due to electroosmotic flow.

CE was realized as an analytical tool by Mikkers and then Jorgenson in the early 1980's.^{28, 29} In nearly three decades since its inception, CE has been used for the separation and analysis of a wide range of analytes. Compared to traditional bioanalytical electrophoretic techniques such as gel electrophoresis, CE provides advantages of lower detection limits, higher applied field strengths, better quantitative capabilities, and the ability to easily detect small biomolecules such as amino and nucleic acids.³⁰ Furthermore, CE consumes low volumes of sample and buffer compared to other methods. CE also benefits from a user interface and instrument control similar to that used for HPLC.³¹

There are two CE-based immunoassay methods that are relevant to the discussion of multianalyte immunoassay techniques, immunoaffinity capillary

electrophoresis (IACE) and capillary electrophoresis immunoassay (CEIA). Immunoaffinity capillary electrophoresis was developed by Guzman and others for preconcentration and detection of trace analytes in complex samples.³² In this technique, antibodies are first immobilized on a solid phase, often the walls of the capillary tubing. Sample is passed over the immobilized antibodies, and target molecules are captured and retained on the solid phase as excess sample is washed away. This step can be used to enrich trace analytes that would otherwise not be detectable at physiological concentrations. After preconcentration, the immunocomplex is dissociated using a strong acid, allowing the analyte to diffuse from the solid phase into solution. Next, CE is performed on the released targets. Enrichment factors of 10^3 have been reported using the method.³³ IACE is an attractive analytical tool as it is two dimensional: analytes are selected during an affinity step and separated during an electrophoretic step. For example, two analytes possessing the same epitope could both be captured in the immunoaffinity step, and then separated and quantified during CE. In contrast, ELISA would only select for the epitope and therefore recognize the two targets as a single analyte, leading to errors in quantification.³³ Note that in some cases, quantification of a single epitope across several biomolecular species may be desirable, such as in the investigation of oxidative deglycosylation in proteins by monitoring carboxymethyl lysine modified residues.³⁴ In such cases ELISA may be a more simple and desirable technique. IACE can be further augmented with the addition of a mass spectrometric step following CE, affording increased selectivity and qualitative data for the analysis.

Shaw and Guzman used IACE-MS to detect neurotensin and angiotensin II in a urine sample.³⁵ IACE may be most relevant for the study of small molecule targets that are more resistive to degradation in the elution step than larger analytes such as proteins. An excellent example of IACE in practice was demonstrated by Phillips and Wellner. Antibodies for 12 different neuropeptides were immobilized in the well of a microfluidic device. Targets were captured from the sample onto the solid phase, and labeled with a fluorescent tracer following the wash step. After acid elution, all 12 labeled neuropeptides were separated using CE on the microchip. In comparing their IACE method to an electrokinetic immunoassay, the authors showed their method could process and detect all analytes in 5 minutes, while an electrokinetic assay could detect only four analytes in 10 minutes.³⁶ This work also demonstrated the ability of IACE to be performed in microchip format where reaction and separation times are reduced compared to those in a conventional instrument.

Capillary electrophoresis immunoassay is a technique that uses CE to separate products from a solution-phase immunoanalytical reaction. Use of electrophoresis to perform such separations has a historical precedent in Yalow and Berson's early immunoassays, which used paper electrophoresis to separate radioimmunoassay products.² Modern CEIA involves labeling of one or more reagent with a detectable tracer group, typically a fluorophore. After reaction with the sample, products are separated and quantified with CE. A competitive or "excess reagent" format is usually employed as this method will result in a peak for tracer and a peak for tracer-antibody immunocomplex for each analyte in the

system. CEIA is an appealing alternative to conventional immunoassay methods for several reasons. CE uses little sample and buffer, which is important when dealing with biological samples that are often of low volume or expensive. Solution-phase reaction kinetics are employed and separations usually take place on the order of minutes, drastically decreasing analysis time over solid-phase methods such as ELISA. Finally, CEIA has the potential to be used for multianalyte analysis from a single sample.³⁷

Separation of antibody-antigen complexes using CE was first described by Nielsen et al. for the separation of human growth hormone (hGH) from monoclonal anti-hGH.³⁸ Soon after, Schultz and Kennedy described both competitive and non-competitive CEIA for insulin using fluorescein isothiocyanate (FITC)-labeled tracers and a laser-induced fluorescence (LIF) detection method.³⁹ Continued research on CEIA has resulted in attempts to multiplex the method and improve separations. Miki et al. demonstrated CEIA for human serum albumin (HSA) in which the immunological reaction was performed on-column by consecutive injection of antibody and tracer which reacted upon application of the separation potential.⁴⁰ They reported a detection limit for HSA 14 times lower than that found with off-column mixing. CEIA for IgM was investigated by Feng et al. using anti-IgM conjugated to a quantum dot to both label the tracer and to improve resolution.⁴¹ This was demonstrated as resolution of the tracer and tracer-antigen complex was improved using the method. Using CE with laser-induced fluorescence, Caslavská et al. developed a CEIA protocol for detection of urinary drugs of abuse. Simultaneous quantitative analysis of

methadone, morphine, benzoylceognin and D-amphetamine was demonstrated by competitive CEIA using the method.⁴² In another attempt to multiplex CEIA, Guillo and Roper used a novel two-color immunoassay for the detection of insulin and glucagon.⁴³ An insulin tracer was prepared using the FITC label, while glucagon was labeled with Cy5. Two different LIF detectors were utilized for detection. This work showed that problems with peak resolution in CEIA could be avoided by using spectrally resolvable tracers. CEIA has also been adapted to microchip format, most notably for the detection of insulin secreted by islets of Langerhans.⁴⁴ Separations were performed in only 5 seconds, and sampling could be performed every 15 seconds. This work also demonstrated the ability to monitor insulin secretion from live cells on-chip.

1.3 Micromosaic Immunoassays

Micromosaic immunoassays have been explored as a way to miniaturize protein microarrays by eliminating the largest and most expensive component—the microarrayer machinery. Micromosaic immunoassays were developed as a way to deliver immunoassay reagents to defined locations on a solid phase using a network of microchannels instead of a robotic spotter. Microchannels with features on the order of tens of microns can be easily fabricated using soft lithography and the polymer poly-(dimethylsiloxane) (PDMS).⁴⁵⁻⁴⁷ A hole punch can be used to create wells in a PDMS microfluidic network that allow the introduction of solution to the channels with a micropipetter.

As in a traditional protein microarray experiment, micromosaic immunoassays typically involve a minimum of two steps: substrate sensitization and immunological reaction. First, a PDMS microfluidic network is made hydrophilic through the use of an air plasma. This treatment allows for a reversible seal between the network and substrate, and for capillary flow of solution through the channels. In this scenario, the channels are defined on three sides by PDMS and on the bottom by the substrate. Upon sealing to the substrate, sensitizing reagent is introduced to channel wells and flows through the channels across the substrate. Because solution flows under capillary action, no mechanical pumps are necessary. After removal and rinsing, a defined pattern of adsorbed proteins remains on the substrate. Following a blocking step, a second set of microfluidic channels is placed perpendicularly over the patterned proteins. Fluorescently labeled affinity reagent is introduced to the channel, allowing reaction at sensitized spots on the surface. The second set of channels is removed, and the substrate imaged using fluorescence microscopy. An example from the literature of this procedure is shown in Figure 1.1.⁴⁸

Micromosaics were described by Rowe et al. for the detection of staphylococcal enterotoxin B, plague F1 antigen, and D-dimer.⁴⁹ Each could be detected within 35 minutes using the method and with LODs similar to other detection methods. Wolf et al. demonstrated the quantitative detection of C-Reactive Protein (CRP) within 10 minutes with an LOD of 30 ng/mL.⁵⁰ The dynamic range of this assay easily covered the clinical reference range for CRP.

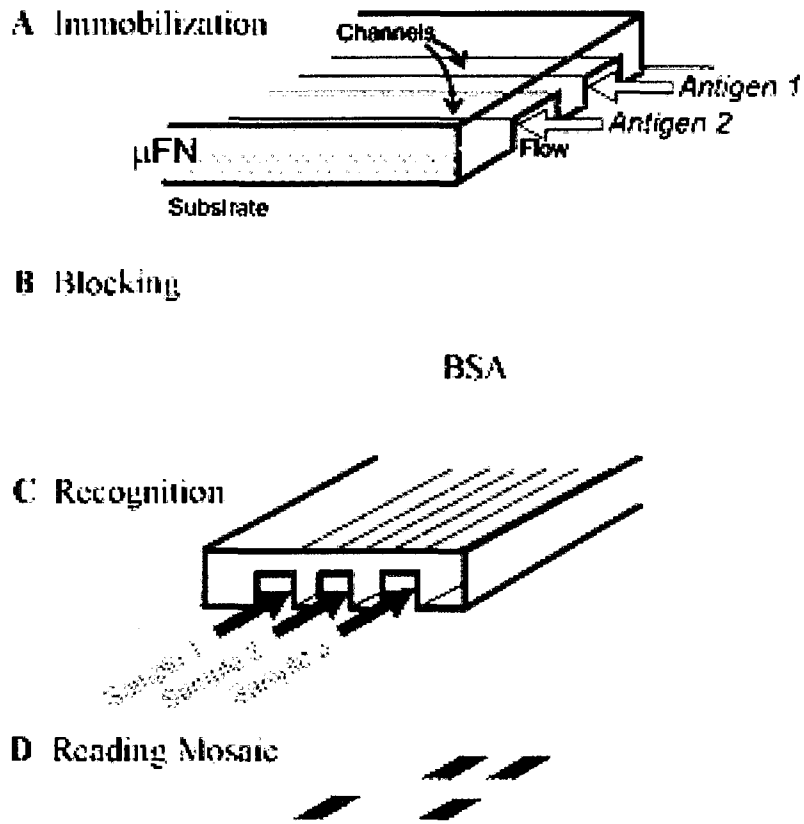


Figure 1.1. Schematic of micromosaic immunoassay. A. Substrate is sensitized during first dimension patterning. B. Substrate is blocked from non-specific binding with BSA. C. Second dimension pattern with fluorescent affinity reagent. D. Completed micromosaic.⁴⁸

Micromosaics have been applied for the screening of cell surface receptors and for the detection of viral and bacterial antigens as well.^{51, 52}

1.4 Cleavable Tag Immunoassay

Despite the advances in CEIA technology, there are several pitfalls which prevent CEIA from becoming a universal method for multianalyte immunoassays. CEIA for a single analyte will produce at least two peaks in each electropherogram, one for free tracer and one for tracer-immunocomplex. In a multianalyte immunoassay, the presence of multiple peaks can lead to electropherogram crowding and resolution problems. Impurities and unreacted labeling reagent can further increase the number of peaks required for the analysis of a single analyte.^{53, 54} If a labeled antibody is employed, steps must be taken to ensure the electrophoretic homogeneity of the tracer to prevent the appearance of additional peaks. This means that monoclonal antibodies should be used instead of polyclonal antibodies.³⁷ Likewise, the heterogeneity of the antigen itself could prove problematic, especially for larger targets such as proteins.

Peak resolution is also a potential problem for multianalyte CEIA. If direct quantification of immunocomplexes is required, the bound target must impart enough of a change in charge and/or mass to the immunocomplex so that it can be resolved from free tracer and from other immunocomplexes in the system. This could prove especially difficult for smaller analytes. Disassociation of the immunocomplex over the course of the separation can also have a negative

impact on peak shape and resolution.^{39, 55} This is an especially difficult problem as the buffer conditions most favorable to the stability of the immunocomplex are not always the best conditions for separation by CE.⁵⁶

Cleavable Tag Immunoassay (CTI) has been introduced as a solution to several of the problems of multianalyte CEIA.⁵⁷ Many of the problems stem from the fact that CEIA utilizes the affinity reagents themselves as the signaling molecules necessary for quantification. In contrast, reaction and detection steps in ELISA are decoupled in such a way that the nature of the antibody and antigen do not affect the way the signal is observed by the operator. CTI seeks to bring the same decoupling strategy to electrophoretic immunoassays through the implementation of unique antibody-fluorophore conjugates. First, a fluorophore is conjugated to an antibody through a spacer group and a disulfide bond. This conjugate is then used as a detection antibody in either a sandwich or indirect competitive solid phase immunoassay. After rinsing, the solid phase is exposed to a solution containing a disulfide reducing reagent such as tris (2-carboxyethyl) phosphine (TCEP). This reduces the external disulfides on the antibody, allowing the fluorophores to diffuse into solution. CE is then performed on this solution. The technique is multiplexed through the use of different fluorophore-antibody conjugates which produce fluorescent tracers of differing electrophoretic mobilities when chemically cleaved. This gives the analyst synthetic control over the mobilities of the signaling molecules. Furthermore, fluorophores can be conjugated to any IgG class antibody, suggesting that the method can be applied to any desired target analyte. Recently, CTI was used for the detection of four

markers of cardiac inflammation.⁵⁸ A schematic of this procedure from the literature is shown in Figure 1.2.

1.5 Dissertation Summary

This dissertation describes recent advancements in both micromosaic immunoassay and CTI technology. Research described here was undertaken with the goal of developing both methods towards universal multianalyte analysis. The first chapter details the background necessary for understanding immunoassays in general, and the history of assay development that has led us to techniques of today. In Chapter 2, the first micromosaic immunoassay utilizing two competitive formats is presented. Discussion of micromosaics is continued in Chapter 3 in which the method is adapted for the simultaneous analysis of small molecules by competitive assay and macromolecules such as proteins by sandwich immunoassay. Chapter 4 is a discussion on the synthesis of two CTI tags used for a sandwich immunoassay in our laboratory. Chapter 5 describes a new method for bioconjugation of fluorophores to antibodies used in CTI, and demonstrates the first competitive immunoassays using the CTI method. Chapter 6 summarizes the work to date on both research projects, and examines future directions for micromosaic and CTI research.

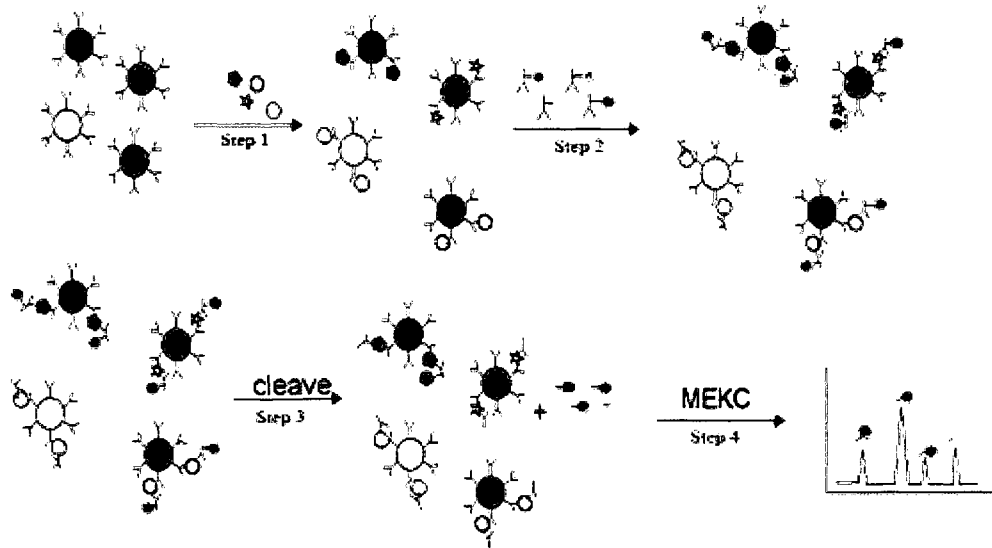


Figure 1.2. CTI, sandwich immunoassay format. Step 1: targets are captured on antibody-conjugated particles. Step 2: Detection antibodies are introduced to particles. Step 3: TCEP is exposed to the particles, allowing diffusion of tracers into solution. Step 4: tracers are analyzed by CE.⁵⁸

1.6 References

- (1) Berson, S. A.; Yalow, R. S.; Bauman, A.; Rothschild, M. A.; Newerly, K. *Journal of Clinical Investigation* **1956**, *35*, 170-190.
- (2) Yalow, R. S.; Berson, S. A. *Nature* **1959**, *184*, 1648-1649.
- (3) Ekins, R. P. *Clinica Chimica Acta* **1960**, *5*, 453-459.
- (4) Yalow, R. S. *Nobel Lecture* **1977**.
- (5) Diamandis, E., Christopoulos, T.K., In *Immunoassay*; Academic Press: San Diego, 1996, pp 1-3.
- (6) Wood, L. G.; Gibson, P. G.; Garg, M. L. *J Sci Food Agr* **2006**, *86*, 2057-2066.
- (7) Mateos, R.; Bravo, L. *J Sep Sci* **2007**, *30*, 175-191.
- (8) Halliwell, B.; Whiteman, M. *Brit J Pharmacol* **2004**, *142*, 231-255.
- (9) Nielsen, U. B.; Geierstanger, B. H. *Journal of Immunological Methods* **2004**, *290*, 107-120.
- (10) Engvall, E.; Perlmann, P. *Immunochemistry* **1971**, *8*, 871-&.
- (11) Avrameas, S. *Immunochemistry* **1969**, *6*, 43-&.
- (12) Kemeny, D. M., Challacombe, S.J. *ELISA and Other Solid Phase Immunoassays*; Wiley Medical: Chichester, 1988.
- (13) Wiese, R.; Belosludtsev, Y.; Powdrill, T.; Thompson, P.; Hogan, M. *Clin Chem* **2001**, *47*, 1451-1457.

- (14) Adrian, J.; Pinacho, D. G.; Granier, B.; Diserens, J. M.; Sanchez-Baeza, F.; Marco, M. P. *Analytical and Bioanalytical Chemistry* **2008**, *391*, 1703-1712.
- (15) Kricka, L. J. In *Immunoassay*; Diamandis, E., Christopoulos, T., Ed.: San Diego, 1996, pp 389-404.
- (16) Spencer, K.; Macri, J. N.; Anderson, R. W.; Aitken, D. A.; Berry, E.; Crossley, J. A.; Wood, P. J.; Coombes, E. J.; Stroud, M.; Worthington, D. J.; Doran, J.; Barbour, H.; Wilmot, R. *Annals of Clinical Biochemistry* **1993**, *30*, 394-401.
- (17) Ekins, R. P. *Journal of Pharmaceutical and Biomedical Analysis* **1989**, *7*, 155-168.
- (18) Stoll, D.; Templin, M. F.; Schrenk, M.; Traub, P. C.; Vohringer, C. F.; Joos, T. O. *Frontiers in Bioscience* **2002**, *7*, C13-C32.
- (19) Templin, M. F.; Stoll, D.; Schrenk, M.; Traub, P. C.; Vohringer, C. F.; Joos, T. O. *Trends in Biotechnology* **2002**, *20*, 160-166.
- (20) Ekins, R.; Chu, F. *Annales De Biologie Clinique* **1992**, *50*, 337-353.
- (21) Wilson, D. S.; Nock, S. *Angew Chem Int Ed Engl* **2003**, *42*, 494-500.
- (22) Anderson, L.; Seilhamer, J. *Electrophoresis* **1997**, *18*, 533-537.
- (23) Gygi, S. P.; Rochon, Y.; Franza, B. R.; Aebersold, R. *Molecular and Cellular Biology* **1999**, *19*, 1720-1730.
- (24) MacBeath, G.; Schreiber, S. L. *Science* **2000**, *289*, 1760-1763.

- (25) Zhu, H.; Bilgin, M.; Bangham, R.; Hall, D.; Casamayor, A.; Bertone, P.; Lan, N.; Jansen, R.; Bidlingmaier, S.; Houfek, T.; Mitchell, T.; Miller, P.; Dean, R. A.; Gerstein, M.; Snyder, M. *Science* **2001**, *293*, 2101-2105.
- (26) Mitchell, P. *Nature Biotechnology* **2002**, *20*, 225-229.
- (27) Landers, J. P. In *Capillary and Microchip Electrophoresis and Associated Microtechniques*
3rd ed.; Landers, J. P., Ed.; CRC Press: Boca Raton, 2008, pp 4-69.
- (28) Mikkers, F. E. P.; Everaerts, F. M.; Verheggen, T. P. E. M. *Journal of Chromatography* **1979**, *169*, 11-20.
- (29) Jorgenson, J. W.; Lukacs, K. D. *Analytical Chemistry* **1981**, *53*, 1298-1302.
- (30) Deyl, Z.; Tagliaro, F.; Miksik, I. *Journal of Chromatography B-Biomedical Applications* **1994**, *656*, 3-27.
- (31) Landers, J. P. *Clinical Chemistry* **1995**, *41*, 495-509.
- (32) Guzman, N. A.; Trebilcock, M. A.; Advis, J. P. *Journal of Liquid Chromatography* **1991**, *14*, 997-1015.
- (33) Guzman, N. A.; Blanc, T.; Phillips, T. M. *Electrophoresis* **2008**, *29*, 3259-3278.
- (34) Baynes, J. W. *Diabetes* **1991**, *40*, 405-412.
- (35) Shaw, C. J., Gusman, N.A. In *Handbook of Pharmaceutical Analysis*;
Ohannesian, L., Streeter, A.J., Ed.; Marcel Dekker: New York, 2002, pp 313-386.
- (36) Phillips, T. M.; Wellner, E. F. *Electrophoresis* **2007**, *28*, 3041-3048.

- (37) Yeung, W. S. B.; Luo, G. A.; Wang, Q. G.; Ou, J. P. *Journal of Chromatography B-Analytical Technologies in the Biomedical and Life Sciences* **2003**, *797*, 217-228.
- (38) Nielsen, R. G.; Rickard, E. C.; Santa, P. F.; Sharknas, D. A.; Sittampalam, G. S. *Journal of Chromatography* **1991**, *539*, 177-185.
- (39) Schultz, N. M.; Kennedy, R. T. *Analytical Chemistry* **1993**, *65*, 3161-3165.
- (40) Miki, S.; Kaneta, T.; Imasaka, T. *J Chromatogr A* **2005**, *1066*, 197-203.
- (41) Feng, H. T.; Law, W. S.; Yu, L.; Li, S. F. Y. *Journal of Chromatography A* **2007**, *1156*, 75-79.
- (42) Caslavská, J.; Allemann, D.; Thormann, W. *Journal of Chromatography A* **1999**, *838*, 197-211.
- (43) Guillo, C.; Roper, M. G. *Electrophoresis* **2008**, *29*, 410-416.
- (44) Roper, M. G.; Shackman, J. G.; Dahlgren, G. M.; Kennedy, R. T. *Analytical Chemistry* **2003**, *75*, 4711-4717.
- (45) Bernard, A.; Delamarche, E.; Schmid, H.; Michel, B.; Bosshard, H. R.; Biebuyck, H. *Langmuir* **1998**, *14*, 2225-2229.
- (46) Kane, R. S.; Takayama, S.; Ostuni, E.; Ingber, D. E.; Whitesides, G. M. *Biomaterials* **1999**, *20*, 2363-2376.
- (47) Xia, Y. N.; Kim, E.; Zhao, X. M.; Rogers, J. A.; Prentiss, M.; Whitesides, G. M. *Science* **1996**, *273*, 347-349.
- (48) Bernard, A.; Michel, B.; Delamarche, E. *Anal Chem* **2001**, *73*, 8-12.
- (49) Rowe, C. A.; Scruggs, S. B.; Feldstein, M. J.; Golden, J. P.; Ligler, F. S. *Anal Chem* **1999**, *71*, 433-439.

- (50) Wolf, M.; Michel, B.; Hunziker, P.; Delamarche, E. *Biosensors & Bioelectronics* **2004**, *19*, 1193-1202.
- (51) Wolf, M.; Zimmermann, M.; Delamarche, E.; Hunziker, P. *Biomed Microdevices* **2007**, *9*, 135-141.
- (52) Rowe, C. A.; Tender, L. M.; Feldstein, M. J.; Golden, J. P.; Scruggs, S. B.; MacCraith, B. D.; Cras, J. J.; Ligler, F. S. *Analytical Chemistry* **1999**, *71*, 3846-3852.
- (53) Chen, F. T. A.; Evangelista, R. A. *Clinical Chemistry* **1994**, *40*, 1819-1822.
- (54) Ye, L. W.; Le, X. C.; Xing, J. Z.; Ma, M. S.; Yatscoff, R. *Journal of Chromatography B-Analytical Technologies in the Biomedical and Life Sciences* **1998**, *714*, 59-67.
- (55) German, I.; Kennedy, R. T. *Journal of Chromatography B-Analytical Technologies in the Biomedical and Life Sciences* **2000**, *742*, 353-362.
- (56) Schou, C.; Heegaard, N. H. H. *Electrophoresis* **2006**, *27*, 44-59.
- (57) Caulum, M. M.; Henry, C. S. *Analyst* **2006**, *131*, 1091-1093.
- (58) Caulum, M. M.; Murphy, B. M.; Ramsay, L. M.; Henry, C. S. *Analytical Chemistry* **2007**, *79*, 5249-5256.

Chapter 2

Competitive Immunoassay Methods for Detection of Metabolites and Proteins Using Micromosaic Patterning

2.1 Introduction.

Following Berson and Yalow's pioneering work in the late 1950's, immunoassay techniques have become the primary tool for analysis of complex biological samples in clinical laboratory settings.¹ Antibodies are the essential reagent for immunoassay testing, providing high selectivity, specificity, and affinity necessary to assay complex samples such as whole blood or serum. Thousands of antibodies and other affinity reagents are available commercially for a variety of analytes, ranging from large proteins to small molecules. Although many affinity assays have been developed, heterogeneous immunoassay protocols have become increasingly popular in both clinical and research labs. These procedures require one or more affinity capture reagents to be bound to a solid phase to capture target analytes. This design proves advantageous because excess or unreacted reagent and sample can be separated from the desired immunocomplex by washing the surface following the capture reaction.² Heterogeneous methods concentrate reagent on the surface thereby increasing the observed signal. Solid-phase heterogeneous formats have been superseded by modern techniques such as the enzyme-labeled immunosorbent assay (ELISA.) The micromosaic strategy has recently been developed as a high-density heterogeneous immunoassay.^{3,4} In the micromosaic patterning approach,

micron-scale channels are fabricated in a polymer, normally poly(dimethylsiloxane) (PDMS), using soft lithography.⁵ Completed microfluidic networks (μ FNs) are then formed when the network is reversibly sealed to a flat substrate such as a silicon wafer or PDMS. Solutions carrying reagent are introduced to the microfluidic network through ports in the polymer mold.^{4, 6} During first-dimension patterning, a receptor molecule flows through the network and binds to the substrate, either through passive adsorption, affinity interaction, or covalent attachment.⁴ This creates a pattern of the receptor on the substrate that replicates the pattern of the microfluidic channels. After removal of the first microfluidic channel, remaining reactive sites on the substrate are passivated with a blocking agent to minimize non-specific adsorption. For second-dimension patterning, the reagents are delivered to the substrate via channels perpendicular to the initial pattern of the immobilized capture molecules. Binding between analytes in the sample and surface-bound affinity reagents is observed after the removal of the second stamp, usually via fluorescence. Affinity interactions produce a pattern of squares on the substrate, thus the term “micromosaic” has been used to describe the pattern. Micromosaic immunoassays offer an appealing alternative to traditional immunoassays for several reasons. Required sample volumes are sub-microliter, and the flow of solution through the network is driven by capillary and hydrodynamic flow eliminating the need for pressurized or electrokinetic pumps. Furthermore, the method allows for precise localization of reagents onto the substrate at the micron scale, while the sample ports provide an interface for macroscopic control of microscopic phenomena. Lastly,

such assays are rapid because they take advantage of micron-scale diffusion distances.^{7, 8} Micromosaics have been used to measure DNA hybridization rates, detect cell surface receptors, detect cardiac markers, and simultaneously analyze samples for different analyte classes including bacteria, viruses, and proteins.⁹⁻¹² To date, however, they have not been used for competitive immunoassays.

This chapter demonstrates the first competitive micromosaic immunoassays using thyroxine (T4), C-Reactive Protein (CRP) and bovine serum albumin labeled 3-nitrotyrosine (BSA-3NT) as model analytes. Surface-activated silicon nitride is employed as the substrate, a unique material for heterogeneous immunoassays with direct applications to waveguide technology.¹³ It is shown that both direct (surface-bound antibody) and indirect (surface-bound hapten) competitive formats can be performed simultaneously.¹⁴ Analyte binding curves allow detection over the reference ranges for T4 (60 to 140 nM) and CRP (<10 µg/mL) and over ng/mL concentrations of BSA-3NT. Finally, detection of all three analytes in affinity-purified human serum is successfully demonstrated. This work attempts to introduce multiplexed analysis of metabolites and proteins using the micromosaic platform as an important step in bioassay development.¹⁵ This chapter was originally published in *Analytical Chemistry*.¹⁶

2.2 Materials and Methods

2.2.1 Chemicals and Materials

CRP (#30-AC05), CRP monoclonal antibody (mAb) (mouse IgG₁, M701289), and T4 mAb (mouse IgG_{2b}, M94208) were purchased from Fitzgerald (Concord, MA). 3NT pAb (rabbit IgG A-21285) was purchased from Invitrogen (Carlsbad, CA). N-(2-aminoethyl)-3-aminopropyl-trimethoxysilane (EDS) was obtained from Gelest (Morrisville, PA). Sulfo-SMCC, all dialysis materials, and BCA protein assay materials were purchased from Pierce (Rockford, IL). Silicon nitride coated silicon wafers (500 Å thickness) were received as a gift from Thermo-Electron (Waltham, MA), and silicon wafers coated with 100nm of thermal oxide were purchased from University Wafer (South Boston, MA). SU8-2035 photoresist was purchased from Microchem (Newton, MA). PDMS monomer and crosslinker (Sylgard 184) were received from Dow Corning (Midland, MI) and used at the recommended 10:1 ratio. Biopsy punches used for creating entrance and exit wells in the μ FNs were purchased from Technical Innovations (Brazoria, TX). Serum samples were affinity-purified in our laboratory against antibody-coated particles.¹⁷ Purified samples were spiked with analyte to the desired concentrations. All other chemicals and reagents were obtained from Sigma (St. Louis, MO) and used as received. Fluorescent measurements were made using a Photometrics HQ² CCD camera from Roper Scientific (Tuscon, AZ) and Metamorph software from Molecular Devices (Sunnyvale, CA) on a Nikon Eclipse TE2000-U epifluorescence microscope assembly (Melville, NY).

2.2.2. Fabrication of Microfluidic Networks

Photolithographic molds for microfluidic networks were made according to previous reports.^{18, 19} Masks were designed using Adobe Illustrator and printed by Photoplot Store at 40,000 dpi (Colorado Springs, CO.) It was observed that silicon wafers with a 100nm layer of thermal oxide bonded strongly to SU-8 photoresist, providing stability and reproducibility for features below 30 μm in width. Each mold was designed as a negative relief for a network containing twelve separate channels, each 20 μm wide with 40 μm spacing between channels. Profilometry was used to measure actual channel cross-sectional dimensions, and these were found to be 26 μm wide and 16.1 μm high. PDMS μFNs made from this mold were prepared for sample introduction with a 1.65mm diameter punch to create inlet and outlet ports. All μFNs were subjected to sequential solvent extraction using toluene, ethyl acetate, and acetone for two hours each with stirring. Residual solvent was removed from the μFNs by overnight baking at 65°C. Solvent compatibility with PDMS has been established previously.²⁰

2.2.3. Preparation of Labeled Proteins and Protein Conjugates

Prior to use, all proteins were purified by dialysis against PBS (150mM NaCl, 50mM Na₂HPO₄ pH 7.4) at 4°C for 8 hours using a Pierce Slide-a-Lyzer kit with a 3.5kDa molecular weight cutoff. BSA-T4 and BSA-3NT conjugates were prepared according to the literature, however the haptens were solubilized using

DMSO and 50mM phosphate pH 8.5 prior to conjugation due to low solubility at lower pH values.²¹ It was found that conjugates could also be synthesized effectively according to the Pierce instructions for EDC-based coupling as an alternative method. Conjugates were dialyzed against PBS and water at room temperature ($22\pm 1^\circ\text{C}$) extensively to remove unreacted hapten and EDC, which could interfere with assay performance. T4-mAb, 3NT-pAb as well as CRP were labeled with the amine-reactive fluorophore fluorescein isothiocyanate (FITC) according to the established procedure (Sigma). FITC conjugates were purified using Pall Omega Nanosep 3kDa centrifuge filters. Final concentrations of all stock protein solutions were determined by bicinchoninic acid assay (BCA).²²

2.2.4. Micromosaic Immunoassays on Silicon Nitride Substrates

All silicon nitride substrates were modified with a thiol-reactive maleimide group to facilitate covalent surface immobilization of affinity reagents as previously reported.²³ Briefly, substrates were first silanized using EDS which functionalized the surface with a primary amine. Derivatization of the amine with the heterobifunctional crosslinker Sulfo-SMCC produced a maleimide modified substrate capable of reaction with protein sulfhydryls. Protein attached in such a manner was expected to present the sample with a population of heterogeneously oriented receptors. BSA conjugate adsorption on both modified and unmodified silicon nitride was found to adsorb to modified and unmodified substrates, however functional levels of mAb-CRP bound only to modified substrates. μFNs were rendered hydrophilic by exposure to air plasma (18W) for

30 seconds (first-dimension patterning) or 40 seconds (second dimension patterning) at 25 torr. Hydrophilic μ FNs were sealed to 2cm x 2cm silicon nitride substrates using very light pressure. Sample ports were filled with $<1\mu\text{L}$ of solution, which could subsequently be observed with the naked eye traversing the length of the channel under capillary action. First-dimension patterning was allowed to proceed for 10 minutes, at which time the μ FN was removed under a constant flow of PBS containing 0.05% Tween 20 (PBS-T) to prevent further surface patterning. Substrates were rinsed copiously with PBS-T solution and water. Remaining reactive sites on the surface were blocked with a solution of 5% BSA and 1mM 8-anilino-1-naphthalene sulfonic acid (ANS) in PBS for 5 minutes. The concentration of BSA in the blocking solution required for a complete surface passivation in 5 minutes time was determined empirically. The same rinse procedure followed the blocking step, and substrates were then dried under a stream of nitrogen. Orthogonal second-dimension patterning followed the same parameters as the first, with μ FN removal after 20 minutes. Substrates were given a final wash then dried under nitrogen before fluorescence measurements were made. A schematic of the overall procedure for an indirect competitive T4 assay is show in Figure 2.1.

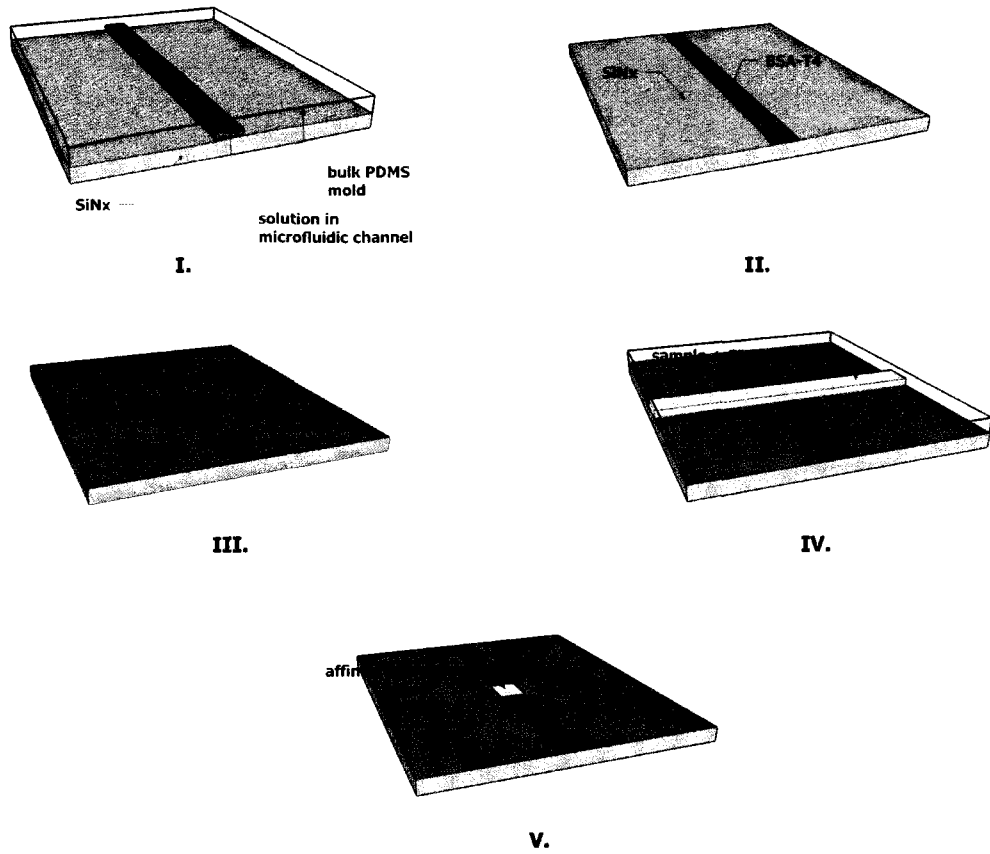


Figure 2.1. Schematic of patterning steps for T4 immunoassay. (I) BSA-T4 is patterned through a microfluidic network on the substrate. (II) The substrate is washed, leaving the patterned feature. (III) Remaining reactive sites are blocked from non-specific adsorption using BSA. (IV) A sample containing FITC-labeled monoclonal antibody for T4 is patterned perpendicular to the first feature using a second microfluidic network. (V) Affinity interactions are observed in a mosaic pattern on the substrate using fluorescence imaging.

2.3. Results and Discussion

2.3.1. Specificity of Fluorescent Tracers for Surface-Bound Capture

Reagents

Immunoassays derive much of their usefulness from the high specificity of antibodies for antigens or haptens in complex samples. However, cross-reactivity between antibodies and other non-target serum metabolites, solutes or proteins is a concern in every immunoassay. It is therefore important to assess reagent cross-reactivity before a multianalyte immunoassay can be performed. An experiment was designed to examine cross-reactivity between the two competitive immunoassay formats and three fluorescent reagents. For first-dimension patterning, BSA-T4 (0.24 mg/mL), CRP mAb (0.025 mg/mL), and BSA-3NT (0.14 mg/mL) were patterned in triplicate in one direction across a silicon nitride substrate. Channels containing 2mg/mL BSA in PBS were used as a negative control between channels containing conjugates and antibody. After washing and blocking, four dilutions each of FITC-T4-mAb, FITC-CRP, and FITC-3NT-pAb were patterned perpendicular to and over the surface bound receptors. A representative fluorescent image of this micromosaic is shown in Figure 2.2. Labeled ligands in this system clearly bind only to their intended targets on the substrate, as indicated by each fluorescent signal at mosaics where there is a matched affinity pair. Non-specific binding at BSA-blocked locations outside of the mosaic was also below a detectable level, and did not interfere with the experiment at the protein concentrations employed. This result demonstrates that all three corresponding analytes can be assayed

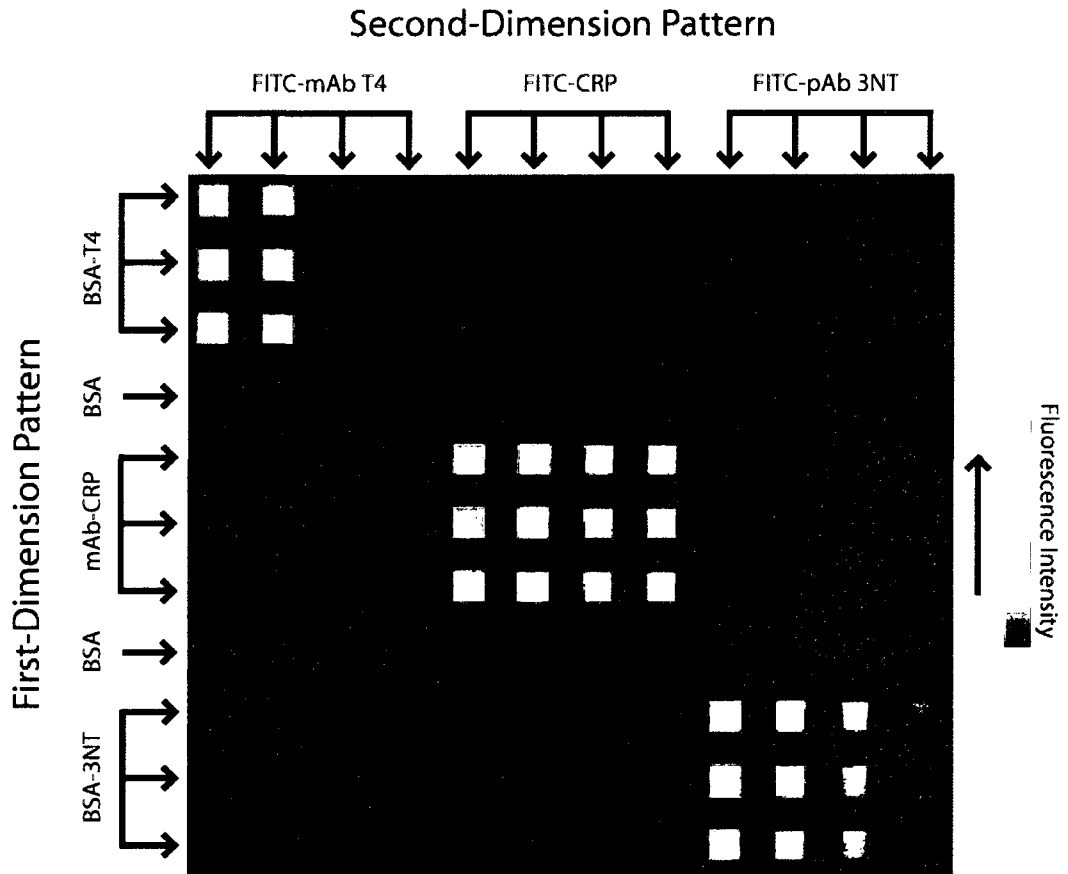


Figure 2.2. Specificity assessment of the three surface receptor/fluorescent ligand pairs. Receptors were immobilized to the substrate during first dimension patterning. Dilutions of fluorescent ligands patterned orthogonally to the first dimension demonstrate the affinity and specificity properties of the system. Cross-reactivity and non-specific binding were below the fluorescent detection limit employed here.

simultaneously using the micromosaic approach, without interference due to reagent cross-reactivity.

2.3.2 Optimization of Competitive Immunoassays

All competitive immunoassays rely on the premise that a labeled or immobilized reagent can compete with sample analyte for the same binding site on an antibody. Dose-response curves produced in this manner show an inverse relationship between signal and analyte concentration.²⁴ These sigmoidal curves have a variable slope, the steeper part of the curve being the most useful for quantitation. One advantage of competitive immunoassays is that dose-response curves can be adjusted so that signal response is most sensitive over the concentration range of interest, often defined by the reference range.²⁴ The position of the curve in relation to analyte concentration is determined by several factors, most notably the ratio of labeled reagent to analyte. This parameter was easily manipulated for competitive micromosaic immunoassays used in this study. Determination of the appropriate labeled reagent or “tracer” concentration was accomplished empirically. Analyte standards spanning the appropriate reference range were spiked with different concentrations of tracer, and the resulting signals evaluated for dose-response sensitivity. Finally, solutions containing all three standards were spiked with tracer at concentrations of 23.3 µg/mL FITC-mAb T4, 7.3 µg/mL FITC-CRP, and 17.8 µg/mL FITC-pAb 3NT. Solutions also contained 0.2mM ANS, a molecule used to displace T4 from binding with serum proteins.²⁵ It should be noted that the original intent of this

study was to assay the unconjugated 3NT amino acid as a marker for oxidative damage.²⁶ However, after labeling pAb-3NT with FITC, the specific antibody used in these experiments did not respond to the free amino acid in solution. FITC-pAb 3NT did respond competitively to the BSA-3NT conjugate in solution, and thus for the purpose of these experiments the conjugate was used as an analyte. This phenomenon has been previously reported in other immunoassays for 3NT.²⁷

2.3.3. Competitive Immunoassay for T4, CRP, and BSA-3NT

Standard buffer solutions (PBS, 45 mg/mL human serum albumin) containing each of the three analytes were prepared and spiked with the appropriate amounts of tracer and ANS. Affinity purified human serum spiked with known values of each analyte was prepared similarly to evaluate assay applicability with true biological samples. First-dimension affinity reagent patterning was undertaken as in Figure 2.2., followed by second-dimension patterning of the eleven standard solutions of known concentrations and one serum sample (Figure 2.3). Relative fluorescent signals for each standard solution mosaic were plotted against their respective analyte concentrations, shown in Figure 2.4. Error bars represent signal variation between each of the three mosaic squares for each standard. Each curve was fit to a four-parameter logistic model equation:

$$Y = \frac{a - d}{1 + \left(\frac{T}{c}\right)^b} + d \quad (2.1)$$

Second Dimension Pattern - Competitive Immunoassay

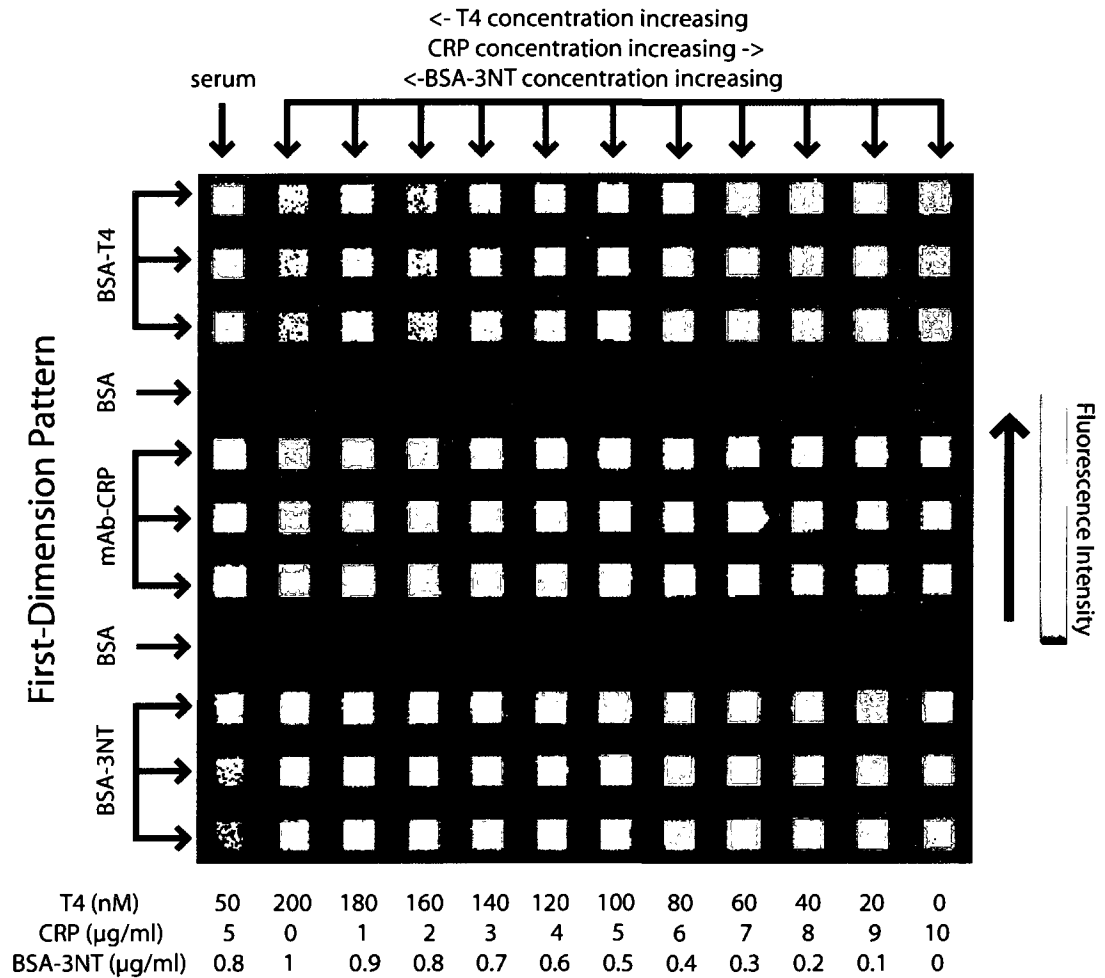


Figure 2.3. Fluorescent image of the competitive immunoassay for T4, CRP and BSA-3NT. Solutions containing each analyte were prepared with a fluorescent tracer for each analyte at a constant, empirically-determined concentration. Decreasing signal with increasing analyte concentration demonstrates the competitive effect for each analyte. An affinity purified serum sample was prepared at known concentrations of each analyte, which is analyzed in the far left column.

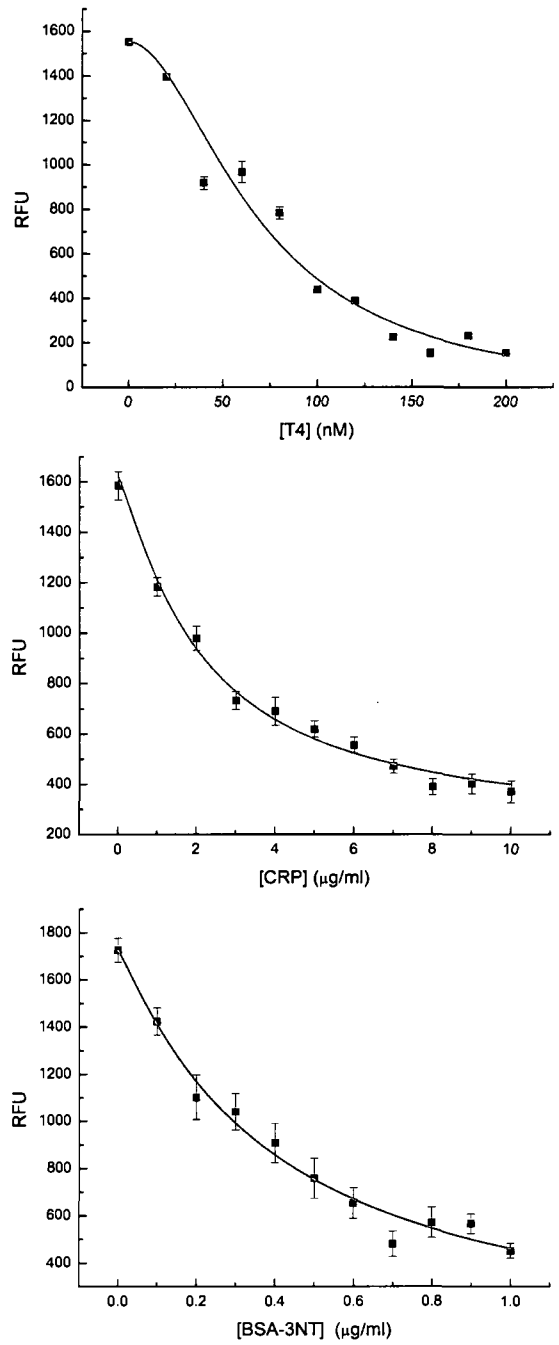


Figure 2.4. Dose-response curves for each analyte. Each fluorescent intensity plot was constructed from fluorescence data taken from the image in Fig. 2.3 as described in the text.

where Y is the fluorescent signal, a is the signal response in the absence of analyte, d is the response at infinite analyte concentration (non-specific binding of tracer), c is the concentration of analyte which gives a signal $Y = (a+d)/2$, T is the analyte concentration, and b is the absolute value of the slope of the curve when expressed in a log-logit format.²⁴ Curves were fit using the non-linear curve fit function in OriginPro 7 (Logistic, 100 iterations). The logistic equation curve fits were used to determine the detection limits (LOD) at both extremes of each curve. LOD at the low concentration/high signal end of the curve was calculated as the concentration that produced signal 2 standard deviations of the zero-analyte signal below the zero-analyte signal. At the opposite end of the curve, LOD was calculated as the concentration which produced a signal 3 times that of the non-specific binding (parameter d in the logistic equation.) These results are listed in Table 2.1. While the assay for CRP does not cover the entire clinical range of interest, 0 to 100 $\mu\text{g/mL}$, it is noted that dilution of samples above the upper LOD may allow for quantification on this curve.¹⁰ All errors were calculated as a single standard deviation of the three mosaic signals for each standard solution and analyte.

Spiked serum samples gave readings for T4 (49 ± 1.4 nM) and CRP (5.0 ± 0.7 $\mu\text{g/mL}$) that were within error of the intended standard concentrations (50 nM T4, 5 $\mu\text{g/mL}$ CRP). BSA-3NT was spiked into the serum at 0.8 $\mu\text{g/mL}$ but produced a signal reading 2.3 ± 0.47 $\mu\text{g/mL}$. As with CRP, a more accurate result might be obtained through dilution of the sample to a concentration producing a

	T4 (nM)	CRP (µg/ml)	BSA-3NT(µg/ml)
LOD's	7.7-257.2	0.3-4.2	0.03-22.4
Serum value	49 ± 1.4nM	5.0 ± 0.7	2.3 ± 0.47
Actual value	50	5	0.8

Table 2.1. Detection limits and serum response for the analytes T4, CRP, and BSA-3NT.

signal on the more sensitive portion of the dose-response curve. The difference between measured and spiked levels of BSA-3NT may be the result of systematic error and/or non-specific cross-reactivity of the antibody with another sample component. In Figure 2.3., signal from the BSA-3NT mosaics appear to decrease descending vertically. This effect could be due to depletion of the antibody/immunocomplex in solution as it binds to the mosaic, combined with a slower diffusion rate. The problems associated with this particular assay, including the low reactivity with free 3NT, could be addressed by examining assay performance using different antibodies.

2.3.4 Estimation of Affinity Constants

If a Langmuir-type adsorption model is assumed (concentration of analyte \gg immobilized affinity reagent), data from Figure 2.2. and Figure 2.3. can be used to estimate the dissociation constants (K_D) between each affinity pair in the system. Similar calculations have been used for SPR-based competitive immunoassays.²⁸ These calculations are straightforward because they do not require quantification of the surface affinity reagent. It is important to mention that the notation used below assumes a direct format such as that used here for CRP, although the same calculations were used for indirect format assays such as those performed for T4 and BSA-3NT.

The amount of receptor-ligand immunocomplex [RL] can be expressed as

$$[RL] = \frac{[R][L]}{K_{D(L)}} \quad (2.2)$$

where $[R]$ denotes the concentration of free surface binding sites and $[L]$ the ligand, with $K_{D(L)}$ as the dissociation constant. A mass balance for the surface receptor can be written as

$$[R_T] = [RL] + [R] \quad (2.3)$$

where $[R_T]$ is the total concentration of binding sites on the surface over a given area. Combining and rearranging the two equations gives

$$\frac{[RL]}{[R_T]} = \frac{[R][L]/K_{D(L)}}{[RL] + [R]} \quad (2.4)$$

The relationship of this ratio with the fluorescent signal can be written as

$$\frac{\Delta F}{\Delta F_{0\max}} = \frac{[RL]}{[R_T]} \quad (2.5)$$

where ΔF is the fluorescent signal at a given $[L]$ (and thus $[RL]$), and $\Delta F_{0\max}$ is the signal when the surface receptor binding sites are saturated with labeled ligand.

After rearrangement, this becomes

$$\frac{1}{\Delta F} = \left(\frac{K_{D(L)}}{\Delta F_{0\max}} \right) \left(\frac{1}{[L]} \right) + \frac{1}{\Delta F_{0\max}} \quad (2.6)$$

A plot of $1/[L]$ versus $1/\Delta F$ allows the calculation of $K_{D(L)}$ and $\Delta F_{0\max}$ from the slope and intercept. The dilutions of fluorescent reagent and the signals taken

from Fig. 2.1. were used to produce the plots in Fig. 2.5. using Eq(6). The $K_{D(L)}$ between the ligand and surface receptor was calculated for each pair in the three analyte system.

During a competitive immunoassay, the labeled reagent is held at a fixed concentration while the analyte concentration varies. Under these conditions, concentration and affinity constants determine fractional binding of each competitor to the antibody. When an analyte [A] competes with labeled ligand [L] a new equilibrium expression may be written as

$$[RA] = \frac{[R][A]}{K_{D(A)}} \quad (2.7)$$

where [A] is the analyte concentration, [RA] the receptor-analyte immunocomplex, and $K_{D(A)}$ the dissociation constant for [RA]. A mass balance for the three component system can be written for the surface receptor as

$$[R_T] = [RL] + [R] + [RA] \quad (2.8)$$

Combining equations (2), (3), (5) and (8), we can write

$$\frac{\Delta F}{\Delta F_{0\max}} = \frac{[RL]}{[R_T]} = \frac{[R][L]/K_{D(L)}}{[RL] + [R] + [RA]} \quad (2.9)$$

Finally, by substituting equation (7) and rearranging, we can write

$$\frac{1}{\Delta F} = \left(\frac{K_{D(L)}}{K_{D(A)} \Delta F_{0\max} [L]} \right) ([A]) + \frac{1 + K_{D(L)}/[L]}{\Delta F_{0\max}} \quad (2.10)$$

A plot of [A] versus $1/\Delta F$ produces a slope from which $K_{D(A)}$ can be calculated, as $K_{D(L)}$, $\Delta F_{0\max}$, and [L] (now constant) are known (data not shown). Dissociation

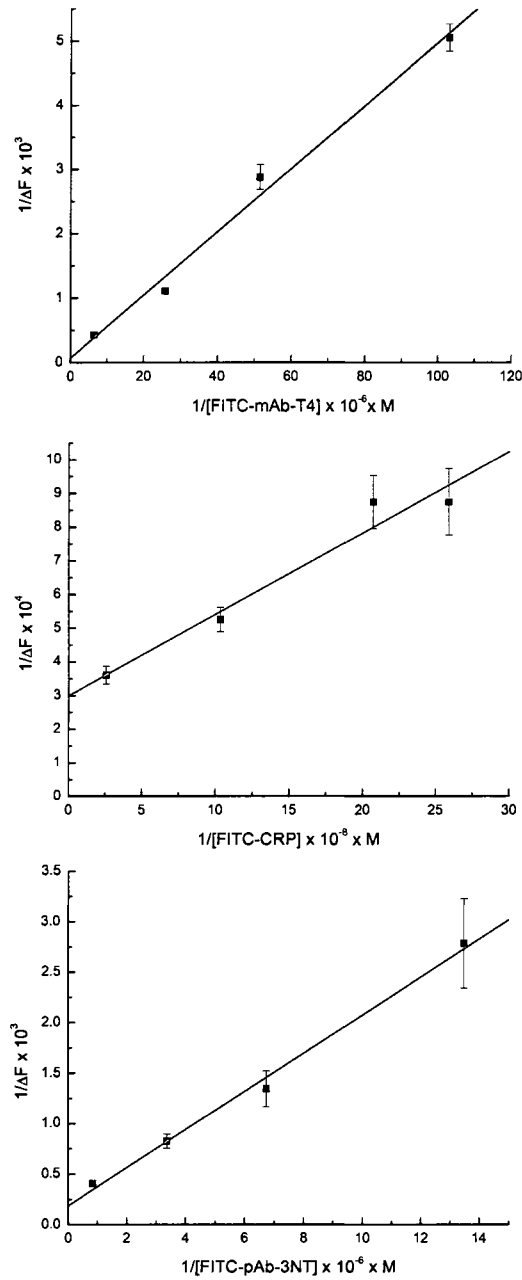


Figure 2.5. Plots of $1/\Delta F$ versus $1/[L]$ for each antibody-antigen system shown in Fig. 2.2. The slope and intercept for each curve can be used to estimate the dissociation constants (K_D) between a tracer and its surface receptor.

constants calculated as described are presented in Table 2.2. Values found for these dissociation constants are typical for antibody-antigen/hapten interactions.²⁴ This result shows that neither labeling with fluorophore nor surface immobilization significantly detracted from reagent performance. Furthermore, these results show that the competitive format is entirely compatible with the micromosaic immunoassay technique.

Affinity Pair	Est. K_D (M)
BSA-T4 (substrate) and FITC-mAb-T4	6.4 x 10 ⁻⁷
T4 and FITC-mAb-T4	1.0 x 10 ⁻⁸
mAb-CRP (substrate) and FITC-CRP	8.1 x 10 ⁻¹⁰
mAb-CRP (substrate) and CRP	1.6 x 10 ⁻¹⁰
BSA-3NT (substrate) and FITC-pAb-3NT	1.0 x 10 ⁻⁶
BSA-3NT (solution) and FITC-pAb-3NT	1.6 x 10 ⁻⁹

Table 2.2. Estimated K_D values for each affinity pair assayed.

2.4. Conclusions

Previous research involving micromosaic immunoassays has utilized as many as eight independent microchannels in each dimension allowing for simultaneous detection of protein biomarkers.^{3, 10} This work demonstrates the first implementation of a 12-channel approach for analysis of both proteins and metabolites by competitive immunoassay. Because small molecules such as T4 are epitope-limited for antibody capture, the sandwich immunoassay format was inappropriate and competitive strategies were used. Therefore, an indirect format competitive assay has been developed to demonstrate small-molecule analysis. Addition of a direct-format competitive assay for CRP indicates that the micromosaic platform can host both competitive assay formats and can be used for protein analysis as well. Complementary analysis of BSA-3NT suggests that this technology can address the demand for multianalyte analysis, particularly for clinically grouped biomarkers.

2.5. References

- (1) Yalow, R. S.; Berson, S. A. *Nature* **1959**, *184*, 1648-1649.
- (2) Butler, J. E. In *Immunoassay*; Diamandis, E., Christopoulos, T., Ed.; Academic Press: San Diego, 1996.
- (3) Bernard, A.; Michel, B.; Delamarche, E. *Anal Chem* **2001**, *73*, 8-12.
- (4) Delamarche, E.; Bernard, A.; Schmid, H.; Michel, B.; Biebuyck, H. *Science* **1997**, *276*, 779-781.
- (5) Whitesides, G. M.; Ostuni, E.; Takayama, S.; Jiang, X. Y.; Ingber, D. E. *Annual Review of Biomedical Engineering* **2001**, *3*, 335-373.

- (6) Juncker, D.; Schmid, H.; Bernard, A.; Caelen, I.; Michel, B.; de Rooij, N.; Delamarche, E. *J Micromech Microeng* **2001**, *11*, 532-541.
- (7) Delamarche, E.; Bernard, A.; Schmid, H.; Bietsch, A.; Michel, B.; Biebuyck, H. *Journal of the American Chemical Society* **1998**, *120*, 500-508.
- (8) Dandy, D. S.; Wu, P.; Grainger, D. W. *Proceedings of the National Academy of Sciences of the United States of America* **2007**, *104*, 8223-8228.
- (9) Benn, J. A.; Hu, J.; Hogan, B. J.; Fry, R. C.; Samson, L. D.; Thorsen, T. *Analytical Biochemistry* **2006**, *348*, 284-293.
- (10) Juncker, D.; Michel, B.; Hunziker, P.; Delamarche, E. *Biosens Bioelectron* **2004**, *19*, 1193-1202.
- (11) Rowe, C. A.; Tender, L. M.; Feldstein, M. J.; Golden, J. P.; Scruggs, S. B.; MacCraith, B. D.; Cras, J. J.; Ligler, F. S. *Analytical Chemistry* **1999**, *71*, 3846-3852.
- (12) Wolf, M.; Zimmermann, M.; Delamarche, E.; Hunziker, P. *Biomed Microdevices* **2007**, *9*, 135-141.
- (13) Yuan, G. W.; Lear, K. L.; Stephens, M. D.; Dandy, D. S. *Applied Physics Letters* **2005**, *87*, -.
- (14) Gonzalez-Martinez, M. A.; Morais, S.; Puchades, R.; Maquieira, A.; Abad, A.; Montoya, A. *Analytical Chemistry* **1997**, *69*, 2812-2818.
- (15) Wu, A. H. B. *Clinica Chimica Acta* **2006**, *369*, 119-124.

- (16) Murphy, B. M.; He, X. Y.; Dandy, D.; Henry, C. S. *Anal Chem* **2008**, *80*, 444-450.
- (17) Caulum, M. M.; Henry, C. S. *Analyst* **2006**, *131*, 1091-1093.
- (18) McDonald, J. C.; Duffy, D. C.; Anderson, J. R.; Chiu, D. T.; Wu, H. K.; Schueller, O. J. A.; Whitesides, G. M. *Electrophoresis* **2000**, *21*, 27-40.
- (19) Vickers, J. A.; Henry, C. S. *Electrophoresis* **2005**, *26*, 4641-4647.
- (20) Lee, J. N.; Park, C.; Whitesides, G. M. *Analytical Chemistry* **2003**, *75*, 6544-6554.
- (21) Englebienne, P. *Immune and Receptor Assays in Theory and Practice*; CRC Press: Boca Raton, 2000.
- (22) Smith, P. K.; Krohn, R. I.; Hermanson, G. T.; Mallia, A. K.; Gartner, F. H.; Provenzano, M. D.; Fujimoto, E. K.; Goeke, N. M.; Olson, B. J.; Klenk, D. C. *Anal Biochem* **1985**, *150*, 76-85.
- (23) Wu, P.; Hoglebe, P.; Grainger, D. W. *Biosensors & Bioelectronics* **2006**, *21*, 1252-1263.
- (24) Diamandis, E., Christopoulos, T.K., In *Immunoassay*; Academic Press: San Diego, 1996, pp 44-45.
- (25) Matsuda, M.; Sakata, S.; Komaki, T.; Nakamura, S.; Kojima, N.; Takuno, H.; Miura, K. *Clinica Chimica Acta* **1989**, *185*, 139-146.
- (26) Schwemmer, M.; Fink, B.; Kockerbauer, R.; Bassenge, E. *Clinica Chimica Acta* **2000**, *297*, 207-216.
- (27) Khan, J.; Brennan, D. M.; Bradley, N.; Gao, B. R.; Bruckdorfer, R.; Jacobs, M. *Biochemical Journal* **1998**, *330*, 795-801.

- (28) Sakai, G.; Ogata, K.; Uda, T.; Miura, N.; Yamazoe, N. *Sensors and Actuators B-Chemical* **1998**, *49*, 5-12.

Chapter 3

Analysis of Oxidative Stress Biomarkers Using a Simultaneous Competitive/Non-Competitive Micromosaic Immunoassay

3.1 Introduction

In this chapter, the development of a simultaneous competitive/non-competitive immunoassay for the detection of metabolites and proteins is presented. As a model system, three markers of oxidative stress are detected.

The presence of molecular oxygen in the atmosphere presents a double-edged sword for humans and other species. The superoxide anion, O_2^- , and other reactive oxygen species (ROS) are essential for cellular signaling¹ and the antimicrobial action of phagocytes², but are harmful at higher levels. ROS have been observed to cause oxidative damage to proteins³, DNA⁴, lipids⁵, and other biomolecules, and have also been associated with numerous diseases including cancer⁶, diabetes⁷, atherosclerosis⁸, and play a role in aging⁹. When the antioxidant system is overcome by oxidative processes, the organism is said to be under oxidative stress during which oxidative damage can occur¹⁰. Antioxidants and products of oxidative stress have received much attention due to the implication of oxidative damage in disease. As analytical targets, these species can be used to assess antioxidant capacity or oxidative status in vitro¹¹. However, due to the complexity of the antioxidant system and because a universal marker for oxidative stress has not been identified, analysis of multiple markers is preferred when assessing oxidative status¹²⁻¹⁵. Therefore, there is a

need for bioanalytical methods capable of parallel, high-throughput analysis of oxidative stress biomarkers.

An analysis of three oxidative stress biomarkers using a micromosaic immunoassay is presented ¹⁶. The micromosaic format has been previously demonstrated for the analysis of cardiac biomarkers (sandwich immunoassay) ¹⁷, cell surface receptors ¹⁸, and most recently the thyroid hormone thyroxine (competitive immunoassay)¹⁹. However, no micromosaic method has been developed for concerted analysis of both metabolites and macromolecules. This development is important because it will provide the ability to simultaneously measure both small and large molecules from a single sample. Here, the small molecule 3-nitrotyrosine (3NT) is examined by indirect competitive immunoassay, while bovine enzyme antioxidants catalase (CAT) and superoxide dismutase (Cu,Zn SOD/SOD1) are analyzed by sandwich (non-competitive) immunoassay. Each of the analytes has been proposed as a marker of oxidative status. By adding a third patterning step to the micromosaic assay, it is demonstrated for the first time that competitive and sandwich immunoassays can be performed in parallel using the micromosaic method. This work demonstrates that micromosaic immunoassays can function as a rapid, high throughput method for simultaneous competitive and non-competitive analysis of biomarkers. A majority of the data presented here was submitted for publication in *Analytical Chimica Acta*.

3.2 Materials and Methods

3.2.1 Chemicals and Materials

Unless otherwise noted, all chemicals were purchased from Sigma (St. Louis, MO). Anti-bovine SOD (Cu,Zn) (rabbit pAb IgG, S8060-11), anti-bovine catalase (rabbit pAb IgG, C2096-06), and anti-3-nitrotyrosine (mouse mAb IgG1, N2700-09) were purchased from United States Biological (Swampscott, MA). Catalase from bovine liver (C9322), bovine superoxide dismutase (S7571), and 3-nitro-L-tyrosine (N7389) were purchased from Sigma. Fluorescent measurements were made using a Photometrics HQ2 CCD camera from Roper Scientific (Tuscon, AZ) and MetaMorph 7.1.7 software from Molecular Devices (Sunnyvale, CA) using a Nikon Eclipse TE2000-U epifluorescence microscope (Melville, NY). Poly (dimethylsiloxane) (PDMS, Sylgard 184) was obtained from Dow Corning (Midland, MI) and used at a 10:1 ratio of monomer to crosslinker. SU8-2035 photoresist was purchased from Microchem (Newton, MA). AlexaFluor® 488 Monoclonal Antibody Labeling Kit (A20181) was purchased from Invitrogen (Carlsbad, CA). Slide-A-Lyzer MINI Dialysis Units were purchased from Pierce (Rockford, IL). Silicon nitride wafers with a proprietary coating were received as a gift from Biostar (Boulder, CO).²⁰ 1.5mm biopsy punches were obtained from Robbins Instruments (Chatham, NJ). All chemicals were used as received.

3.2.2 Protein Labeling and Conjugation

Prior to use, all antibodies were purified by dialysis for 2 hours against 1L of 25 mM phosphate, 150 mM NaCl pH 7.4 (PBS). Capture antibodies (pAb SOD, pAb CAT) were diluted to the specified concentrations using deionized water. Detection antibodies for both competitive (mAb 3NT) and sandwich assays (pAb SOD, pAb CAT) were prepared at 1 mg/mL in 100 μ L of the above mentioned buffer and labeled with AlexaFluor® 488 (AF) using the AlexaFluor® 488 Monoclonal Antibody Labeling Kit. Labeled antibodies were purified according to the directions included with the kit and were stored at 4°C until use. 3NT was conjugated to bovine serum albumin (BSA) using carbodiimide chemistry as described in the literature.²¹ The hapten was solubilized for conjugation in a 1:1 mixture of dimethylsulfoxide and 50 mM sodium phosphate, pH 8.5. The BSA-3NT conjugate was dialyzed against PBS to remove unreacted hapten and EDC carbodiimide, stored at 0°C prior to use in immunoassays and diluted with deionized water (Millipore, 18 Ω) to the final concentration prior to use.

3.2.3 Microfluidic Network Fabrication and Substrate Preparation

Microfluidic networks (μ FNs) made from the polymer poly-(dimethylsiloxane) (PDMS) were used to pattern capture reagents and deliver analytes and affinity probes to the substrate. Negative relief molds for each network of channels were made using photolithography according to the literature^{22, 23}. Photolithography masks were designed in Adobe Illustrator and

printed at 40,640 DPI by Fineline Imaging, Inc (Colorado Springs, CO). First and second dimension channels were designed with a 40 μm width and 20 μm spacing between channels. Actual channel dimensions were found to be 25 μm with a spacing of 35 μm and a height of 20 μm using profilometry. Third dimension μFNs were designed with single entry and exit ports and a 1.5 mm channel containing a central 3.0 mm diameter “bubble cell” design for patterning over the entire affinity mosaic. μFN designs used for each patterning step are shown in Figure 3.1. PDMS networks made using these molds were punched with a 1.5 mm biopsy punch to create wells for sample introduction. T-poly coated silicon nitride wafers (SiNx) were rinsed in Millipore water and dried under a stream of nitrogen prior to use. Wafers were scored and cut into pieces approximately 1.5 cm \times 1.5 cm for each assay.

3.2.4 Micromosaic Immunoassays. All assays were performed using three patterning steps or “dimensions.” μFNs were made hydrophilic before each patterning step by oxidation in an air plasma cleaner for 50 seconds at 18 W. A volume of 0.9 μL of reagent was introduced to each well at each step. First dimension patterning was used to sensitize the substrate with patterns of receptor proteins. The BSA conjugate of 3NT (BSA-3NT, 0.35 mg/mL) along with pAb SOD (0.66 mg/mL) and pAb CAT (0.30 mg/mL) in deionized water were patterned in triplicate for a 10 min incubation. Because the sensitizing agents were passively adsorbed, random orientation of the protein on the substrate was expected. μFNs were removed under PBS containing 0.05% Tween 20 (PBS-T),

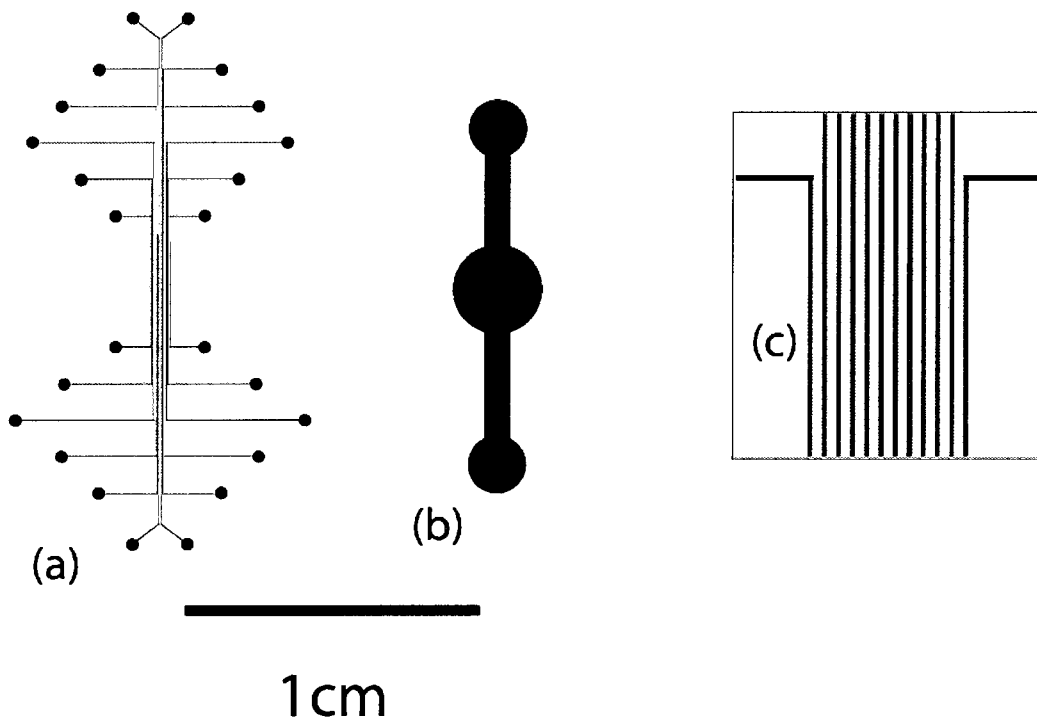


Fig. 3.1. Schematic showing microfluidic channel shape for first and second dimension patterning (a) and for third dimension pattern (b). Inset of 12 channel design is shown in (c), where each channel is 20 microns wide with 40 micron spacing.

then rinsed copiously with PBS-T and water. Remaining reactive adsorption sites were passivated by a 5 min incubation with 0.5 mL 45 mg/mL BSA in PBS covering the entire substrate. This was followed by repeating the above rinse procedure. Solutions containing all three analytes and competitive assay tracer AF mAb 3NT (25 μ g/mL) in 45 mg/mL human serum albumin (HSA) were patterned orthogonal to the first dimension pattern for 15 min and rinsed. Finally, detection reagents for the two sandwich assays (AF pAb SOD, 50 μ g/mL and AF pAb CAT, 50 μ g/mL) in 45 mg/mL BSA/PBS were patterned for 2.5 min using the “bubble cell” μ FN that covered the entire mosaic area. Epifluorescence measurement parameters were a 4 \times 4 binning, 10 \times objective, unmodified gain, and an exposure time of 1.5 s. Fluorescence measurements were taken directly from the image; no image processing or smoothing was applied. The average signal from each mosaic was recorded. Total assay time from the first patterning step to the fluorescence measurement was less than 45 min.

3.3 Results and Discussion

3.3.1 Cross Reactivity Analysis. Prior to quantification of analyte in the multi-analyte immunoassay, a patterning experiment was carried out to determine possible cross-reactivity between tracer/detection antibodies and surface receptors/captured antigens. This was particularly important given the nature of the simultaneous competitive/non-competitive assays to be done in these experiments. Following sensitization, the competitive assay tracer (25 μ g/ml AF

pAb 3NT) and each antigen (10 ng/mL SOD, 125 ng/mL CAT) were patterned independently in triplicate, and the third dimension pattern followed this step as described above. A fluorescent image of this mosaic is shown in Figure 3.2.

Cross reactivity may be assessed by examining the fluorescent signal across each row. For example, signal from the middle three rows, in which AF mAb 3NT was patterned, shows that binding of the tracer to affinity mismatch coordinates (immobilized pAb CAT, pAb SOD) is below the sensitivity of the camera. In the bottom set of rows, pAb CAT captures only CAT, while the pAb CAT columns show only pAb CAT captures CAT. Specificity of detection antibodies for SOD and CAT were verified in a similar experiment utilizing only one detection antibody in the third patterning step in the presence of both captured targets. The results of this experiment show low cross reactivity for the prescribed antibodies and antigens, and therefore demonstrate that these three analytes can be measured simultaneously in the micromosaic format.

3.3.2 Multiplexed Immunoassay for CAT, 3NT, and SOD

Dilutions of CAT, 3NT, and SOD were prepared in 45 mg/mL HSA dissolved in phosphate buffered saline. While this is not a biological sample, it does represent a complex system containing physiologically relevant levels of albumin as thus serves as a good model system during experimental development. Prior to the multiplexed assay, each analyte was assayed individually to determine a working concentration range estimate. The appropriate titer of AF mAb 3NT was also determined experimentally¹⁹. These

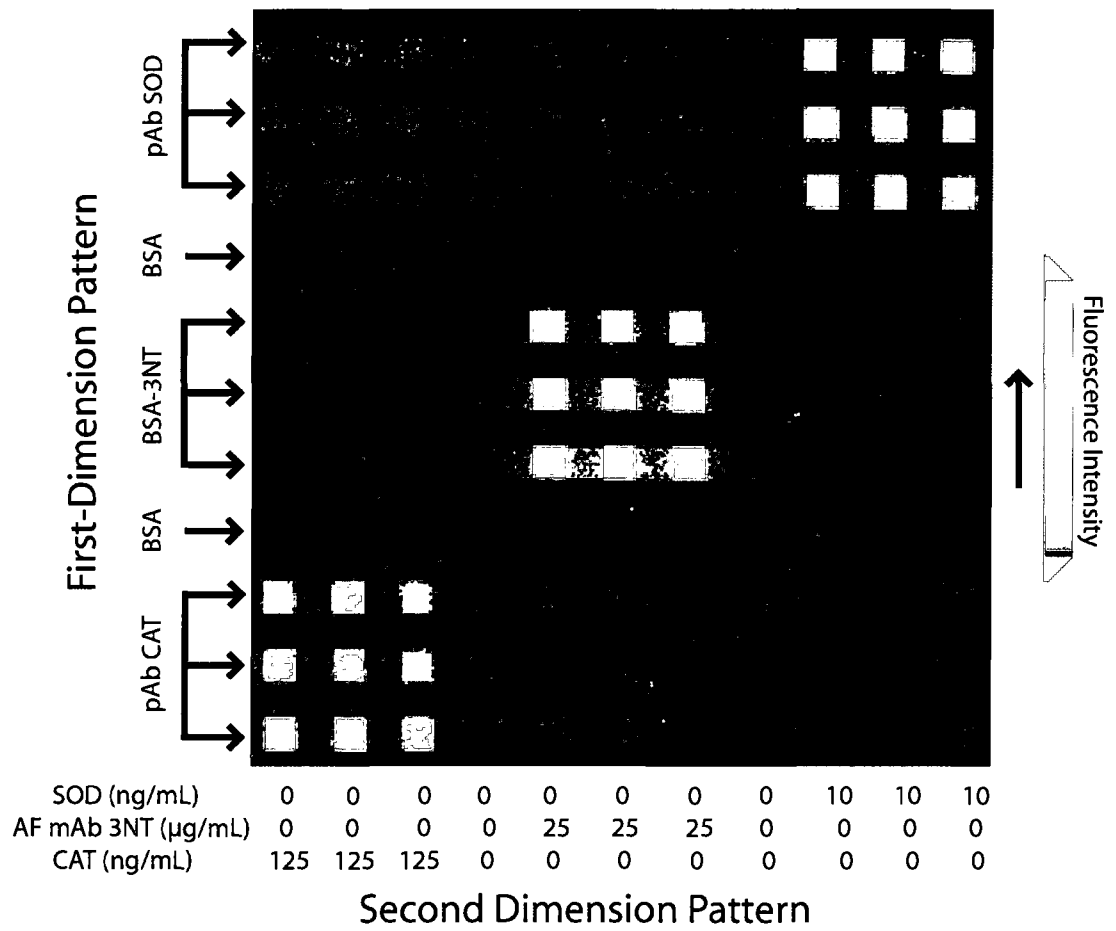


Fig. 3.2. Micromosaic demonstrating tracer specificity for patterned and captured proteins for each of the three analytical targets CAT, 3NT and SOD.

values were used to create dilutions containing the appropriate amount of each analyte. The fluorescent image of the three-analyte assay is shown in Figure 3.3 with the corresponding concentrations of each analyte used in the second dimension pattern listed below. In the case of 3NT, the competitive effect is observed as signal decreases with increasing analyte concentration. In the cases of SOD and CAT, signal increases with increasing analyte concentration as expected until capture antibodies are saturated.

Dose-response curves for each assay were fit to the four-parameter logistic equation:

$$Y = \frac{a - d}{1 + \left(\frac{T}{c}\right)^b} + d \quad (1)$$

where Y is the fluorescent signal (F/F_{\max} where F_{\max} is the highest signal observed for each analyte set), a is the response in absence of analyte, d is the response due to non-specific adsorption of tracer, c is the concentration of analyte that produces a signal $Y = (a+d)/2$, T is the analyte concentration, and b is the absolute value of the slope of the curve in a log-logit format²⁴. Curves were fit using OriginPro 7's non-linear curve fitting tool for a four-parameter logistic equation using 300 iterations. Correlation

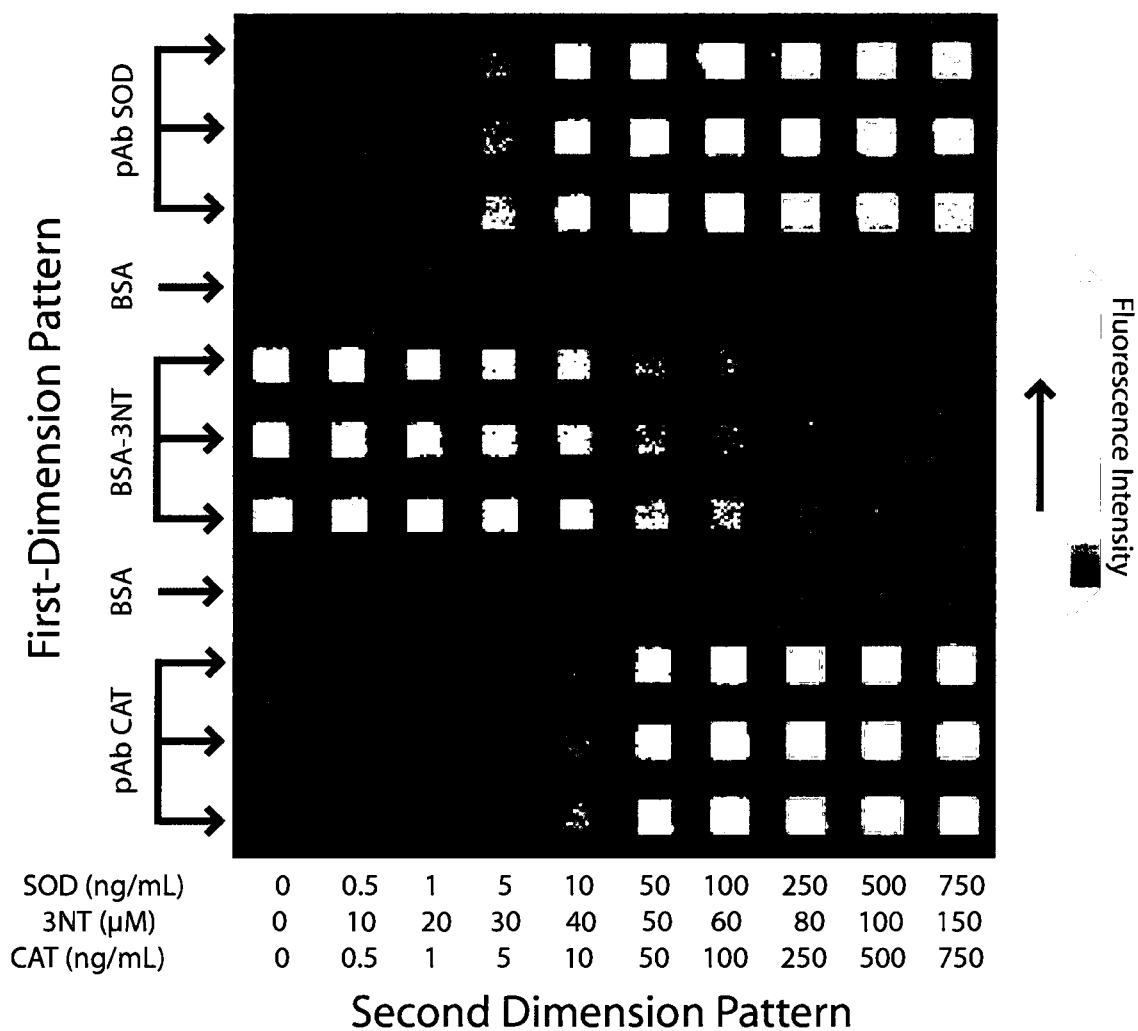


Fig. 3.3. Micromosaic immunoassay for simultaneous detection of CAT, 3NT, and SOD. Solutions patterned in the first and second dimension are indicated. The entire mosaic was patterned in the third dimension with 50μg/ml AF pAb CAT and 50μg/ml AF pAb SOD detection antibodies.

coefficients were 0.999, 0.996, and 0.999 and reduced χ^2 values were 1×10^{-4} , 2×10^{-5} , and 4×10^{-5} for CAT, 3NT and SOD, respectively.

Dose-response curves are shown in Figure 3.4. Error bars represent a single standard deviation for each set of three mosaic squares that correspond to one concentration of analyte. Error may be partially attributed to depletion of captured reagent (target protein or competitive assay tracer) during flow across the substrate. This phenomenon has been documented previously during a micromosaic immunoassay for C-Reactive Protein ²⁵. The direction of flow in Figure 3.3 was from the bottom of the image to the top. The depletion effect is most pronounced for CAT although it also contributes to the variability for 3NT. A fluorescence intensity profile linescan for the 100 ng/mL CAT mosaic in Figure 3.3 is shown in Figure 3.5 along with an indication of the direction of flow. This figure shows that depletion of CAT occurs not only between mosaics, but within them as well. SOD is least affected by error, having the lowest absolute signal deviation of all three analytes. These results suggest that depletion in micromosaic immunoassays are an analyte-dependent phenomenon. SOD (32 kDa) is much smaller than both rabbit IgG (150kDa) and CAT (250kDa), and will have a higher Stokes-Einstein diffusion coefficient, making the SOD assay less susceptible to depletion effects inherent to the mass transfer-limited conditions in these experiments.

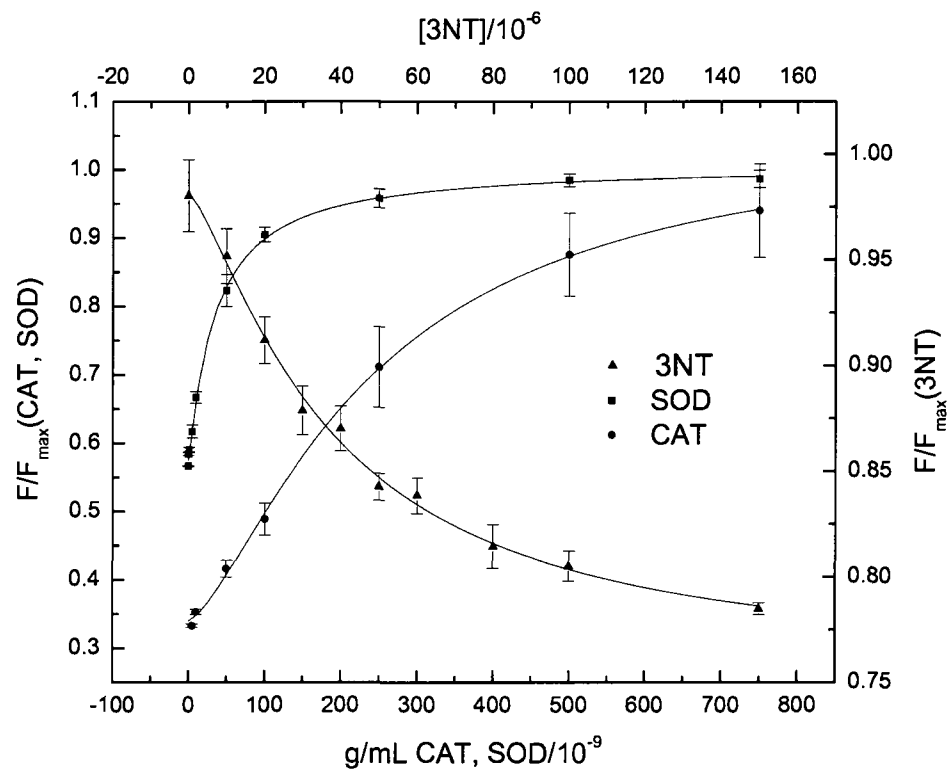


Fig. 3.4. Dose-response curves for CAT, 3NT, and SOD obtained from fluorescent signals in Fig. 3.

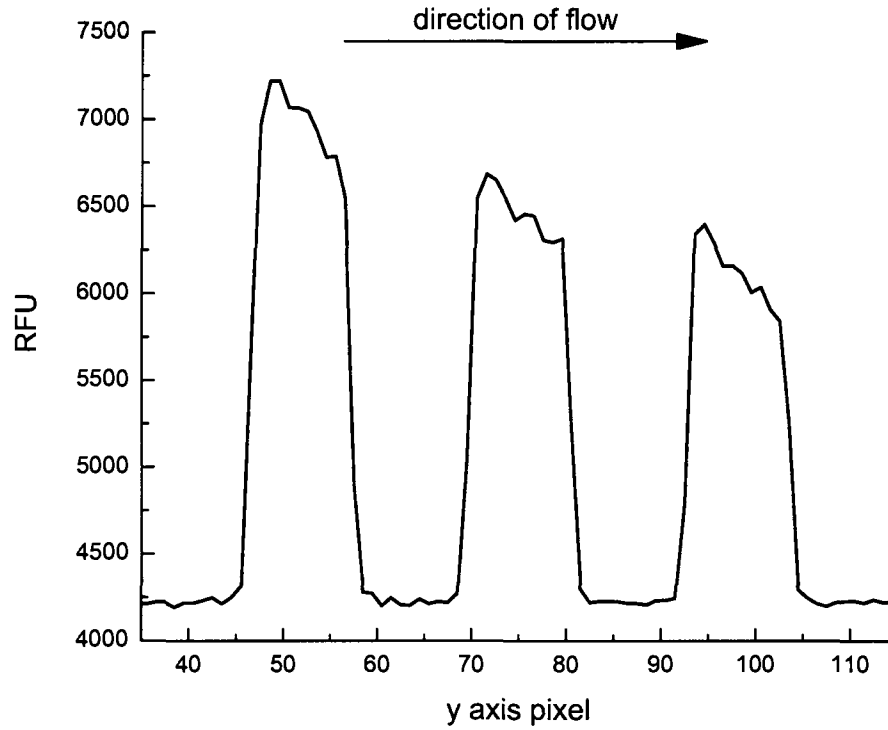


Fig. 3.5. Fluorescence intensity profile of 100ng/ml CAT mosaics with direction of flow indicated. Depletion of analyte from solution occurs along the direction of flow.

3.3.3 Calculation of Limits of Detection

The LOD for an immunoassay is given as the lowest concentration of analyte or dose which gives a signal statistically different from that at zero analyte concentration^{21, 26}. A method for calculating detection limit estimates based on the standard deviation of mean response at zero-dose has been developed²⁷. The expected response at the detection limit (Y_{min}) can be expressed as:

$$Y_{min} = Y_0 \pm ts \left[\frac{1}{n_0} + \frac{1}{n_{min}} \right]^{1/2} \quad (2)$$

where Y_0 is the mean response at zero dose, t is student's t at 95% CI, s is the standard deviation of the response near zero dose, and n_0 and n_{min} are the number of replicates performed at zero dose and at the theoretical LOD. In the case of a negative slope near zero dose (as in a competitive assay), the (+) is used in Eq. 2. In the case of a positive slope near zero dose (a two-site or sandwich assay), the (-) is used instead. Y_{min} can be substituted into the dose-response curve to obtain the calculated detection limit. In this work, s is taken as the average standard deviation from all data points assayed, except for the case of CAT where high-dose standard deviations were much larger than those found closer to zero dose; only the deviations from the lowest four responses were averaged. CAT also differs in that the signal at zero dose was below the camera sensitivity, so $Y = 5$ ng/ml was used in place of Y_0 . After determining the response at the minimum detectable dose and substituting into the logistic curve

fits (including error to those curve fits), the detection limits at 95% CI were found to be 35 ± 4.8 ng/mL CAT, 8 ± 1.4 μ M 3NT, and 1.7 ± 0.14 ng/mL SOD.

3.3.4 Mitigating Depletion Effect with Selective Geometries

The reagent depletion phenomenon described above was investigated using a linear fluid dynamics model by Scott Lynn in CSU's Chemical Engineering department. Figure 3.6 shows the predicted reagent concentration gradient in a microchannel cross section during flow over several reactive spots for an association constant of $K_a = 1 \times 10^{-8}$. This model was designed to mimic conditions during micromosaic immunoassay second dimension patterning. The model predicts that binding of reagent to the first reactive spot forms a concentration gradient of that reagent in the channel which affects binding to subsequent reactive spots. If this model is correct, there should be several strategies available to address reagent depletion which leads to increased error in analyte quantitation. One possible solution is to change the spacing between reactive spots. This would provide a longer distance over which the reagent gradient could be overcome by diffusion. To investigate this theory, surfaces were sensitized with BSA-3NT over spacings of 0, 1, 2, 3, and 4 empty channels between each sensitized channel. After blocking, AF mAb 3NT was patterned perpendicular to the first pattern. Reagent concentrations and reaction times were preserved from the competitive immunoassay above. Sample images for a spacing of 0 and a spacing of 4 channels are shown in Figure 3.7. The RSD between signal in each row for each image was recorded and is displayed in

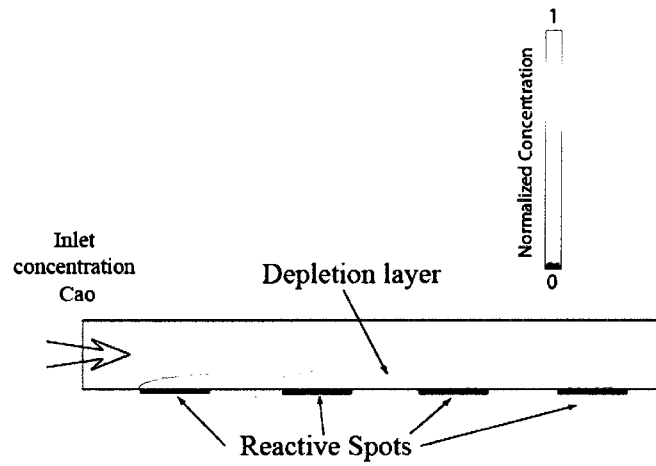


Figure 3.6. Reagent depletion effect can be predicted using linear fluid dynamics. Cross section of microchannel with reagent flowing over reactive spots. Image courtesy of Scott Lynn, CSU Department of Chemical Engineering.

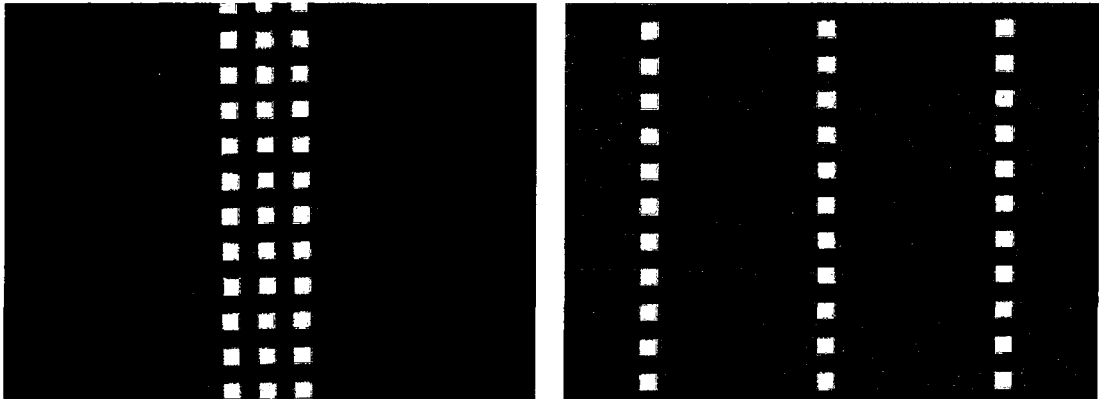


Figure 3.7. Examination of the effect of microchannel spacing on analyte depletion using AF mAb 3NT. BSA-3NT spacing of 0 (left) and 4 empty microchannels (right).

Figure 3.8. For the 3NT system, the RSD decreased by 53.3% between a spacing of 0 and 4 empty channels. This decrease in RSD suggests that geometrical optimization of channel spacing could be an easy way to decrease micromosaic immunoassay error associated with analyte depletion in microchannels. Other possible solutions to depletion-associated error include increased incubation time during the capture step and the use of microchannels designed to mix solution during flow over sensitized spots.

3.4 Conclusions

Bernard et al. has demonstrated the use of micromosaics for detection of antigens using non-competitive sandwich immunoassay, while our lab has developed methodology for micromosaic competitive immunoassays^{16, 19}. In this work, the merging of the two micromosaic techniques is examined for the combined simultaneous competitive and sandwich immunoassay of a small molecule metabolite and two enzyme biomarkers for oxidative stress. The micromosaic method is shown to detect each analyte with low cross reactivity in a HSA/PBS matrix containing the other two analytes. Detection limits for catalase and superoxide dismutase were 35 ± 4.8 ng/mL and 1.7 ± 0.14 ng/mL, while for 3-nitrotyrosine the detection limit was 8 ± 1.4 μ M. The immunoassay required less

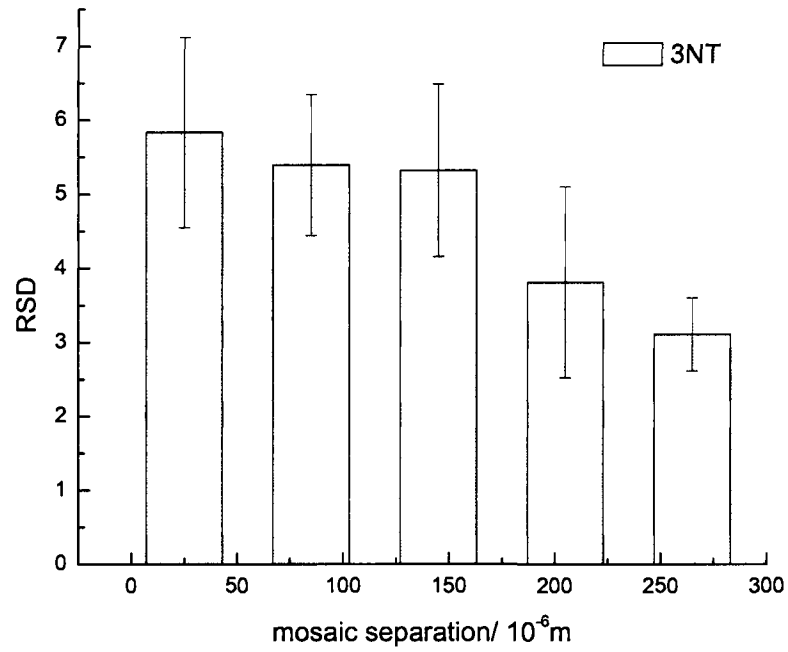


Figure 3.8. RSD versus channel spacing (in microns) for AF mAb 3NT geometrical optimization experiment.

than 1 μL of sample, needed minimal user optimization, and could be completed within 45 min.

3.5 Acknowledgments. I thank the Dandy research group for their crucial advice and support and N. Scott Lynn for his help with photolithography mask design and understanding of the depletion phenomenon.

3.6 References.

- (1) Wolin, M., Mohazzab-H, K. In *Oxidative Stress and the Molecular Biology of Antioxidant Defenses*; Scandalios, J. G., Ed.; Cold Spring Harbor Laboratory Press: Plainview, NY., 1997, pp 21-48.
- (2) Klebanoff, S. J. *Ann Intern Med* **1980**, *93*, 480-489.
- (3) Zhang, Y. J.; Xu, Y. F.; Chen, X. Q.; Wang, X. C.; Wang, J. Z. *Febs Lett* **2005**, *579*, 2421-2427.
- (4) Dizdaroglu, M.; Jaruga, P.; Birincioglu, M.; Rodriguez, H. *Free Radical Bio Med* **2002**, *32*, 1102-1115.
- (5) Inouye, M.; Mio, T.; Sumino, K. *Atherosclerosis* **2000**, *148*, 197-202.
- (6) Hagen, T. M.; Huang, S.; Curnutte, J.; Fowler, P.; Martinez, V.; Wehr, C. M.; Ames, B. N.; Chisari, F. V. *P Natl Acad Sci USA* **1994**, *91*, 12808-12812.
- (7) Chowienczyk, P. J.; Brett, S. E.; Gopaul, N. K.; Meeking, D.; Marchetti, M.; Russell-Jones, D. L.; Anggard, E. E.; Ritter, J. M. *Diabetologia* **2000**, *43*, 974-977.

- (8) Esterbauer, H., Schmidt, R., Hayn, M. In *Advances in Pharmacology*; Sies, H., Ed.; Academic Press: San Diego, 1997; Vol. 38, pp 425-456.
- (9) Finkel, T.; Holbrook, N. J. *Nature* **2000**, *408*, 239-247.
- (10) Sies, H., Ed. *Oxidative Stress*; Academic Press: London, 1985.
- (11) Smith, P. K.; Krohn, R. I.; Hermanson, G. T.; Mallia, A. K.; Gartner, F. H.; Provenzano, M. D.; Fujimoto, E. K.; Goeke, N. M.; Olson, B. J.; Klenk, D. C. *Anal Biochem* **1985**, *150*, 76-85.
- (12) Wood, L. G.; Gibson, P. G.; Garg, M. L. *J Sci Food Agr* **2006**, *86*, 2057-2066.
- (13) Mateos, R.; Bravo, L. *J Sep Sci* **2007**, *30*, 175-191.
- (14) Halliwell, B.; Whiteman, M. *Brit J Pharmacol* **2004**, *142*, 231-255.
- (15) England, T.; Beatty, E.; Rehman, A.; Nourooz-Zadeh, J.; Pereira, P.; O'Reilly, J.; Wiseman, H.; Geissler, C.; Halliwell, B. *Free Radical Res* **2000**, *32*, 355-362.
- (16) Bernard, A.; Michel, B.; Delamarche, E. *Anal Chem* **2001**, *73*, 8-12.
- (17) Juncker, D.; Michel, B.; Hunziker, P.; Delamarche, E. *Biosens Bioelectron* **2004**, *19*, 1193-1202.
- (18) Wolf, M.; Zimmermann, M.; Delamarche, E.; Hunziker, P. *Biomed Microdevices* **2007**, *9*, 135-141.
- (19) Murphy, B. M.; He, X. Y.; Dandy, D.; Henry, C. S. *Anal Chem* **2008**, *80*, 444-450.
- (20) Trotter, B.; Moddel, G.; Ostroff, R.; Bogart, G. R. *Opt Eng* **1999**, *38*, 902-907.

- (21) Englebienne, P. *Immune and Receptor Assays in Theory and Practice*; CRC Press: Boca Raton, 2000.
- (22) McDonald, J. C.; Duffy, D. C.; Anderson, J. R.; Chiu, D. T.; Wu, H. K.; Schueller, O. J. A.; Whitesides, G. M. *Electrophoresis* **2000**, *21*, 27-40.
- (23) Vickers, J. A.; Henry, C. S. *Electrophoresis* **2005**, *26*, 4641-4647.
- (24) Diamandis, E., Christopoulos, T.K., In *Immunoassay*; Academic Press: San Diego, 1996, pp 44-45.
- (25) Ziegler, J.; Zimmermann, M.; Hunziker, P.; Delamarche, E. *Anal Chem* **2008**, *80*, 1763-1769.
- (26) Diamandis, E., Christopoulos, T.K., In *Immunoassay*; Academic Press: San Diego, 1996, pp 47-49.
- (27) Rodbard, D. *Anal Biochem* **1978**, *90*, 1-12.

Chapter 4

Fluorescent CTI Tags for Avidin-Biotin Based Immunoconjugation Schemes

4.1 Introduction.

At this juncture in the dissertation, the focus will move from micromosaic immunoassays to cleavable tag immunoassays (CTI). This project was begun by Dr. Meghan Caulum in our laboratory and continues today under myself. Like our work on micromosaics, CTI has been researched as a technique to measure multiple biomarkers from a complex sample using immunochemical means. While micromosaics has been used to resolve different affinity reactions spatially on a solid substrate, CTI seeks to resolve similar reactions in solution using electrophoresis. Unlike traditional electrophoretic immunoassays which simply separate immunocomplex from free tracer, CTI relies on the resolution of different cleavable fluorescent reporter groups as signaling molecules. To perform a multianalyte immunoassay using CTI, each detection antibody must be conjugated to a fluorophore in such a way that following cleavage of fluorophores from the antibodies, the resulting solution will contain reporter groups which are electrophoretically resolvable. One of the primary tasks in starting this project was devising conjugation and cleavage chemistry which would make this type of immunoassay possible.

This chapter details early efforts to assemble a CTI tag library using avidin-biotin chemistry to conjugate cleavable fluorophores to the detection

antibodies used for CTI. The first tag assembled in our laboratory utilized fluorescein-ethylenediamine (FTED) which was described in the literature by Bertram et al.¹ The same chemistry used to produce FTED is examined for the synthesis of fluorescein- hexamethylenediamine (FTHD) and fluorescein-cystamine (FAM) in an effort to build a CTI tag library for multianalyte immunoassay. Fluorophore products are conjugated to NHS-SS-biotin, which provided both a cleavable disulfide and a biotin linkage for attachment to avidin-labeled antibodies. CE-UV is used to examine the reaction products. The goal of this work was to build a tag library for the first CTI experiments. These three tags were included in the synthetic library used for the first published multianalyte CTI by Caulum et al.²

4.2 Materials and Methods

4.2.1 Chemicals and Materials.

Fluorescein isothiocyanate (FITC), ethylene diamine, hexamethylenediamine, cystamine dihydrochloride, and tris(2-carboxyethyl)-phosphine (TCEP) were purchased from Sigma-Aldrich (St. Louis, MO). Sulfo-NHS-SS-biotin and NHS-biotin were purchased from Pierce (Rockford, IL). Glass capillary for CE was purchased from Polymicro Technologies (Phoenix, AZ).

4.2.2 Synthesis of FTHD and FAM Tags.

200 mg of hexamethylenediamine was dissolved in 5 mL of methanol containing 10 mL/L triethylamine. 100 mg of FITC was dissolved in 5 mL of the

same solvent, and added dropwise to the hexamethylenediamine solution while stirring over a 30 minute period. The solution was then covered and protected from light during overnight incubation. Solvent was evaporated to 5 mL with an air stream, then precipitated upon the addition of acetone. Solid was washed with acetone three times, then dried under an air stream. FTHD solid was stored at 0°C until further use. To form the complete biotinylated tag, FTHD was incubated with sulfo-NHS-SS-biotin at a 1:1 ratio for 4 hours at 4°C in 20 mM sodium phosphate pH 7.4. Tag was stored at 4°C until further use. The synthesis steps are shown in Figure 4.1.

180 mg of cystamine dihydrochloride was dissolved in 5 mL methanol, 2 mL deionized water, and 40 µL triethylamine. 51 µg FITC was dissolved in 5 mL methanol, 50 µL triethylamine and added dropwise over 30 minutes to the cystamine. After overnight reaction at room temperature, solution was evaporated to a volume of 5 mL and product precipitated with a 10:1 mixture of acetonitrile:methanol. Solid was washed several times with this solution and dried under an air hose. FAM solid was stored at 0°C until further use. To form the complete biotinylated tag, FAM was incubated with NHS-biotin at a 1:1 ratio overnight at 4°C in 20 mM sodium phosphate pH 7.4. Tag was stored at 4°C until further use. This synthesis is shown in Figure 4.2.

4.2.3 Capillary Electrophoresis.

All separations were performed on a Beckman-Coulter P/ACE MDQ Capillary Electrophoresis System. 40 cm capillary (50 micron inner diameter) with a detection window at 30 cm was used for all separations. Unless otherwise

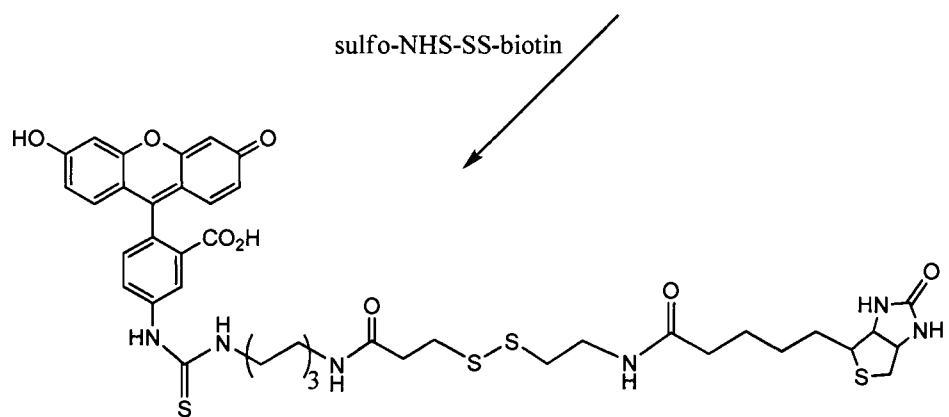
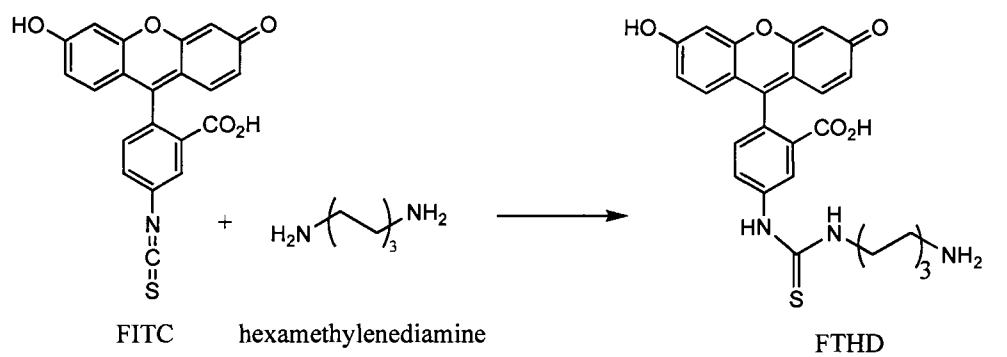


Figure 4.1. Synthesis of FTHD and FHB.

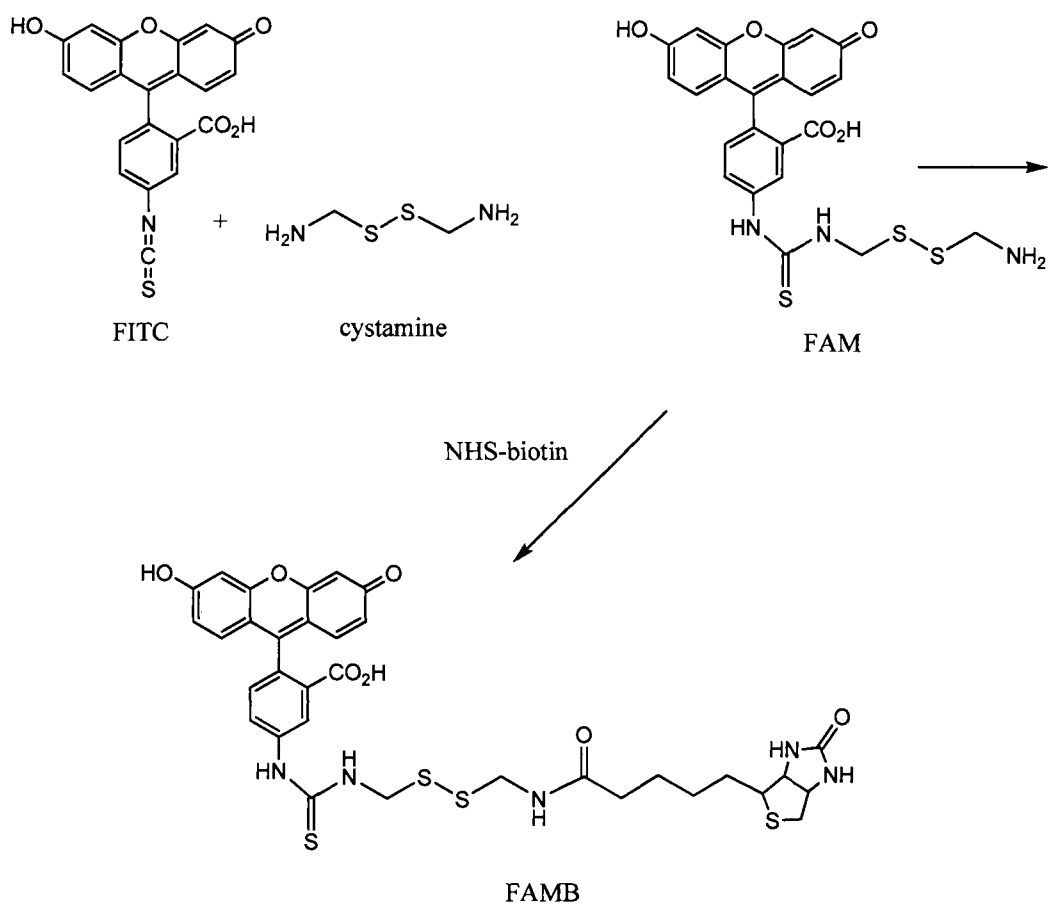


Figure 4.2. Synthesis of FAM and FAMB.

noted, run buffer was 20 mM sodium tetraborate pH 9.2. A separation potential of 20kV was employed for all separations, and a pressure injection of 8 seconds at 0.5 psi was used to load the column with sample. Detection was performed at 214 nm with a data collection rate of 4Hz. A caffeine neutral marker was added to each sample.

4.3 Results and Discussion

4.3.1 Capillary Electrophoresis of CTI Tag Products

Capillary electrophoresis was used to examine CTI reaction products. First, the FTHD product was examined for purity and for the ability of CE to resolve FTHD and FTED. The FTHD electropherogram gave two peaks, one for caffeine and one for the product. Caffeine was added as an internal mobility standard. Mobility of the product was higher than for FTED as expected. An example electropherogram is shown in Figure 4.3. This experiment shows that hexamethylenediamine can be used for a reaction with FITC in the same manner as ethylene diamine. Previous work in our lab had demonstrated the successful reaction of FTED with sulfo-NHS-SS-biotin. The same reaction was undertaken using FTHD, and the products were examined using CE. In the electropherograms shown in Figure 4.4, it is shown that FTHD is consumed by the reaction and a new peak not present in the FTHD or sulfo-NHS-SS-biotin electropherograms is formed.

Due to the success of FTHD and FTED synthesis, a new type of reaction was performed in which the necessary disulfide was incorporated into the

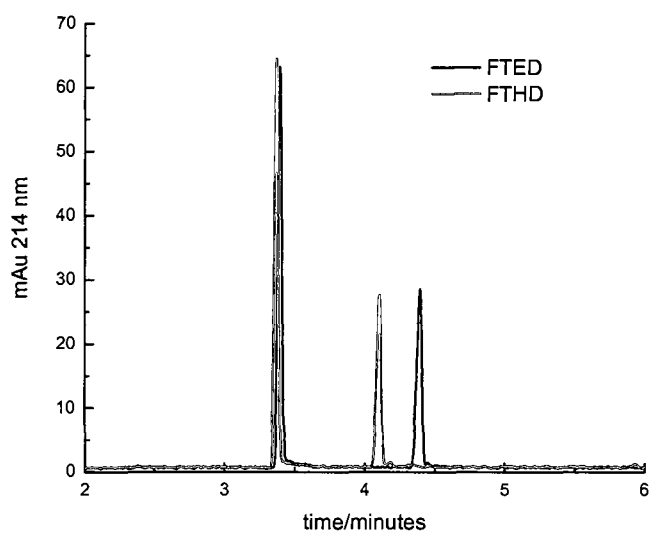


Figure 4.3. Electropherograms for FTED and FTHD using caffeine as a neutral marker. Both products exhibit a single product peak, and can be easily resolved from one another.

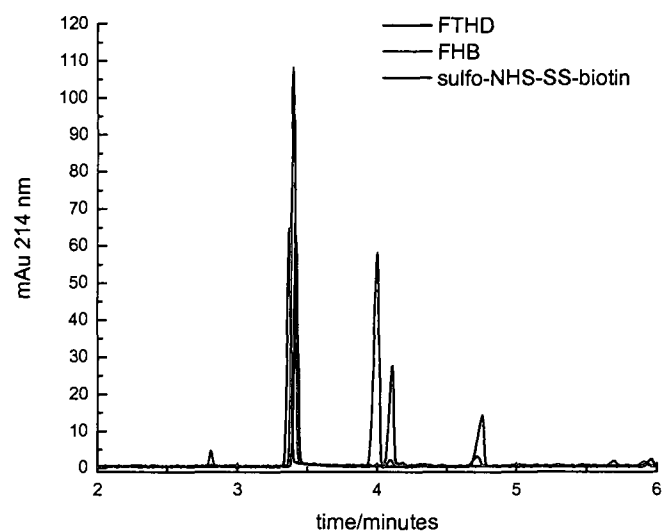


Figure 4.4. Electropherograms for the reaction of FTHD and sulfo-NHS-SS-biotin. FTHD is consumed, and a new product peak is formed.

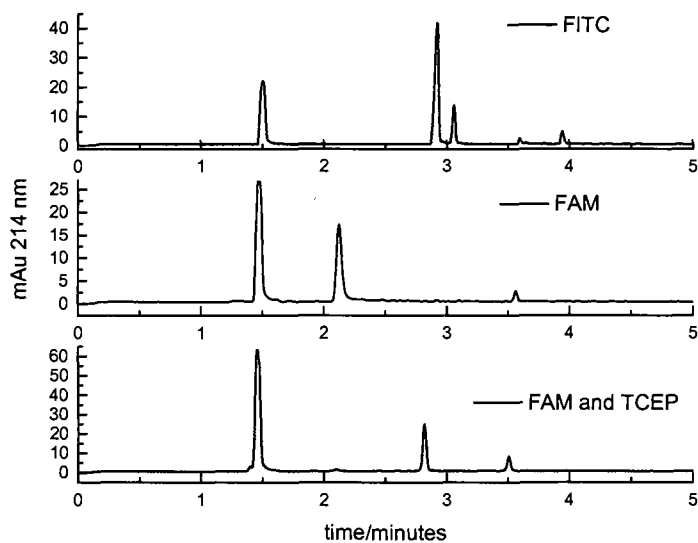


Figure 4.5. Formation of FAM using FITC and cystamine. Cleavage of the final product is observed after addition of disulfide reducing reagent TCEP.

diamine. The symmetric diamine and disulfide cystamine was therefore examined for reactivity towards FITC. Following reaction, CE was performed on FITC, FAM, and FAM after exposure to 20mM TCEP. In Figure 4.5, the reaction of FITC with cystamine is confirmed, as is the cleavage of the disulfide due to exposure to TCEP. A reaction of FAM with NHS-biotin was found to produce the desired biotinylated CTI tag.

4.4 Conclusions

Synthesis of two new biotin-based CTI tags was performed to build a library for avidin-biotin CTI conjugates and immunoassay experiments. It was found that both hexamethylenediamine and cystamine would react with FITC in the same manner as ethylene diamine. Furthermore, both FITC derivatives could be incorporated to amine-reactive forms of biotin. These two synthetic protocols were ultimately used for the detection of cardiac biomarkers using sandwich CTI by a colleague in our laboratory.²

4.5 References

- (1) Bertram, V. M.; Bailey, M. P.; Rocks, B. F. *Annals of Clinical Biochemistry* **1991**, 28, 487-491.
- (2) Caulum, M. M.; Murphy, B. M.; Ramsay, L. M.; Henry, C. S. *Analytical Chemistry* **2007**, 79, 5249-5256.

Chapter 5

Competitive Microplate CTI for 3NT, T4, and BSA-CML

5.1 Introduction

Enzyme-linked immunosorbant assay (ELISA) is the current industry standard for making a variety of immunochemical measurements from complex samples such as human serum. While ELISA is a proven technology, it is a slow process and is used to measure only a single analyte from a single sample at a time in clinical settings. Electrophoretic separation methods for multianalyte immunoassays have several distinct advantages over traditional ELISA. Capillary electrophoresis immunoassays (CEIA) take advantage of solution-phase kinetics to decrease analysis time, and the high separation efficiency of CE to examine multiple biomarkers in a single sample.¹ Immunoaffinity capillary electrophoresis (IACE) uses a solid phase to extract the target from complex media, then analyses eluted analytes using CE.² While some multianalyte experiments have been demonstrated using these methods, they are not suitable as a universal tool for multianalyte CE analysis of immunoassay products. Problems with resolution of immunocomplexes and electropherogram crowding are the main challenges to CEIA and IACE.

Caulum et al recently developed a novel approach to CE immunoassays.³ A sandwich immunoassay is performed on a solid phase using a unique detection antibody possessing a fluorophore conjugated to the antibody through a reducible disulfide bond. After capture and detection steps, the disulfide is

reduced and the fluorophore allowed diffusing into solution where it can be examined by CE. Termed a Cleavable Tag Immunoassay (CTI), this method can be multiplexed by using antibody conjugates that produce different fluorophores when the disulfide is reduced. Unlike CEIA and IACE, the affinity reagents themselves do not need to be separated, and the mobility of the signaling molecules can be controlled through synthesis.

This chapter presents the adaptation of CTI to the indirect competitive immunoassay format. As CTI is intended as a multiplexing technique, the versatility of the method should be demonstrated not only for traditional sandwich immunoassays which are used primarily for larger targets such as proteins, but for smaller analytes such as metabolites, which are usually assayed by competitive means. Analytes examined here include 3-nitrotyrosine (3NT), BSA-carboxymethyl lysine (BSA-CML), and thyroxine (T4). Thyroxine is a thyroid hormone traditionally measured by competitive immunoassay, and our laboratory has shown detection of this compound over the clinical reference range using micromosaics (see Chapter 2). 3-nitrotyrosine is a potential biomarker for oxidative damage by peroxy nitrite, and has also been previously examined in our laboratory. Carboxymethyl lysine (CML) is a protein glycoxidation product also associated with oxidative stress.⁴ Because CML exists as modified lysine residues on proteins, it is assayed here as the BSA conjugate of CML (BSA-CML). CML is a particularly interesting target to examine by competitive CTI. Immunochemical measurement of CML must be done in competitive format as low amounts of CML residues on a protein would make sandwich immunoassay

methods impossible. Furthermore, any glycosylated protein could be oxidized to possess CML modifications. Analysis by CEIA would likely produce many peaks due to analyte heterogeneity, while CTI would produce only one peak.

This chapter also details improvements and other changes to CTI methodology which focus on simplification of the technique and an alternate procedure for the creation of CTI antibody conjugates. Here, microtiter plate wells are introduced as a solid phase on which assays can be performed. The use of this traditional immunoassay platform should make the method more practical for implementation by other labs. The popular heterobifunctional crosslinker N-succinimidyl 3-(2-pyridyldithio) propionate (SPDP) is used here to modify IgG and thus introduce a thiol-reactive group which easily forms new disulfides with the addition of a thiol-amine. An amine-reactive fluorophore is used in the final conjugation step to produce a unique CTI conjugate. This approach to CTI conjugation should allow for the generation of fragments which have much more diverse charge-to-mass ratios than those from earlier CTI experiments, and will thus be easier to resolve using electrophoretic means. Using the new conjugation method, detection of all three analytes is demonstrated.

5.2 Materials and Methods

5.2.1 Chemicals and Materials

Unless otherwise noted, all chemicals were obtained from Sigma-Aldrich (St. Louis, MO) and used as received. Monoclonal mouse anti-thyroxine (M94208) was purchased from Fitzgerald (Concord, MA). Polyclonal goat anti-3-

nitrotyrosine (NT 50, pAb 3NT) was obtained from Oxford Biomedical Research (Oxford, MI). Polyclonal goat anti-carboxymethyl lysine (K97135G, pAb CML) was obtained from Biodesign International (Saco, ME). Polyclonal rabbit anti-bovine catalase (C2096-06, pAb CAT) was obtained from United States Biological (Swampscott, MA). N-succinimidyl 3-(2-pyridyldithio) propionate (SPDP) (21857), 3-3'-dithiobis(sulfosuccinimidylpropionate) (DTSSP) (21579), (21578) Slide-A-Lyzer Mini Dialysis Unit (69550), BCA Protein Assay Kit (23227), 2,4,6-trinitrobenzene sulfonic acid (TNBSA) (28997), SuperBlock blocking buffer (37516), EZ-Link Maleimide-PEO Solid Phase Biotinylation Kit (21930), and Zeba Desalt Spin Columns (89882) were obtained from Pierce (Rockford, IL). Microcon Ultracel YM-3 centrifugal devices (42403) were obtained from Millipore (Bedford, MA). F96 MaxiSorp Microtiter Plates (439454) were obtained from Nalge Nunc International (Rochester, NY). Thermal oxide silicon wafers were purchased from University Wafer (South Boston, MA). PDMS monomer and crosslinker (Sylgard 184) were purchased from Dow Corning (Midland, MI). SU8-3025 photoresist was obtained from Microchem (Newton, MA). All fluorescence measurements were performed using a Photometrics HQ² CCD camera from Roper Scientific (Tucson, AZ) and Metamorph software from Molecular Devices (Sunnyvale, CA) on a Nikon Eclipse TE2000-U epifluorescence microscope assembly (Melville, NY).

5.2.2 Preparation of IgGs for Conjugation

Prior to conjugation, all antibodies were dialyzed extensively against 50 mM sodium phosphate, 150 mM sodium chloride, and 1 mM EDTA pH 7.4 (PBS-EDTA) using a Slide-A-Lyzer MINI dialysis kit. EDTA was included in the antibody samples to prevent metal catalyzed reduction of disulfides.

5.2.3 One Step CTI Conjugates Using DTSSP Crosslinker

pAb CAT was used as a test IgG for CTI conjugation experiments. Two different methods were investigated using a one-step conjugation procedure. 0.5 mg pAb CAT was diluted to 500 μ l in PBS. A 20-fold molar excess of FITC-ethylene diamine (FTED) and a 60-fold excess of homobifunctional crosslinker DTSSP was added to the protein solution. This solution was allowed to mix for two hours in the dark at room temperature. Following reaction, unbound fluorophore and crosslinker were removed from solution by centrifugation using a Microcon 3,000 MWCO centrifuge tube. Centrifugation continued until the retained solution was either no longer fluorescent to the eye or ceased to change in color from continued purification. PBS was added to solution as necessary to prevent centrifugation to dryness. Finally, the solution was diluted to 500 μ l in PBS and stored at 4°C until further use. A schematic of this one-step CTI conjugation is shown in Figure 5.1.

Conjugation of pAb CAT to FTED using DTSSP was also attempted on a nickel affinity resin. 0.5 mg pAb CAT in 400 μ l was added to a centrifuge tube containing one Swell Gel nickel affinity disc obtained in an EZ-Link Maleimide

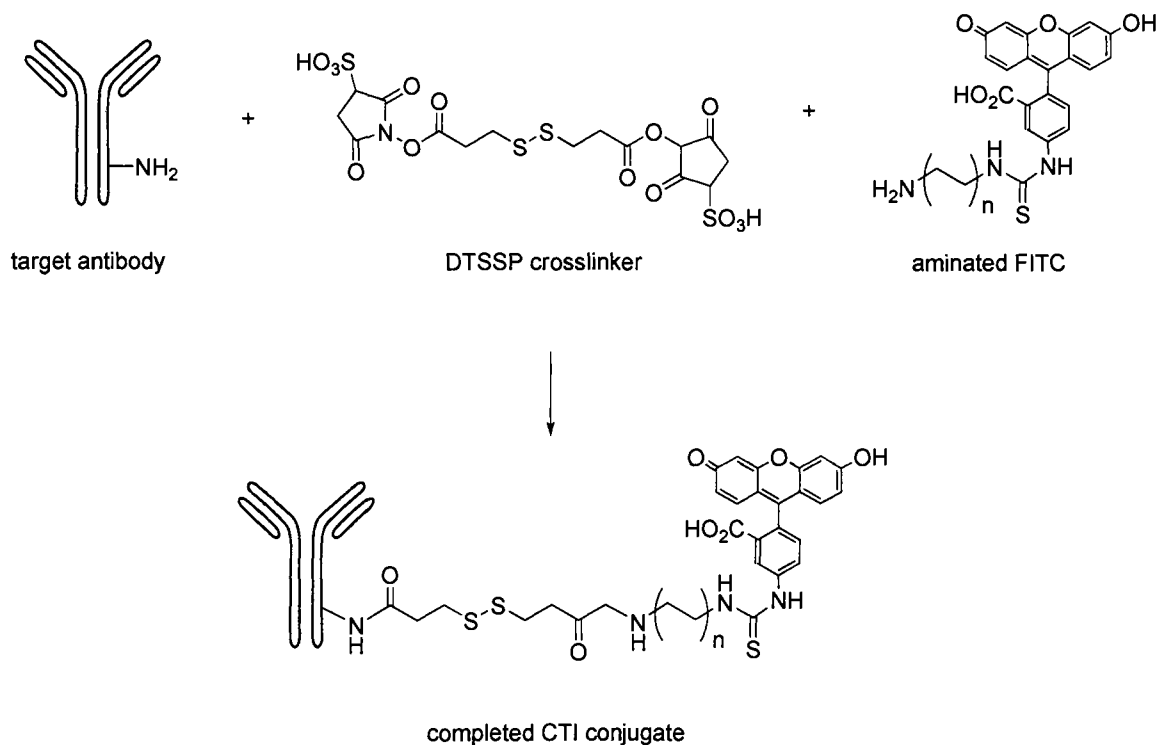


Figure 5.1. Schematic for one-step CTI conjugation using the homobifunctional crosslinker DTSSP and FITC derived with a diamine.

PEO Solid Phase Biotinylation Kit. The disc was allowed to hydrate for 30 seconds, and then was suspended through several inversions. The resin was mixed for 10 minutes to allow binding of the antibody to the solid phase. The tube was then centrifuged to pellet the resin. Solution was removed, and the resin washed with 1 ml PBS and pelleted two more times. Next, 200 μ l 5 mM DTSSP in PBS was added to the resin and allowed to mix for 30 minutes. Again the resin was pelleted and washed three times with PBS. 200 μ l 1 mM FTED in PBS was added to the resin and allowed to mix for one hour. Resin was again pelleted and rinsed with 1 ml aliquots of PBS until solution no longer was colored. Finally, 200 μ l of 200 μ M imidazole solution was added to the resin and incubated for 10 minutes to remove modified antibody from the affinity resin. Solution was stored at 4°C until further use.

5.2.4 Modification of IgG with SPDP Crosslinker

In this conjugation scheme, pAb CAT was again used as a test IgG to determine method viability. 0.5 mg pAb CAT in 100 μ l PBS-EDTA was added to 2.5 μ l 40 mM SPDP in DMSO, a 30-fold excess of crosslinker to protein. The solution was mixed for two hours at room temperature. To remove unbound SPDP, the protein solution was buffer exchanged using a Zeba desalt spin column according to manufacturer's instructions and using PBS-EDTA as the exchange buffer. A control solution containing only SPDP and no protein was buffer exchanged in parallel. To determine the extent of protein-SPDP crosslinking, an aliquot of modified pAb CAT was reacted with dithiothreitol (DTT)

according to the Pierce instructions included with SPDP, and the SPDP-protein molar ratio was calculated. A schematic of the first step of antibody modification by SPDP and cleavage with DTT is shown in Figure 5.2.

5.2.5 Thiol-Amine Conjugation to SPDP Modified IgG

Modification of pAb CAT with SPDP allowed for further conjugation of the protein to a thiol-containing molecule through reaction with the 2-pyridyldithio group of SPDP. Two 30 μ l aliquots of 6.55 mg/ml pAb CAT SPDP were prepared. Following quantification of the molar SPDP/protein ratio, the thiol-amine cysteamine was added to the two samples in either a 1.5-fold or 5-fold excess over SPDP. This reaction was allowed to proceed overnight at 4°C. The protein samples were purified using Zeba desalt spin columns pre-equilibrated with PBS.

5.2.6 Fluorescence Derivatization of Thiol-Amine Modified IgG

After modification of pAb CAT with the thiol-amine cysteamine, 1 μ l 20mM FITC in DMSO was added to each of the two aliquots and mixed. Again the reaction was allowed to proceed overnight at 4°C. Following reaction, the samples were again purified by buffer exchange into PBS. A control solution containing only FITC was also buffer exchanged into PBS to determine the quality of the purification method. Modification of SPDP labeled antibody with thiol-amine and FITC fluorophore is shown in Figure 5.3.

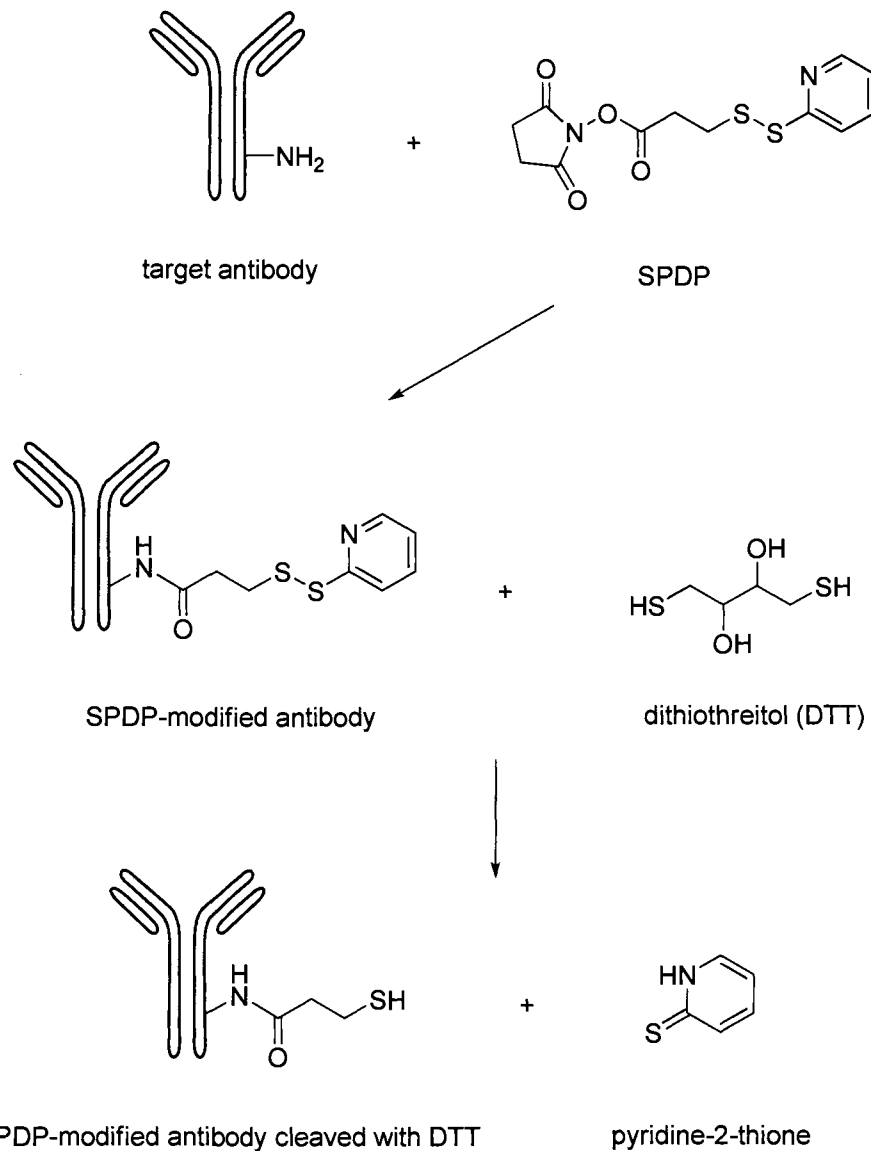


Figure 5.2. Schematic for modification of target antibody with SPDP crosslinker.

Exposure of the conjugate to DTT results in cleavage of the disulfide and release of pyridine-2-thione.

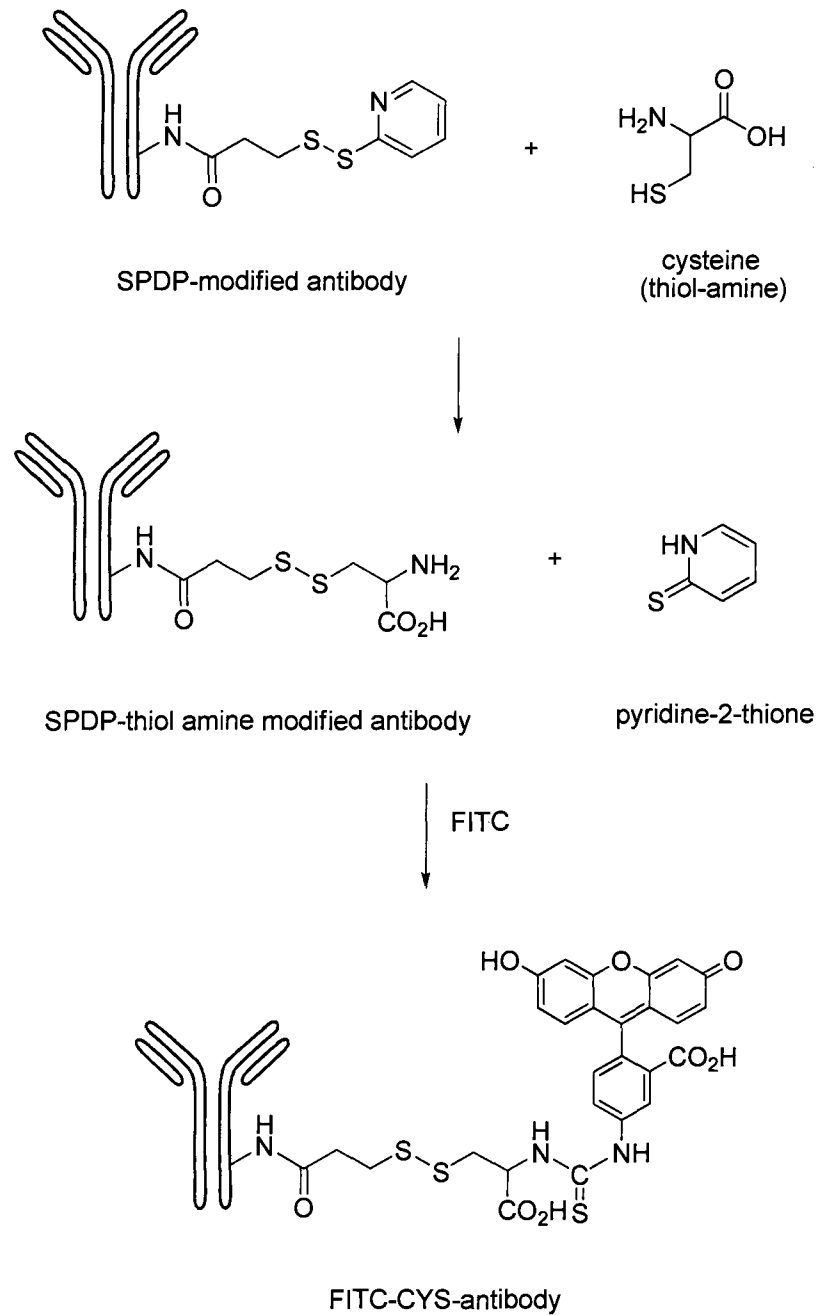


Figure 5.3. Conjugation of SPDP modified antibody to thiol-amine and FITC fluorophore.

Some thiol-amine modified IgGs were also labeled with the AlexaFluor 488 fluorophore for CTI use. This was performed using the AlexaFluor 488 antibody labeling kit according to instructions provided by Invitrogen.

5.2.7 PDMS Microchip Fabrication

PDMS microchips used for CE were constructed in our lab using in-house procedures. A 3 inch thermal oxide coated silicon wafer was used as a base for making a chip mold. These were used either out of the box with no cleaning (new wafers) or after washing with soap and water, rinsing with deionized water and blowing dry with an air stream (reused wafers). Wafer was placed into a spin coater (Laurell Model WS-400A-6NPP/LITE) and held under vacuum while approximately 2 mL of SU-8 3025 photoresist was added to the center of the wafer. The wafer was spin coated at 900 RPM for 30 seconds followed by 1000 RPM for 45 seconds. The wafer was then soft baked at 65°C for 3 minutes and 95°C for 5 minutes. The appropriate photomask was then placed on the coated wafer and under a ¼ inch piece of glass to ensure contact between wafer and mask. The wafer was then exposed to UV light for 7 seconds using an Intelli-Ray 400 Shuttered UV Floodlight. A second soft bake incubation was performed on the wafer at 65°C for 2 minutes, followed by 95°C for 6 minutes. Unreacted photoresist was then removed by immersion of the wafer in a propylene glycol monomethyl ether acetate developer solution for 10 minutes. Wafer was then rinsed with developer and finally with isopropanol. Remaining solution was blown off of the wafer with an air stream. The new mold was then incubated at 95°C for

at least 30 minutes to complete the curing of photoresist. Sylgard 184 elastomer was mixed at a 10:1 ratio with crosslinker, and degassed in a vacuum chamber. This mixture was poured onto the new mold and was spin coated onto a glass slide at 2000 RPM for 30 second. Both mold and slide were placed into an oven at 65°C for at least 60 minutes. Cured PDMS was then cut from the mold, and circular wells of 5 mm diameter were punched at four defined locations. The PDMS piece and the coated glass slide were cleaned with tape and then placed into a Harrick Plasma Cleaner/Sterilizer PDS-32G and treated with air plasma for 30 seconds. The plasma treated sides of the two pieces were then placed together, creating a permanent seal. The completed microchip was then placed in the oven at 65°C for 24 hours before use.

5.2.8 Microplate Competitive Immunoassay

Conjugates of BSA and either T4 or 3NT were prepared according to the literature.^{5, 6} Lysine residues on native BSA were modified by glyoxylic acid to become carboxymethyl lysine residues according to the literature.⁷ To coat microplate wells, BSA conjugates were diluted in PBS to between 2.5 and 7.5 µg/mL depending on the experiment and added to each microplate well at 70 µL for overnight incubation at room temperature. Each well was then blocked twice using Pierce Superblock according to manufacturer instructions. After tapping the microplate dry on a Kimwipe, 50 µL of sample containing 45 mg/mL BSA in PBS was added to each well. Appropriate amounts of CTI immunoconjugate tracers (usually between 2.5 and 10 µg/mL) were then spiked into each well. Microplate

was covered and placed on a plate shaker for 4 hours. The plate was then rinsed twice with PBS + 0.05% Tween 20 and twice with 10 mM HEPPSO buffer at pH 7.5 or pH 8.5 depending on the experiment. Finally, each well was exposed to 50 μ L 10 mM HEPPSO, 1 mM TCEP for two hours on the plate shaker before evaluation using microchip fluorescence CE.

5.2.9 Separation Parameters for Microchip Fluorescence CE

All separations were performed on a straight-T PDMS microchip with a 5 cm separation channel 50 microns high by 50 microns wide. Microchips were pretreated with 0.5 M NaOH for one hour, followed by rinse and incubation with separation buffer for at least 30 minutes. A power supply used for electrophoresis was set up according to Garcia.⁸ During injection, both buffer and sample waste reservoirs were held at a variable potential (+700 V) to prevent sample introduction to the channels leading to the two reservoirs. Separation potential was +1200 V, and injection time was 5 seconds unless otherwise noted. Each well was loaded with 40 μ L of the indicated buffer or sample solution. Detection was performed at a distance of 4.5 cm from the straight T injection point. Metamorph imaging software settings were a binning of 8, gain of 3, and an exposure time of 75 ms/frame.

5.3 Results and Discussion

5.3.1 Examination of One-Step CTI Conjugation Using DTSSP

Conjugates formed using the one-step method (both in situ and using nickel affinity resin) were quantified using BCA assay. The IgG conjugate formed in solution was found to have a concentration of 0.75 mg/ml in a 0.5 ml solution, or 0.325 mg total protein. The experiment began with 0.5 mg of protein, meaning 25% of protein was lost during conjugation, mostly likely during the purification using centrifugal filters. The conjugate formed using the nickel affinity resin showed even lower recovery with only 0.10 mg/ml in 0.5 ml, or 0.05 mg total protein (10% recovery). Because of the low recovery of this method, one-step conjugation on a nickel affinity resin was not further pursued as a CTI conjugation method.

When a one-step conjugation method is explored using a homobifunctional crosslinker such as DTSSP, undesired products such as antibody-antibody or fluorophore-fluorophore can cause a low yield of the desired antibody-fluorophore products. During the one-step conjugation of pAb CAT and FTED in solution, a stoichiometric excess of both FTED and DTSSP is used to prevent antibody-antibody conjugates, although some fluorophore-fluorophore conjugation would be expected. To examine the level of antibody-antibody crosslinking using this method, the sample was examined by size exclusion chromatography (SEC). Conjugate and native protein were prepared at 1 mg/ml in PBS. 20 μ l of sample was injected onto a Biosep SEC-S 3000 column and

separated at 1 ml/min using 100 mM sodium phosphate pH 6.8 as the mobile phase.

The SEC chromatogram in Figure 5.4 includes traces from both the FTED-DTSSP-pAb CAT and native pAb CAT. The prominent peak of both traces appears at 18.5 minutes, while a much smaller peak is seen at 17 minutes. While the peak at 17 minutes could be indicative of dimerization of IgG, it is clearly not the main product of conjugation. Also, conjugation of the small molecules onto pAb CAT did not change the retention time in a significant way, which was expected.

One-step in situ conjugation of target antibodies to aminated fluorophores using DTSSP appears to be a viable method for formation of CTI conjugates. However, this strategy is limited by the small number of diamines commercially available to the user. Conjugates made using diamines such as ethylenediamine, cystamine, and 1,6 hexanediamine produce TCEP-cleaved CTI fragments that differ only by a few (CH_2) groups and would be expected to be more difficult to resolve electrophoretically than groups differing in charge. These fragments have been resolved previously, but required extensive separation method development.³ For these reasons, one-step conjugation of IgG to aminated fluorophores using DTSSP was discontinued in favor of SPDP mediated conjugation, discussed below.

5.3.2 Quantification of Crosslinking of IgG to SPDP.

The conjugation of proteins and other biomolecules to antibodies through SPDP has been firmly established in the literature, most notably for the formation

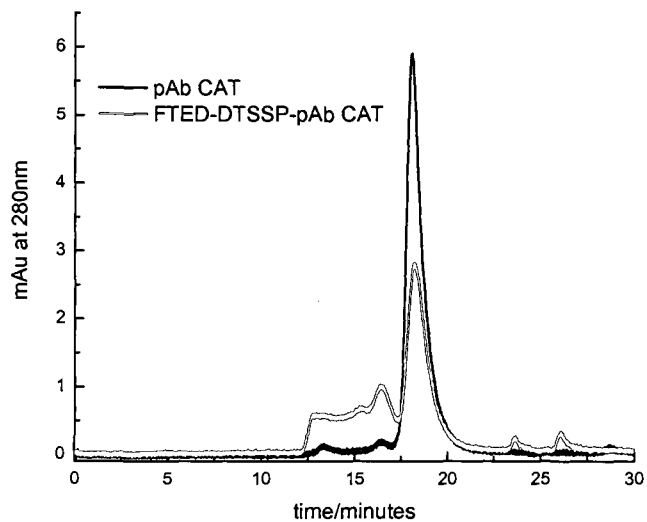


Figure 5.4. Size-exclusion chromatogram of native pAb CAT and pAb CAT conjugated to FTED using DTSSP in a one-step procedure. Flow rate was 1 ml/min in 100 mM sodium phosphate pH 6 run buffer. Injection was 20 μ l of 1 mg/ml antibody.

of immunotoxins.⁹ Toxins are conjugated to an antibody so that the toxin can be directed to a certain location in a biological system (defined by the antibody's specificity for target), as opposed to exposing the entire system to large amounts of toxin in a non-specific manner.

The heterobifunctionality of SPDP is defined by an amine-reactive N-hydroxysuccinimide group and a thiol-reactive 2-pyridyldithio group. When a thiol reacts with a SPDP-protein conjugate, it forms a new disulfide linkage with the protein while pyridine-2-thione leaves the SPDP residue as a byproduct.¹⁰ This leaving group is not reactive towards the newly formed disulfide, so the reverse reaction cannot threaten the stability of the new conjugate. SPDP is an appealing crosslinker for the formation of immunotoxins for several reasons. As a heterobifunctional crosslinker, a target protein can be modified through the NHS ester of SPDP without concern for homopolymerization of the protein due to a lack of free thiols on the protein surface. Thiolated toxin can then be added to the protein in a specific manner. The final conjugate contains a disulfide separating the antibody and the toxin, which can be reduced to release the toxin once inside a cell.¹¹ Disulfides can undergo disulfide exchange in the presence of free thiols. Cleavage of disulfides using excess DTT is an example of disulfide exchange. It is necessary to understand the degree of protein modification by SPDP so that reaction with free thiol-amine in the second conjugation step can be controlled in such a way to prevent undesired disulfide reduction and preserve newly formed disulfides. Quantification of SPDP residues in a protein sample is most easily

accomplished by measuring the absorbance of pyridine-2-thione at 343 nm following cleavage of disulfides in the sample by DTT.

In experiments with pAb CAT SPDP conjugates, both the conjugate and a control containing only SPDP were purified by column buffer exchange using a desalting resin. The control was included to examine the ability of the desalting resin to remove unbound SPDP. 5 μ l of each sample was diluted to 500 μ l in PBS and absorbances were recorded at 280 nm and 343 nm. Each sample was then mixed with 5 μ l 15 mg/ml DTT in PBS. After 15 minutes, samples absorbances were again measured at 343 nm. The absorbance at 343nm of the pAb CAT SPDP sample went from 0.001 A before reaction to 0.049 A following the reaction, while the control sample went from 0.004 A to 0.007 A. The degree of SPDP labeling can be measured using the following formula:

$$\frac{\Delta A}{8080} \frac{MW_{protein}}{mg/ml} = SPDP / protein \quad (5.1)$$

where ΔA is the change in absorbance at 343 nm, 8080 is the extinction coefficient of pyridine-2-thione at 343 nm, and $SPDP/protein$ is the molar ratio. The concentration in mg/ml of the IgG is estimated using the absorbance at 280 nm.¹²

The modified pAb CAT sample was found to contain 12.9 moles SPDP per mol of protein. Furthermore, the very small change in absorbance at 343 nm of the control SPDP sample indicates that the buffer exchange resin does remove most of the unreacted SPDP from solution. With the SPDP content of the protein

now known, aliquots from the sample were reacted with different molar excesses of thiol amine, 1.5-fold and 5-fold excesses. A low molar excess would be expected to modify the protein without the risk of further disulfide exchange, while a higher ratio could result in the undesired cleaved SPDP modified protein product.

5.3.3 Primary Amine Concentration on Modified and Unmodified IgG

The CTI tracer conjugation methodology described here utilizes newly introduced primary amines for reaction with fluorophore after SPDP reaction with a thiol-amine. Therefore, quantification of primary amine content in a conjugated protein sample can reveal the extent of modification during several of the steps. The reaction of 2,4,6 trinitrobenzene sulfonic acid (TNBSA) with free amino groups to produce a colored derivative provides a convenient method to examine primary amine content in a sample. Following the instructions provided by Pierce for TNBSA assay, native pAb CAT, pAb CAT SPDP, and pAb CAT SPDP-cysteamine samples were examined using glycine as a standard to create a calibration curve. After reaction of the native protein with SPDP, there is a 56.6% reduction in free amine content. Because SPDP reacts with primary amines, a reduction in primary amine content after this step would be expected. Both pAb CAT SPDP cysteamine samples were also examined for amine content. The sample treated with a 1.5-fold excess of cysteamine over SPDP showed a 350.9% increase in amine content. With the maximum amine content expected to be 100% of the original primary amine concentration, this result is likely in error.

It is possible that the buffer exchange procedure did not remove excess cysteamine, however even that scenario should not produce a result this high. Other IgG conjugates made in our lab with a 1.5-fold excess of thiol-amine produced functional CTI conjugates, so this result may simply be an anomaly. The sample with a 5-fold excess of cysteamine gave 98.1% of the original amine content, a more sensible result that shows all SPDP residues have reacted and excess amine has been removed. It would appear that at low millimolar concentrations, displacement of the disulfide by free thiol is not significantly detrimental to the viability of the conjugate. The TNBSA amine quantification assay is an essential experiment which has been used to confirm the functional expectations of the first two steps of CTI bioconjugation.

5.3.4. Molar F/P Ratio Quantification for FITC Labeled Conjugates

After labeling pAb CAT with SPDP and cysteamine, the final modification was performed in which the fluorescent amine-reactive label FITC was used to label the conjugate. Buffer exchange resin was used to remove unbound FITC, which could be seen as a yellow color concentrated at the top of the resin bed. The conjugate was diluted to 500 μ l with PBS, and the absorbances at 280 nm and 495 nm were recorded. The following equation was used to determine the molar fluorophore/protein (or F/P) ratio:¹³

$$\frac{2.77 \times A_{495}}{A_{280} - (0.35 \times A_{495})} = \text{Molar } F / P \quad (5.2)$$

This method was used for molar F/P calculation for conjugates used in the CTI experiments below. An additional experiment was used to examine the FITC-cysteamine pAb CAT conjugate. Two 25 μ l aliquots of that conjugate were prepared. One aliquot was added to 25 μ l 5 mM borate pH 8, 1 mM TCEP. The other aliquot was used as a control, adding 25 μ l 5 mM borate pH 8 with no TCEP. After an hour reaction in the dark, samples were buffer exchanged using a Zeba desalting column into 5 mM borate pH 8 and diluted to 400 μ l in the same buffer. Absorbances were then measured at 495 nm. The solution exposed to TCEP gave an absorbance of 0.000, while the sample that was not exposed to TCEP gave an absorbance of 0.028. Because the buffer exchange procedure allows the protein to pass through the column and retains small molecules on the column, this experiment shows that TCEP does reduce the newly formed disulfide allowing the CTI fragment to diffuse into solution. This key experiment demonstrates the viability of this conjugation method to produce CTI tracers made from any thiol-amine and any amine-reactive fluorophore. The main advantage of this method over previous methods is the increased control it gives to the chemist over the charge-to-mass ratio of the CTI fragments. Furthermore, it vastly expands the number of possible CTI fragments available to the user. Previous methods relied on using different diamines which are limited in number and in the difference in charge-to-mass ratio imparted on the final fragment. Because the CTI fragment is conjugated directly onto the protein step by step, fluorophores which are too costly to use in large quantities can be introduced from much smaller masses. Table 5.1 contains a list of CTI conjugates which

antibody	thiol-amine	fluorophore	abbreviation
thyroxine	cysteine	FITC	FCYS mAb T4
3-nitrotyrosine	cysteamine	FITC	FCAM pAb 3NT
carboxymethyl lysine	cys-gly	FITC	FCG pAb CML
thyroxine	cysteamine	FITC	FCAM mAb T4
3-nitrotyrosine	cysteamine	AlexaFluor 488	AFCAM pAb 3NT
carboxymethyl lysine	cysteine	AlexaFluor 488	AFCYS pAb CML

Table 5.1. CTI conjugates used for competitive immunoassays. Abbreviations used in the text are in the column to the far right.

have been prepared in the lab using various thiols-amines and fluorophores for use in this work. Creation of dozens of other conjugates should be feasible, given the availability of several different thiol-amines and spectrally similar fluorophores that are commercially available.

5.3.5 Competitive CTI for BSA-3NT

To demonstrate competitive microplate CTI, BSA-3NT was selected as an analyte given our successful analysis of the same target using micromosaics. After overnight sensitization using 5 µg/mL BSA-3NT and BSA-T4, the microplate was exposed to samples containing variable amounts of BSA-3NT and 5 µg/mL of the tracers FCAM pAb 3NT and FCYS mAb T4. Having already established peak identities for the FCAM and FCYS fragments, it was theorized that the peak associated with 3NT would decrease in area as a result of competition between surface-bound BSA-3NT and BSA-3NT in solution. Figure 5.5 shows a representative electropherogram from this separation, and a dose-response curve for BSA-3NT. The dose-response curve clearly shows the competitive effect that BSA-3NT in solution has on FCAM peak area over sub-microgram per milliliter concentrations. This proof of concept experiment was used as a basis to justify further competitive CTI experiments where multiple analytes were examined simultaneously.

5.3.6 Three Analyte Competitive CTI

Having demonstrated that CTI was possible for a single analyte, a three analyte system was next devised for targets 3NT, T4, and CML. In the first attempt to perform this assay, the conjugate FCG pAb CML was examined with

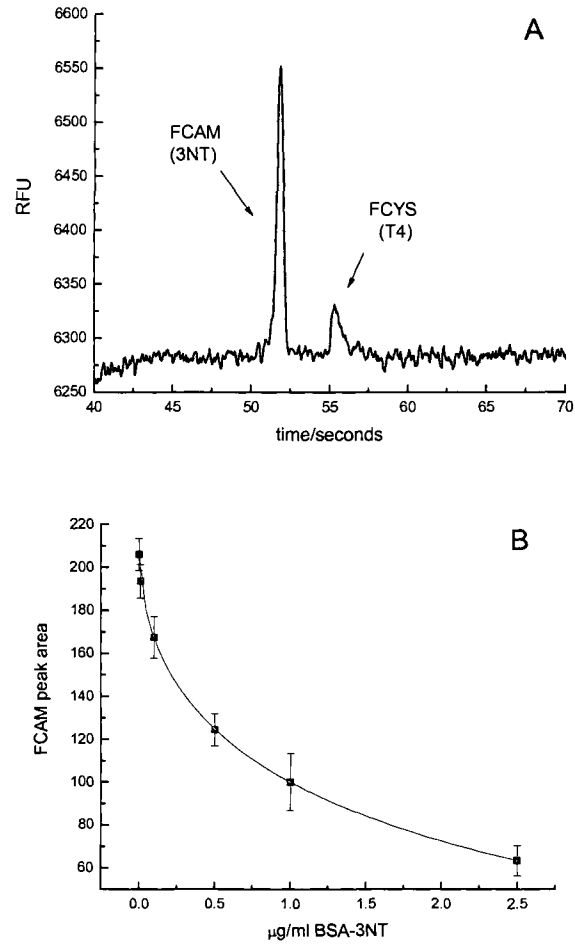


Figure 5.5. Sample electropherogram for separation of FCAM and FCYS tags (A). CTI dose-response curve for BSA-3NT (B). Separation buffer was 10 mM HEPPSO, 5 mM SDS, 0.5 mM TDAPS pH 7.5. Cleavage buffer was 10 mM HEPPSO, 1 mM TCEP pH 7.5.

FCAM pAb 3NT and FCYS mAb T4. Microplates sensitized to all three analytes were incubated with the three conjugates, and the cleavage products examined by CE so that peak resolution could be optimized prior to immunoassay. The HEPPSO buffer used for 3NT immunoassay above was found to be unable to separate the comigrating peaks of FCYS and FCG. Several other buffer conditions were examined for this separation. The most promising separation buffer was found to be 10 mM TAPS, 5 mM SDS, 0.05% Triton-X 100 and 20% acetonitrile. An electropherogram from this separation is seen in Figure 5.6. One of the peaks appears as a small peak shoulder at x seconds. These buffer conditions did not provide sufficient resolution to perform quantitative measurements from the FCYS and FGC peaks.

One of the stated benefits of CTI is the synthetic control of the signaling molecules. Due to the problems associated with simple resolution of FCYS and FCG fragments, a new separation was attempted using conjugates that produced different cleaved tags. The three conjugates examined were AFCAM pAb 3NT, FCAM mAb T4, and AFCYS pAb CML (see Table 5.1). The idea behind this approach to analysis was that problems with resolution of cleaved tags could be addressed by simply using a different synthesis to produce a different, more easily resolved set of cleaved fluorophores. The three new conjugates produced cleaved tags that were found to have baseline resolution using a separation buffer of 10 mM TAPS, 5 mM SDS, 0.05% Triton-X 100. Having established the separation parameters, a specificity experiment was undertaken to both examine cross reactivity and determine peak identities. Microplate wells were sensitized to

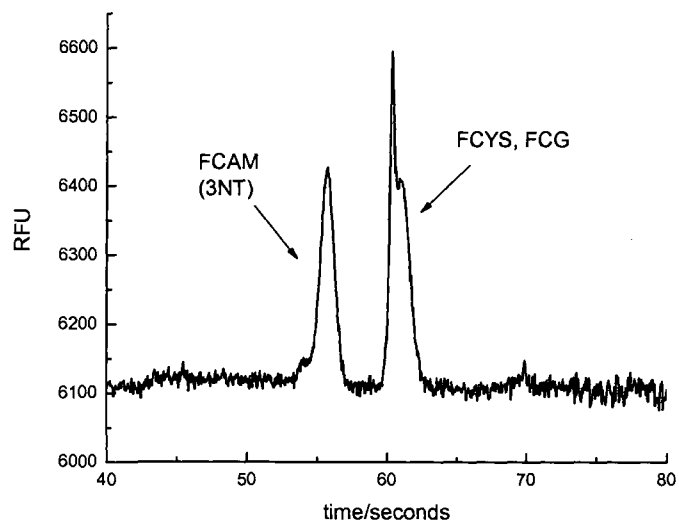


Figure 5.6. Electropherogram for separation of FCAM, FCYS, and FCG CTI fragments. Separation buffer was 10 mM TAPS, 5 mM SDS, 0.05% Triton-X 100, and 20% acetonitrile.

only one of the three analytes in the first step, yet exposed to all three conjugates during the second incubation step. This experiment is similar to the cross reactivity study shown in Figure 2.2. Cleaved solutions were examined by CE, and in each case a single peak appeared. This shows that the three analyte system has low cross reactivity, and could therefore be used for multianalyte analysis. An electropherogram for each of the three sensitized wells is shown in Figure 5.7.

Once both the separation parameters needed for resolution of the three peaks (AFCAM, FCAM, AFCYS) had been determined and the specificity of the affinity reagents demonstrated, a competitive immunoassay for all three analytes 3NT, T4, and BSA-CML was attempted. Figure 5.8 shows two electropherograms. One is from a sample in which no competing analytes were present, and results in the appearance of the three peaks. The second electropherogram is taken from a sample in which 10 μM 3NT, 10 μM T4, and 4 $\mu\text{g/mL}$ of BSA-CML were present. The peaks from AFCAM and FCAM are no longer present, and the peak from AFCYS appears diminished. This is evidence that the competitive effect is occurring and has the expected effect on the three peaks.

At this point in the CTI project, quantification of analytes has been slow due to irreproducibility of the injection of analyte into the capillary during CE. Figure 5.9 shows a dose-response curve for 3NT using the parameters discussed above. The trend of the data (decreasing AFCAM peak area with increasing 3NT concentration) is indicative of competition, but the large error of

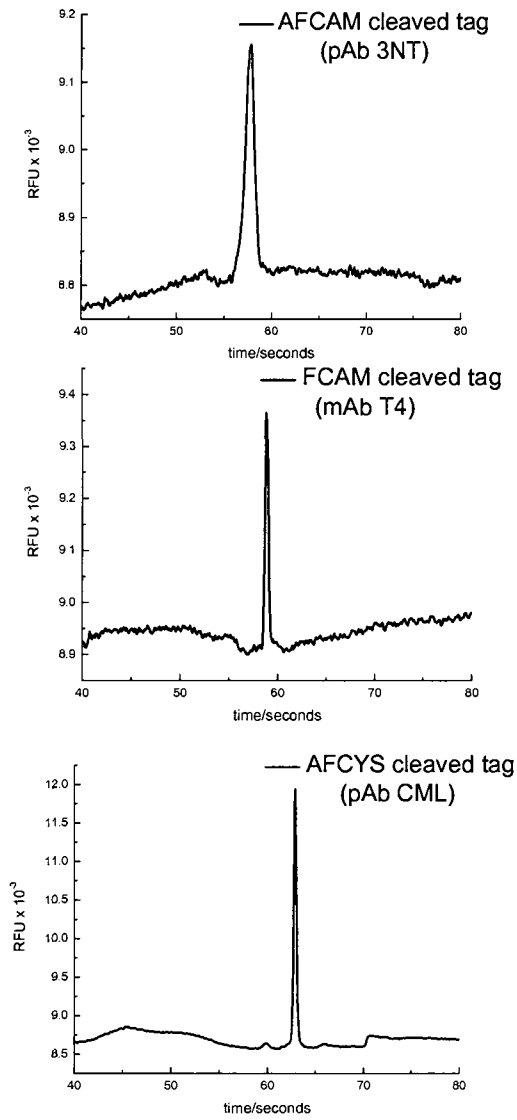


Figure 5.7. Specificity and peak identity experiment. Substrates were sensitized to only one analyte, but incubated with all three CTI immunoconjugates in the second step.

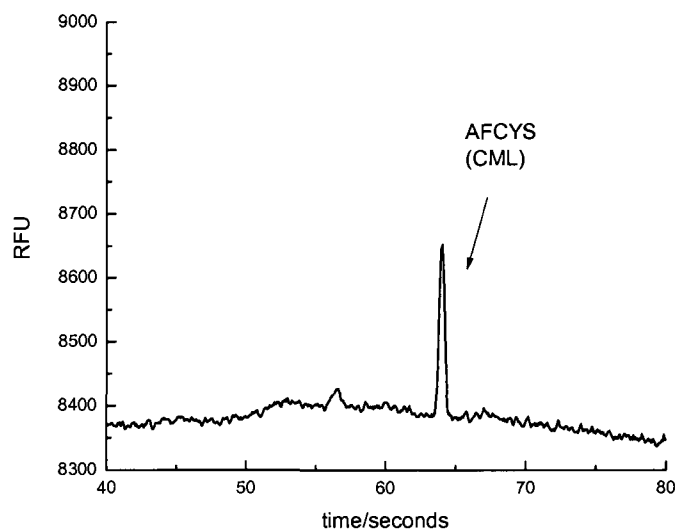
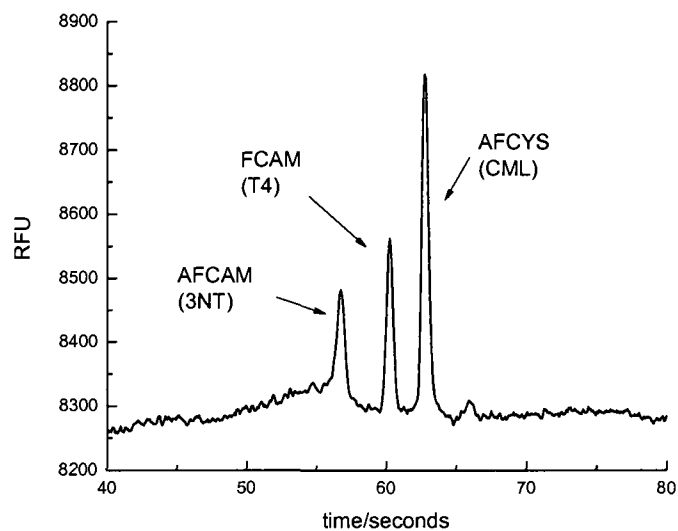


Figure 5.8. Competitive effect of 3NT, T4, and BSA-CML on cleaved tag peaks. Above: 0 μM 3NT, 0 μM T4, 0 $\mu\text{g/mL}$ BSA-CML. Below: 10 μM 3NT, 10 μM T4, 4 $\mu\text{g/mL}$ BSA-CML. Separation buffer was 10 mM TAPS, 5 mM SDS, 0.05% Triton-X 100.

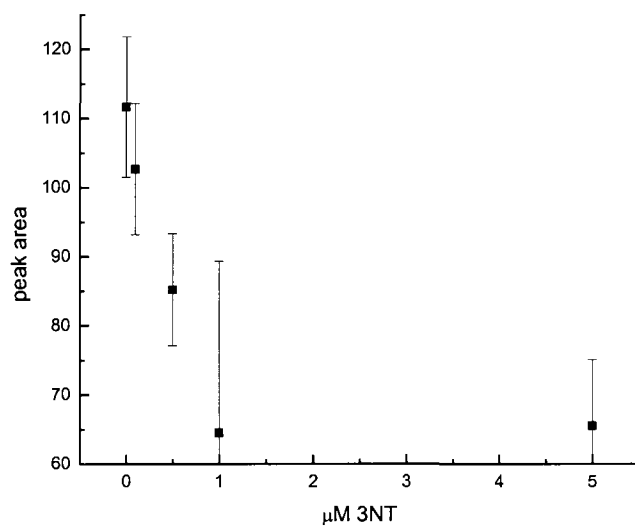


Figure 5.9. Dose-response curve for 3NT in three analyte system. Error bars represent one standard deviation.

the peak area has prevented further characterization of the immunoassay (LOD, etc).

5.4. Conclusion

In this chapter, competitive CTI has been presented as a possible alternative to traditional single analyte immunoassay methods such as ELISA, and multianalyte methods such as CEIA and IACE. A new conjugation scheme has been introduced which utilizes the popular heterobifunctional crosslinker SPDP. Modification of the protein was quantified at each of the three steps to confirm the viability of the procedure. Using this protocol, several different immunoconjugates were prepared in our laboratory. Use of these conjugates in competitive CTI was researched using a microtiter plate as a solid phase and microchip fluorescence CE for cleaved tag detection. Resolution of two tags in a HEPPSO buffer and competitive assay for BSA-3NT was demonstrated. Three different tags were separated using a TAPS buffer and the competitive effect demonstrated, but reproducibility of injection and separation has thus far prevented quantification of analytes.

5.5. References

- (1) Nielsen, R. G.; Rickard, E. C.; Santa, P. F.; Sharknas, D. A.; Sittampalam, G. S. *Journal of Chromatography* **1991**, 539, 177-185.
- (2) Guzman, N. A.; Trebilcock, M. A.; Advis, J. P. *Journal of Liquid Chromatography* **1991**, 14, 997-1015.

- (3) Caulum, M. M.; Murphy, B. M.; Ramsay, L. M.; Henry, C. S. *Analytical Chemistry* **2007**, *79*, 5249-5256.
- (4) Fu, M. X.; Requena, J. R.; Jenkins, A. J.; Lyons, T. J.; Baynes, J. W.; Thorpe, S. R. *Journal of Biological Chemistry* **1996**, *271*, 9982-9986.
- (5) Englebienne, P. *Immune and Receptor Assays in Theory and Practice*; CRC Press: Boca Raton, 2000.
- (6) Murphy, B. M.; He, X. Y.; Dandy, D.; Henry, C. S. *Anal Chem* **2008**, *80*, 444-450.
- (7) Schleicher, E. D.; Wagner, E.; Nerlich, A. G. *Journal of Clinical Investigation* **1997**, *99*, 457-468.
- (8) Garcia, C. D.; Liu, Y.; Anderson, P.; Henry, C. S. *Lab on a Chip* **2003**, *3*, 324-328.
- (9) Marsh, J. W., Srinivasachar, K., Neville, D.M. In *Immunotoxins*; Frankel, A. E., Ed.; Kluwer Academic Publishers: Boston, 1988, pp 213-237.
- (10) Hermanson, G. T. In *Bioconjugate Techniques*; Academic Press: Rockford, 1996, pp 228-232.
- (11) Cattell, L.; Dosio, F.; Brusa, P.; Arpicco, S. *Stp Pharma Sciences* **1999**, *9*, 307-319.
- (12) www.piercenet.com; Thermo Scientific: Rockford, IL; Vol. 2008, pp Procedure for SPDP crosslinker.
- (13) www.sigma-aldrich.com; Sigma: St. Louis, MO; Vol. 2008, pp Fluorescein Isothiocyanate Product Information.

Chapter 6

Research Summary and Future Directions

6.1 Research Summary

This doctoral dissertation discusses two new immunoassay techniques offered as platforms for multianalyte analysis. In this work, resolution of immunochemical reactions was performed both spatially using a micromosaic immunoassay, and electrophoretically using CTI.

Micromosaic research presented here focuses first on development of competitive immunoassays. Indirect competitive assays for T4 and BSA-3NT and a direct competitive assay for CRP are demonstrated simultaneously. Using the method, both T4 and CRP are quantified over their clinical reference range. Next, simultaneous analysis of SOD and CAT by sandwich immunoassay and 3NT by competitive immunoassay is presented. This work shows that both small and large analytes can be examined at the same time, from the same sample but using different assay configurations. As a technique for examining small sets of related biomarkers (2-5 analytes), micromosaics is presented as a versatile and sensitive method.

During micromosaic experiments, a pattern was observed involving decreasing signal across identical mosaics in the direction of flow. This phenomenon, termed the depletion effect, was not only observed in our lab but also predicted by Dr. David Dandy's lab using linear fluid dynamics. This dissertation briefly investigates depletion and proposes a strategy to address

error associated with the effect through geometrical optimization. Using this approach, RSD for signal in the 3NT competitive assay system was reduced by almost 50%. The depletion effect is theorized here to be related to the size of the particle diffusing to the surface in accordance with the Stokes-Einstein equation, and is therefore analyte dependent.

CTI was originally developed in the Henry Lab by Dr. Meghan Caulum for the detection of cardiac biomarkers using a bead-based sandwich immunoassay format. In this dissertation, several new approaches to CTI are examined. Most notably, the bioconjugate protocol for the creation of CTI antibody tracers is investigated using the crosslinker SPDP. This combinatorial approach utilizes various thiol-amines and spectrally similar fluorophores to vastly expand the number of cleavable tags which can be synthesized. Although there are not currently CTI methods which use the dozens of possible tags, the increased number of tags available allows the researcher to pick and choose CTI conjugates which will give more easily resolvable fragments when performing CTI for just a few analytes.

Indirect competitive CTI is demonstrated here using a microtiter plate as a solid phase. Microtiter plates are a standard platform for solid phase assays such as ELISA and could make the CTI technique more appealing for use in other labs. T4, 3NT, and BSA-CML are examined using unique antibody conjugates for each of the targets. Resolution of the three CTI tags is demonstrated using microchip fluorescence CE.

6.2. Future Work

The long term goal for the micromosaics project is to devise a method for examination of metabolites, proteins, and larger targets such as viruses in a simultaneous fashion. Capture and detection strategies for larger targets will have to be developed and incorporated onto the substrate. Another area of interest is patterning across a waveguide surface for label-free detection. Silicon nitride has been used for these detection strategies. Because our patterning methods have been developed on this material, the surface chemistry necessary for these experiments is straightforward.

Further development of CTI can go in several possible directions. The immediate need is to develop a separation chemistry for the cleaved tags that is reproducible and provides for low peak area error. Next, assays for larger numbers of analytes should be investigated. This will likely require more method development in terms of separation strategies. The limit to the number of simultaneous assays possible using CTI currently has an electrophoretic basis. However, this number could be expanded even further through the use of tags that can be resolved spectrally. This would require bioconjugation using labels that fluoresce at a significantly different wavelength than fluorescein. Another aspect of CTI development involves the construction of a micro total analysis system in which each assay step is accomplished on a microfluidic microchip. This would involve a return to a bead-based solid phase for immunocapture. Our laboratory is currently considering many of these possibilities for future research.

Appendix 1: Original Research Proposal

Selection of High Affinity Aptamers Using Imprinted Polymers for Oligonucleotide Extraction

Summary

Functional oligomers or “aptamers” are a class of biopolymers which can catalyze a reaction or bind with high affinity and selectivity to a target molecule [1, 3]. Realization of aptamers as molecular probes and therapeutic agents has been made possible due to aptamer selection methods [4, 5]. Typically, aptamers are selected by exposing an oligomer solution containing a large number of random sequences to an immobilized target molecule. Aptamers bound to the immobilized target are easily separated from the DNA pool by washing. PCR is used to amplify the aptamer, which can then be sequenced. While systematic evolution of ligands by exponential enrichment (SELEX) has provided aptamers for many target molecules, it requires facile target immobilization and a conjugation regime that does not destroy or block the aptameric determinants of the target [6]. The recently developed CE-SELEX method allows for selection in free solution, but requires electrophoretic resolution of aptamer-target complexes [7]. *We propose an in situ selection method in which unbound oligomers are removed from solution using molecularly imprinted polymers (MIP-SELEX).* We hypothesize that a) free solution aptamer-target binding prevents aptamer binding to an imprinted polymer resin due to conformational changes of the given

aptamer or other steric factors and b) a single imprinted polymer resin can serve as a template for an entire oligonucleotide library. Because immobilization of target is not necessary, we expect to create the first truly universal SELEX method which can be applied to any target that can be solubilized with the oligomer library. The method will be demonstrated for the small molecule atrazine. To achieve this goal, the following specific aims will be addressed:

A. Specific Aims

1. Develop an imprinted polymer resin capable of specifically binding a known aptamer for the small molecule pesticide atrazine
2. Determine effects of the presence of target on aptamer binding to the polymer resin. Compare apparent aptamer affinity constants between surface and target.
3. Prepare an imprinted polymer resin using a standard SELEX DNA or RNA library as a template, and expose the new resin to the imprinted SELEX library and a desired target. Perform amplification and sequencing on the eluent to identify potential aptamers to the target.

B. Background

Clinical diagnostics and research require specific reagents for selective detection and quantification of analytes of interest[1]. Affinity reagents are essential for this work, binding with high affinity and specificity to a specific target in the presence of thousands of related molecules. These analytical targets

include proteins and small molecule biomarkers which can be used to understand the mechanisms of biological systems[8]. Affinity reagents are a versatile tool for analysis and clinical diagnostics in highly complex biological samples including blood, serum, and urine.

Immunoglobulins (antibodies) are currently the most widely used affinity reagents [9]. Antibodies are produced in mammalian B cells as a response of the immune system to a foreign molecule [10]. By immunizing a given animal against a chosen antigen or hapten, researchers have been able to isolate antibodies against a wide variety of molecular targets. Using these reagents, immunoassays have become a standard method of biological sample analysis. However, immunoassays face certain limitations due to the nature of antibodies and their production and storage. Polyclonal antibody development is an expensive and time consuming process requiring trained technicians to immunize the animal and collect the serum immunoglobulin fractions [1, 10]. Production of monoclonal antibodies requires further steps to isolate B lymphocytes, fuse them to myeloma cells and grow in a tissue culture. Lastly, the antibody product must be characterized. Antibodies for small molecules must be generated against molecules larger than 5kD, ie molecules large enough to stimulate an immune response [11]. Therefore, small molecule immunogens require conjugation of the small molecule to a carrier protein such as bovine serum albumin (BSA) or keyhole limpet hemocyanin (KLH) [10]. Conjugation can be synthetically challenging, and the process itself can destroy unique antigenic determinants of the target molecule. Finally, as with most protein reagents, antibodies have a

limited shelf life and are at risk for deactivation through denaturation and aggregation.

Aptamers, the name given to single stranded DNA (ssDNA) or single stranded RNA (ssRNA) possessing affinity properties, present an exciting alternative to antibodies and may emerge as the choice affinity reagent for the future of biosensing and analysis. Aptamers possess several interesting advantages over antibodies [1]. For instance, aptamer development does not require immunization of animals or cell cultures. Secondly, aptamer selection and use can proceed under a range of conditions, unlike antibodies which are raised under physiological conditions and can suffer from loss of activity outside this range of conditions. Most importantly, after the sequence of an aptamer has been determined, exact oligomer replicates can be easily synthesized. The key to aptamer utilization lies in the process of selection.

B.1. SELEX

In 1990, three different groups of researchers published descriptions of their efforts to find RNA strands that could bind a specific ligand from a large pool of random sequence RNA oligomers [4, 5, 12]. These researchers theorized that a large population of random sequence oligomers with a wide range of sizes and conformations would contain a select few molecules capable of ligating a target. To test the theory, target ligands were exposed to the diverse RNA pools for a given amount of incubation time. RNA-target complexes were then separated from the RNA pool and enriched by reverse transcription, polymerase chain

reaction (PCR), and transcription. This process was repeated several times using the amplified RNA pools, and resulting oligomers could then be sequenced. The SELEX process is depicted in Figure 1. These sequences (aptamers) were found to bind to the given target with dissociation constants on the order of μM . Tuerk and Gold called their process “Systematic Evolution of Ligands by Exponential Enrichment” or SELEX. This is the modern accepted term for aptamer selection processes [5].

In the years following the debut of SELEX, aptamers have been selected for targets including proteins,[13] amino acids,[14] and even cells [15, 16]. Libraries containing up to 10^{18} different sequences are commonly employed, providing the genetic diversity necessary to select aptamers for a wide range of targets [17]. Aptamers can be selected under a variety of conditions such as differing buffers and temperatures.

Aptamer-target binding has been investigated, primarily through NMR [1]. Yang et al showed that RNA aptamers for arginine and citrulline fold into compact structures upon ligand binding [18]. Likewise, an aptamer for cyanocobalamin is believed to contain a pseudoknot structure which undergoes a conformational change during binding [19].

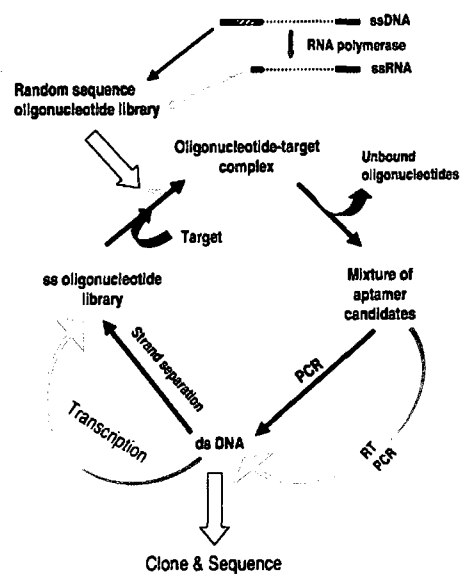


Figure 1. SELEX scheme.[1]

Aptamer conformation changes that generate a signal have been the basis of both colorimetric and fluorometric assays [20, 21].

B.2. CE-SELEX

While the SELEX method has been popularized and aptamers have gained more scientific attention, there have been only a few developments in the fundamental selection methods. One of

the most interesting methodological advancements is capillary electrophoresis SELEX (CE-SELEX) [7, 22-24]. Developed by Mendonsa and Bowser, the method is unique in that target is incubated with the random-sequence nucleic acid library in solution as opposed to on a solid phase. After a period of incubation, the target-library solution is injected onto a capillary column where a separation is performed by CE. Uncomplexed ssDNA migrates as a single band, regardless of size. Aptamer-target complexes migrate at different velocities, as the charge/mass of the target is assumed to impart a mobility shift when complexed with the ligating DNA. Following fraction collection, PCR is used to amplify the DNA pool for the next round of selection as in other SELEX methods.

CE-SELEX has been shown to provide several advantages over conventional SELEX. High-affinity aptamers have been found using this method

after only 2-4 rounds of selection [23]. In direct comparison with conventional SELEX, Tang et al. produced a DNA pool of which 87.2% of oligomers had significant affinity for ricin toxin after four rounds of CE-SELEX, while conventional SELEX produced a pool with only 38.5% of oligomers showing significant affinity after 9 rounds [25]. CE-SELEX has also been found to produce aptamer pools with more sequence heterogeneity than conventional SELEX, which often produces aptamers with common sequence motifs [22]. Several CE-SELEX advantages stem from elimination of the solid phase used for capture of ligating DNA [6]. Conjugation of the target is not required, which eliminates selection bias towards sterically available “epitopes” and crosslinking chemicals. In addition, non-specific binding to the solid phase is eliminated, and high affinity binders don’t need to be eluted prior to PCR amplification. In theory, CE-SELEX could be used to find aptamers for unidentified targets, assuming a control sample with the same matrix was available.

CE-SELEX was not the first method to utilize “free solution” aptamer selection. Tuerk and Gold used free solution selection and captured aptamer-target complexes on a nitrocellulose membrane [5]. This method suffered from low separation efficiencies,[6] and in theory would not work for smaller targets unable to bind to nitrocellulose.

The principle disadvantage of CE-SELEX is evident in the necessary electrophoretic resolution of target-aptamer complex from the bulk nucleotide library. This would be most problematic for smaller targets which would not contribute enough mass or charge to the complex for electrophoretic resolution.

However, larger molecules with electrophoretic mobilities close to that of uncomplexed ssDNA might also lack significant mobility difference to perform CE-SELEX. Finally, aptamer-target peaks are below the limit of detection for CE-UV during selection, requiring researchers to collect all fractions to one side of the unbound oligomer peak.

B.3. Alternatives to CE – Molecularly Imprinted Polymers

CE-SELEX research has demonstrated that free solution selection provides several advantages over traditional affinity purification-type methods. Due to a dependence on electrophoretic resolution, CE-SELEX is not a truly universal method for aptamer selection.

To the best of our knowledge, few other methods for separation of free solution selection products have been explored. We believe that solid-phase extraction of unreacted oligomers from solution could be realized through the use of molecularly imprinted polymers.

Due to the limitations and costs of biologically-based affinity reagents, there has been much interest in synthetic materials that possess similar properties of affinity and selectivity [26]. There has been considerable research focused on the design and use of molecularly templated or imprinted polymers

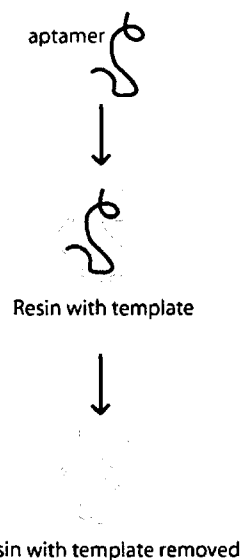


Figure 2. Polymerization of a MIP for target aptamer

(MIPs). Imprinted polymer theory says that a target molecule in the presence of functional monomer will undergo self-assembly such that the molecules' relative orientations will create energetically favorable interactions (hydrogen bonds, hydrophobic interactions, Van-der Waals forces) [26, 27]. A crosslinker is added to aid in polymerization of the monomer into a rigid structure, trapping the target. The templated molecule can then be removed through solvent extraction. Removal of the target leaves a cavity in the polymer capable of recognizing and binding target molecules from a sample, mimicking the hypervariable region of an

antibody. Dissociation constants for the target-MIP complex have been reported in the nM range [26]. These affinity constant values are similar to those observed for antibody-antigen interactions.

To date, MIPs have been synthesized and utilized as receptors for a wide variety of polymer materials, targets, and applications. Popular organic

polymers include polystyrenes and polyacrylates. Methacrylic acid can form hydrogen bonds with the template and allows for easy template removal following polymerization [28]. Inorganic materials have also been investigated, as the sol-gel technique has been used for template entrapment [29]. A potentiometric

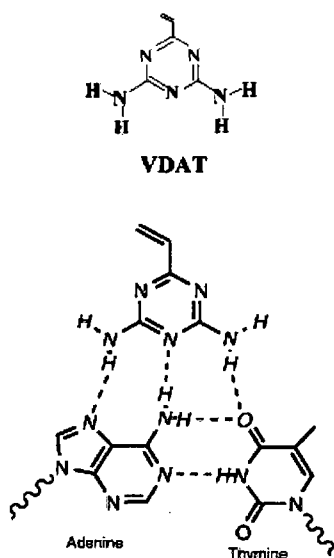


Figure 3. Functional monomer VDAT and theorized interaction with A-T base pair.[2]

sensor for the pesticide atrazine was developed using a polyvinyl chloride sensor matrix formed into a membrane [30]. The sensor was highly selective for atrazine over other common pesticides. Murray et al developed an optical sensor for soman hydrolysis products using a europium-doped MIP [31]. When the target was coordinated to the embedded europium, a fluorescent signal was observed. The hydrolysis product could be detected down to 4 pM. These examples represent only a few of the hundreds of papers currently published on the topic of MIP technology.

MIPs have found the most success in small molecule assays. Prepolymer solutions containing solvent and monomer are generally more compatible with small molecule templates than larger molecules such as proteins. It was not until 1996 that the first MIP for a protein was developed [32]. More recently, Takatsy et al. developed MIPs for two different hemoglobin species in gel granules. Binding of target was observed as a function of granule mobility during free zone electrophoresis [33]. Because the granules were neutrally charged, migration was only observed when hemoglobin protein was present and therefore bound to the MIP receptors on the granules. Selectivity was high, as granules imprinted against human hemoglobin would not recognize bovine hemoglobin, and vice versa.

Recently, Ogiso et al. have developed a system for detection of double-stranded DNA (dsDNA) using a molecularly imprinted gel matrix [2, 34, 35]. The functional monomer 2-vinyl-4,6-diamino-1,3,5-triazine (VDAT) was present in the polyacrylamide polymerization step to provide a site for recognition of A-T base

pairs by hydrogen bonding (Figure 3). A 564 base-pair DNA strand was used as a template molecule. Imprinted polymer gels were compared to non-imprinted gels during electrophoresis of a group of DNA strands including the templated dsDNA. It was found that migration of the templated molecule during electrophoresis was slower in the imprinted gel than in the non-imprinted gel, while the migration of several other DNA strands of various sizes was not affected by the imprinting. This suggests that the imprinted polymer gel specifically recognized the templated molecule as expected. The main challenge of dsDNA recognition by this MIP was that VDAT did not discriminate between A-T and T-A base pairs. DNA with a single point mutation of A-T to T-A also had slowed migration in the templated polymer gel.

B.4. Summary

High-affinity aptamers show potential to be an excellent synthetic alternative to antibodies. SELEX technology has been used for the last decade to find high affinity aptamers for a variety of small and large targets. CE-SELEX represents an important development for aptamer discovery, but is limited to aptamer-target complexes which can be electrophoretically resolved from the SELEX library. MIP-SELEX utilizes *in situ* selection as in CE-SELEX, but would use a templated polymer to remove non-aptamer DNA strands from solution. This method would be the first truly universal procedure for aptamer selection.

C. Research Methods/Experimental Design

Development of a SELEX system using an imprinted polymer resin for removal of non-aptamers from solution is presented. This goal will be accomplished with four specific aims.

1. Use traditional SELEX to select an aptamer for the pesticide atrazine.

Synthesize a pure stock of the aptamer for use in subsequent steps.

2. Prepare an imprinted polymer resin using the atrazine aptamer as a template.

3. Observe the partitioning behavior of the atrazine aptamer between solution and polymer receptor in the presence and absence of atrazine.

4. Prepare an imprinted polymer resin using a SELEX oligomer library as the imprinting molecules, and use the resin to remove non-aptamers from solution during SELEX separation. Compare selected aptamers to those found using traditional SELEX.

C.1. Selection of an atrazine aptamer

Atrazine is an herbicide which has seen widespread use in the United States and can be

found in streams near the point of use [36]. It has been found to induce hemapherotism in frogs [37] and is therefore of interest in aquatic ecological systems [38].

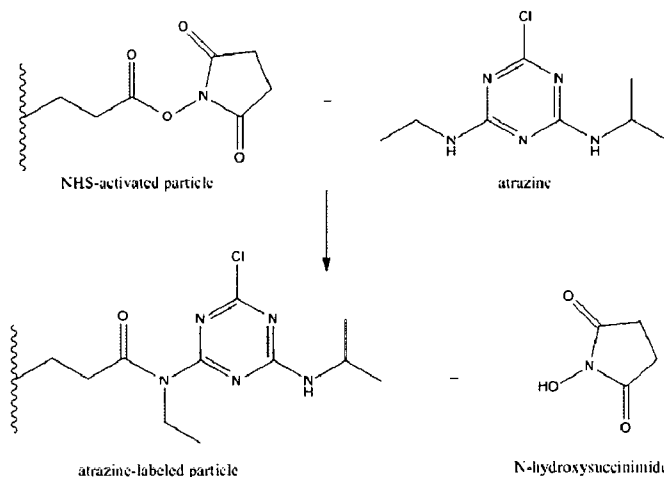


Figure 4. Conjugation of atrazine to a NHS-activated solid phase.

Atrazine is an excellent target to examine in SELEX systems because it is water soluble and can be easily conjugated to a solid phase. Figure 3 shows a reaction scheme for conjugation of atrazine to NHS-activated chromatography particles. Note that atrazine can be conjugated at either secondary amine, imparting heterogeneity in the aptameric determinant resin. Following conjugation, this solid phase will be used for selection of atrazine aptamers using traditional SELEX according to Niu et al [39]. Typical SELEX experiments require as many as 12 rounds of selection, while CE-SELEX requires only 2-4 [7]. Therefore, we will use 12 rounds in our initial SELEX experiments. Individual aptamers will be synthesized and conjugated to 6-carboxyfluorescein for fluorescence detection. Labeled aptamers will be incubated with an atrazine affinity column (as used above) and eluted with free atrazine. Fluorescence analyses of the elutents will be used to determine which aptamer shows the highest affinity for a given amount of atrazine in solution [7]. This aptamer sequence will be used for further experimentation.

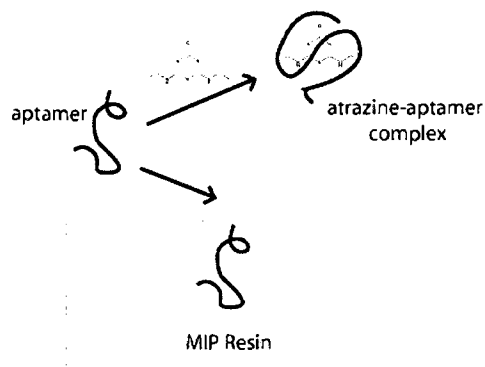


Figure 5. Partition of atrazine aptamer between liquid and solid phases in the presence of atrazine.

C.2. Preparation of an MIP for recognition of ssDNA atrazine aptamer

Atrazine is also an excellent target for free solution MIP SELEX

experiments. Target selection for atrazine using CE-SELEX or free solution SELEX using nitrocellulose for capture could be difficult or impossible due to the molecule's small mass (215.09 D).

Following the selection and synthesis of an atrazine ssDNA aptamer, a MIP resin will be created using the aptamer as a template molecule. The most appropriate resin for this application that has been published is a MIP gel created by Ogiso et al for use in gel electrophoresis. To form this gel, the template aptamer will be incubated with 2-vinyl-4,6-diamino-1,3,5-triazine (VDAT) at a 10:1 molar ratio of VDAT:aptamer and allowed to self-assemble for an incubation period. This solution will then be mixed with the recommended amounts of acrylamide, N,N'-methylenebisacrylamide, N,N,N',N'-tetramethylethylenediamine, and ammonium persulfate in a spin column with a removable frit for elution. Control polymer spin tubes will be prepared without the template aptamer present. Removal of the template will proceed by repeated rinsing with 0.1M guanidine hydrochloride in 50mM HEPES [2].

It is important to note that the VDAT recognition element is expected to recognize A-T and T-A residues on dsDNA. Although aptamers are produced as single strands, they commonly self-hybridize into folded states to create the unique conformations necessary for target binding [40]. It is through these Watson-Crick pairings that aptamers form secondary structures such as stems, pseudoknots and hairpins [3]. Therefore, we should expect that aptamers possess A-T pairings which can be recognized by the templated polymer in the same manner as ssDNA is recognized.

MIP binding affinity will be observed by incubation of the aptamer with both the imprinted polymer and the control. Following incubation, gel spin columns will be rinsed repeatedly with buffer then rinsed with the guanidine solution used above to elute the oligomers. All DNA in the eluent will be labeled with 6-carboxyfluorescein as above after a solvent exchange to remove guanidine. We expect that solutions eluted from the MIP gel will yield much more aptamer than that which is eluted from the non-imprinted gel.

C.3. Aptamer partition between the liquid and solid phases

In the above experiment we will show that the MIP gel can specifically bind an aptamer target. In the presence of a third affinity reagent, atrazine, we expect to see a partitioning of the aptamer between the imprinted polymer and a solution containing atrazine (Figure 5).

The system developed here is a three component competitive scenario, where one of the elements can bind with either of the other two, but in theory not both simultaneously. A similar system is that of the competitive immunoassay in which two ligands compete for binding at the same antibody's antigen-binding site. However, the MIP-SELEX system is different in that the aptamer serves as a ligand for the MIP, while atrazine is a ligand for the aptamer. This investigation will determine if the binding of atrazine to aptamer changes the aptamer conformation in a way that prevents binding to the imprint polymer.

In this system, we will examine three different incubation procedures for competitive binding using the aptamer, MIP spin column, and atrazine.

- a. Atrazine and the aptamer are applied to the column simultaneously, allowing all three components to interact at the same time.
- b. Atrazine and the aptamer are incubated together for a period of time before application to the column.
- c. The aptamer is applied to the column and allowed to incubate, followed by the addition of atrazine.

After the final incubation of each procedure, the columns will be spun down and the oligomer content of each eluate evaluated. It is understood that both MIPs and aptamers can have high affinities on the order of antibody-antigen interactions ($K_d = 10^{-9}$ M). To compensate for affinity differences, a range of atrazine concentrations covering several orders of magnitude will be used in each procedure to derive a dose-response curve where eluted aptamer concentration is plotted as a function of applied atrazine. We expect that the concentration of eluted aptamer will be proportional to applied atrazine concentration.

C.4. Preparation of an MIP for recognition of a SELEX library

SELEX libraries consist of pools of DNA or RNA of over 10^{15} different sequences [40]. Creating receptors for each oligomer in the library using biological systems (ie raising antibodies) would be an impossible task. Using self-assembly and MIPs, receptors for each sequence could be synthesized onto a single resin.

Using a stock ssDNA SELEX library as a template, MIP resins will be prepared in spin columns as described above for a single aptamer. A dilute solution of the same library and a given concentration of atrazine will be prepared. The library will be diluted in order to increase the ratio of available MIP binding sites for each oligomer to individual oligomer in solution. The library-atrazine solution will be incubated to allow for binding before being placed in contact with the spin column. The column will be rinsed several times with the library-atrazine solution to ensure complete non-aptamer extraction. PCR will be applied to the resulting eluent, completing one round of MIP-SELEX. 10 rounds will be performed during early testing. Final products will be sequenced and compared to aptamers discovered using traditional SELEX for both sequence motifs and binding affinity towards atrazine.

As with the single aptamer experiments discussed above, we intent to investigate alternative incubation schemes. These would include incubating the library with the column prior to atrazine exposure and simultaneous exposure of the library and atrazine to the column.

D. Summary

Aptamer selection technology is an emerging field which will likely provide the next generation of affinity reagents for diagnostic and therapeutic applications. CE-SELEX is a recent advancement which addresses several problems encountered during traditional SELEX by performing the selection process in free solution rather than on a solid phase.

The proposed MIP-SELEX system utilizes free solution selection, but does not require electrophoretic resolution of aptamer-target from non-aptamers. MIP-SELEX has potential to be the first universal aptamer selection protocol, capable of producing high affinity aptamers for any target.

E. References

1. Jayasena, S.D., *Aptamers: An emerging class of molecules that rival antibodies in diagnostics*. *Clinical Chemistry*, 1999. **45**(9): p. 1628-1650.
2. Slinchenko, O., et al., *Imprinted polymer layer for recognizing double-stranded DNA*. *Biosensors & Bioelectronics*, 2004. **20**(6): p. 1091-1097.
3. Klussmann, S., *The Aptamer Handbook*. 2006, Weinheim: Wiley-VCH. 490.
4. Ellington, A.D. and J.W. Szostak, *In vitro Selection of Rna Molecules That Bind Specific Ligands*. *Nature*, 1990. **346**(6287): p. 818-822.
5. Tuerk, C. and L. Gold, *Systematic Evolution of Ligands by Exponential Enrichment - Rna Ligands to Bacteriophage-T4 DNA-Polymerase*. *Science*, 1990. **249**(4968): p. 505-510.
6. Hamula, C.L.A., et al., *Selection and analytical applications of aptamers*. *Trac-Trends in Analytical Chemistry*, 2006. **25**(7): p. 681-691.
7. Mendonsa, S.D. and M.T. Bowser, *In vitro selection of high-affinity DNA ligands for human IgE using capillary electrophoresis*. *Analytical Chemistry*, 2004. **76**(18): p. 5387-5392.

8. Vlahou, A. and A. Fountoulakis, *Proteomic approaches in the search for disease biomarkers*. Journal of Chromatography B-Analytical Technologies in the Biomedical and Life Sciences, 2005. **814**(1): p. 11-19.
9. Gosling, J.P., Basso, L.V., *Immunoassay: Laboratory Analysis and Clinical Application*. 1994, Boston: Butterworth-Heinemann. 360.
10. Diamandis, E., Christopoulos, T.K., , *Immunoassay*. 1996, Academic Press: San Diego. p. 44-45.
11. Odell, W.D., Franchimont, P., *Principles of Competitive Protein Binding Assays*. Second ed. 1983, New York.
12. Robertson, D.L. and G.F. Joyce, *Selection Invitro of an Rna Enzyme That Specifically Cleaves Single-Stranded-DNA*. Nature, 1990. **344**(6265): p. 467-468.
13. Klug, S.J., A. Huttenhofer, and M. Famulok, *In vitro selection of RNA aptamers that bind special elongation factor SelB, a protein with multiple RNA-binding sites, reveals one major interaction domain at the carboxyl terminus*. Rna-a Publication of the Rna Society, 1999. **5**(9): p. 1180-1190.
14. Geiger, A., et al., *RNA aptamers that bind L-arginine with sub-micromolar dissociation constants and high enantioselectivity*. Nucleic Acids Research, 1996. **24**(6): p. 1029-1036.
15. Herr, J.K., et al., *Aptamer-conjugated nanoparticles for selective collection and detection of cancer cells*. Analytical Chemistry, 2006. **78**(9): p. 2918-2924.

16. Tombelli, S., M. Minunni, and M. Mascini, *Aptamers-based assays for diagnostics, environmental and food analysis*. Biomolecular Engineering, 2007. **24**(2): p. 191-200.
17. O'Sullivan, C.K., *Aptasensors - the future of biosensing*. Analytical and Bioanalytical Chemistry, 2002. **372**(1): p. 44-48.
18. Yang, Y.S., et al., *Structural basis of ligand discrimination by two related RNA aptamers resolved by NMR spectroscopy*. Science, 1996. **272**(5266): p. 1343-1347.
19. Lorsch, J.R. and J.W. Szostak, *In-Vitro Selection of Rna Aptamers Specific for Cyanocobalamin*. Biochemistry, 1994. **33**(4): p. 973-982.
20. Ho, H.A. and M. Leclerc, *Optical sensors based on hybrid aptamer/conjugated polymer complexes*. Journal of the American Chemical Society, 2004. **126**(5): p. 1384-1387.
21. Hamaguchi, N., A. Ellington, and M. Stanton, *Aptamer beacons for the direct detection of proteins*. Analytical Biochemistry, 2001. **294**(2): p. 126-131.
22. Mendonsa, S.D. and M.T. Bowser, *In vitro evolution of functional DNA using capillary electrophoresis*. Journal of the American Chemical Society, 2004. **126**(1): p. 20-21.
23. Mendonsa, S.D. and M.T. Bowser, *In vitro selection of aptamers with affinity for neuropeptide Y using capillary electrophoresis*. Journal of the American Chemical Society, 2005. **127**(26): p. 9382-9383.

24. Mosing, R.K., S.D. Mendonsa, and M.T. Bowser, *Capillary electrophoresis-SELEX selection of aptamers with affinity for HIV-1 reverse transcriptase*. Analytical Chemistry, 2005. **77**(19): p. 6107-6112.
25. Tang, J.J., et al., *The DNA aptamers that specifically recognize ricin toxin are selected by two in vitro selection methods*. Electrophoresis, 2006. **27**(7): p. 1303-1311.
26. Holthoff, E.L. and F.V. Bright, *Molecularly templated materials in chemical sensing*. Analytica Chimica Acta, 2007. **594**(2): p. 147-161.
27. Avila, M., et al., *Molecularly Imprinted Polymers for Selective Piezoelectric Sensing of Small Molecules*. Trac-Trends in Analytical Chemistry, 2007.
28. Kandimalla, V.B. and H.X. Ju, *Molecular imprinting: a dynamic technique for diverse applications in analytical chemistry*. Analytical and Bioanalytical Chemistry, 2004. **380**(4): p. 587-605.
29. Gupta, R. and N.K. Chaudhury, *Entrapment of biomolecules in sol-gel matrix for applications in biosensors: Problems and future prospects*. Biosensors & Bioelectronics, 2007. **22**(11): p. 2387-2399.
30. Prasad, K., et al., *Molecularly imprinted polymer (biomimetic) based potentiometric sensor for atrazine*. Sensors and Actuators B-Chemical, 2007. **123**(1): p. 65-70.
31. Jenkins, A.L., O.M. Uy, and G.M. Murray, *Polymer-based lanthanide luminescent sensor for detection of the hydrolysis product of the nerve agent Soman in water*. Analytical Chemistry, 1999. **71**(2): p. 373-378.

32. Liao, J.L., Y. Wang, and S. Hjerten, *Novel support with artificially created recognition for the selective removal of proteins and for affinity chromatography*. *Chromatographia*, 1996. **42**(5-6): p. 259-262.
33. Takatsy, A., et al., *Universal method for synthesis of artificial gel antibodies by the imprinting approach combined with a unique electrophoresis technique for detection of minute structural differences of proteins viruses and cells, (bacteria). Ib. Gel antibodies against proteins (hemoglobins)*. *Electrophoresis*, 2007. **28**(14): p. 2345-2350.
34. Ogiso, M., et al., *Detection of a specific DNA sequence by electrophoresis through a molecularly imprinted polymer*. *Biomaterials*, 2006. **27**(22): p. 4177-4182.
35. Ogiso, M., et al., *DNA detection system using molecularly imprinted polymer as the gel matrix in electrophoresis*. *Biosensors & Bioelectronics*, 2007. **22**(9-10): p. 1974-1981.
36. Gruessner, B., N.C. Shambaugh, and M.C. Watzin, *Comparison of an Enzyme-Immunoassay and Gas-Chromatography Mass-Spectrometry for the Detection of Atrazine in Surface Waters*. *Environmental Science & Technology*, 1995. **29**(1): p. 251-254.
37. Hayes, T., et al., *Atrazine-induced hermaphroditism at 0.1 ppb in American leopard frogs (Rana pipiens): Laboratory and field evidence*. *Environmental Health Perspectives*, 2003. **111**(4): p. 568-575.
38. Huber, W., *Ecotoxicological Relevance of Atrazine in Aquatic Systems*. *Environmental Toxicology and Chemistry*, 1993. **12**(10): p. 1865-1881.

39. Niu, W.Z., N. Jiang, and Y.H. Hu, *Detection of proteins based on amino acid sequences by multiple aptamers against tripeptides*. *Analytical Biochemistry*, 2007. **362**(1): p. 126-135.
40. Wilson, D.S. and J.W. Szostak, *In vitro selection of functional nucleic acids*. *Annual Review of Biochemistry*, 1999. **68**: p. 611-647.